

# The Institute of Paper Chemistry

Appleton, Wisconsin

## Doctor's Dissertation

**The Contribution of Charge-Transfer Complexes  
to the Color of Kraft Lignin**

**Gary S. Furman, Jr.**

**June, 1986**

THE CONTRIBUTION OF CHARGE-TRANSFER COMPLEXES  
TO THE COLOR OF KRAFT LIGNIN

A thesis submitted by

Gary S. Furman, Jr.

B.S. 1980, Lebanon Valley College

M.S. 1982, Lawrence University

In partial fulfillment of the requirements  
of The Institute of Paper Chemistry  
for the degree of Doctor of Philosophy  
from Lawrence University,  
Appleton, Wisconsin

Publication rights reserved by  
The Institute of Paper Chemistry

June, 1986

# TABLE OF CONTENTS

	Page
ABSTRACT	1
INTRODUCTION	3
Perspective	3
Literature Survey	4
Review of Chromophoric Structures in Kraft Lignin	4
Electronic Absorption Spectroscopy	5
Transition Metal Complexes	6
Conjugated Unsaturated Systems	8
Quinones	11
Other Chromophores	13
Quinonemethides	13
Free Radicals	13
Charge-Transfer Complexes (CTC's)	14
Theoretical Treatment	14
Classifications of CTC's	15
Structural Considerations	16
Electronic Spectra	19
Factors Influencing CT Absorption Bands	20
Substituents	20
Solvent	22
Temperature	24
Pressure	24
Association Constants	25
Thermodynamic Parameters	26
Selected Examples of CTC's	27
Indication for CTC's in Kraft Lignin	28
Thesis Objectives	30

Experimental Approach	31
Determination of CTC's in Kraft Lignin	31
Evaluation of the Contribution to Color of Various Chromophores	33
MATERIALS AND METHODS	34
Lignin Starting Material	34
Isolation	34
Carbohydrate Removal	36
Lignin Analyses	38
Elemental, Methoxyl, and Ash Analyses	38
Phenolic Hydroxyl Content	39
Catechol Content	40
Instrumental Methods	40
Electronic Absorption Spectroscopy	40
Infrared Spectroscopy	41
Nuclear Magnetic Resonance (NMR) Spectroscopy	41
Proton Spectra	41
Carbon-13 Spectra	43
Metal Analysis	43
Compounds and Synthesis	47
Acetylated Models	47
<u>meta</u> -Nitrobenzenesulfonyl Hydrazide	49
1-Propionyl-Pyrrolidine	51
Lignin Preparations	52
Acetylation	52
Reductive Acetylation	52
Sodium Borohydride Reduction	53

Diimide Reduction	54
Metal Ion Removal	56
Periodate Oxidation	60
Lead Nitrate Addition	60
Sulfur Dioxide Addition	60
Ethylene Glycol Addition	61
High Pressure Spectroscopy	62
Apparatus	62
Sample Preparation	63
Procedure for High Pressure Run	63
Labeling Techniques for Kraft Lignin	64
Carbon-13	64
Carbon-14	65
RESULTS AND DISCUSSION	68
Lignin Materials	68
Kraft Lignin	68
Periodate Oxidized Kraft Lignin	68
Periodate Oxidation with Ethylene Glycol Addition	70
Charge-transfer Complexes in Kraft Lignin	83
CTC's Between Model Compounds and Kraft Lignin	83
Effect of Acetylating the Lignin	85
Effect of Added Quinone Concentration	88
Effect of Solvent	90
CTC Between Model Phenol and Model Quinone	90
CTC Between Model Acetate and Model Quinone	94
Evidence for CTC's in Periodate Oxidized Kraft Lignins	95

Solvent Effect	96
Pressure Effect	101
Derivatization Experiments	108
Evidence for CTC's in Kraft Lignin	112
The Contribution of Various Chromophore Types to the Color of Kraft Lignin	122
Transition Metal Complexes	122
Extended Conjugated Systems	126
Quinones	133
Summary of Chromophore Contributions	136
CONCLUSIONS	138
RECOMMENDATION	139
ACKNOWLEDGMENTS	140
LITERATURE CITED	141
APPENDIX I. CARBOHYDRATE ANALYSES	148
APPENDIX II. PERIODATE OXIDATION OF KRAFT LIGNIN	151
APPENDIX III. ESTIMATION OF SOLVENT COMPRESSION	162
APPENDIX IV. UNIT MOLECULAR WEIGHTS FOR ACETYLATED LIGNINS	166
APPENDIX V. MOLAR ABSORPTIVITY OF QUINONES IN KRAFT LIGNINS	168
APPENDIX VI. SEPARATION OF QUINONE AND CTC ABSORBANCES	170

## ABSTRACT

The dark color of kraft lignin represents a major drawback to the kraft pulping process, since kraft pulps must be subjected to extensive bleaching sequences for many end uses. This dark color has also hindered the use of kraft lignin as a feedstock for the production of more valuable products. Although various chromophores have been identified in kraft lignin, they have not accounted for the total color which is observed. The possible role that charge-transfer complexes play in the color development of kraft lignins was the subject of this investigation. Specifically, work was directed at determining whether charge-transfer complexes occur in kraft lignin, and, if so, what contribution they make to its color.

Electronic absorption spectroscopy was employed as the major investigative tool for determining the presence of charge-transfer complexes in kraft lignin. Spectra clearly revealed the occurrence of a complex between kraft lignin and the added model quinone, 3,5-di-tert-butyl-1,2-benzoquinone. The spectral response of a periodate oxidized kraft lignin to solvent and pressure changes and derivatization (acetylation) demonstrated the likely presence of charge-transfer complexes. The periodate oxidation served to introduce ortho-quinone structures into the lignin.

The determination of the quinone content of an unreacted kraft lignin by a carbon-14 labeling technique showed the presence of approximately three quinone groups per one-hundred lignin C<sub>9</sub> units. The calculated molar absorptivity of these quinones (528 lit/mol-cm) indicated only one-third of the absorbance decrease caused by the sodium borohydride reduction of this lignin could be accounted for by this number of quinones. The remainder of the decrease in absorbance (two-thirds) was assigned to the disruption of charge-transfer

complexes in which the quinones participated as acceptor moieties. The complementary donor species in these lignin complexes apparently were free phenolic structures.

Quinones were a major source of color in the laboratory-produced kraft lignin which was studied. This color resulted from the visible absorption bands of the quinones, as well as from the resultant visible absorption band due to their charge-transfer interactions. The removal of transition metals by chelation with EDTA demonstrated that metal complexes were not a source of color in this lignin. However, the similar examination of an industrial kraft lignin showed that metal complexes did contribute to its color. The difference in behavior may be due to different complexing structures in the two lignins. The hydrogenation of carbon-carbon double bonds with diimide also did not reduce the visible absorbance of the laboratory kraft lignin. The contribution of extended conjugated systems to the color of kraft lignins, therefore, appears to be insignificant.



## INTRODUCTION

### PERSPECTIVE

Of the wood pulp produced in the United States in 1982, 75% was obtained from the kraft pulping process.<sup>1</sup> The kraft process has a number of advantages which have kept it the dominant pulping process in the world today. Two of these advantages are the high strength of the pulp which is obtained and the insensitivity of the process to widely variant wood species. Nonetheless, the process does have some disadvantages, one of which is the low brightness of the resultant pulps, compared, for example, with sulfite pulps. The dark color of kraft pulps necessitates extensive and expensive bleaching treatments for many end uses. Lignin remaining in and on the fibers after pulping is the source of this color.

Approximately 20 million tons of kraft lignin were produced in the United States in 1986 as a byproduct of the kraft pulping process.<sup>2</sup> The vast majority of this lignin was burned in recovery boilers, and, therefore, was used as a major fuel source for many pulp and paper mills. In any proposition to utilize this abundant raw material source as a feedstock for the production of more valuable chemicals, the product produced must be worth more than the corresponding replacement fuel cost. Again, a major stumbling block to the use of kraft lignin in such higher quality, value-added products is its dark color.

The dark color of residual and isolated kraft lignins can therefore be seen as both an important and a wide-ranging problem. Not until recently have the structural aspects of residual kraft lignin been explored.<sup>3-7</sup> Much more information is available on the structure of isolated kraft lignins, and this has

been used in determining some of the chromophoric structures present in it. Structures including transition metal complexes, conjugated unsaturated systems, and quinones have been cited as sources of color in isolated kraft lignins. In spite of this effort, the individual structures responsible for the color of both residual and isolated kraft lignins are still not fully understood.

Previous work on isolated kraft lignin (referred to from now on as simply "kraft lignin"), performed in order to determine the origin of its color, has made it apparent that the identified chromophores were not present in sufficient quantities to account for the total color observed. This has led to speculation on the possible presence of other chromophores in kraft lignin, including occasional references to charge-transfer complexes.

A charge-transfer complex (CTC) may be defined as a weak interaction between an electron donor and an electron acceptor. Characteristic of CTC's is the appearance of an additional electronic absorption band(s), separate from the absorption bands of both the donor and acceptor molecules. With the appropriate combination of donor and acceptor, the CT absorption band occurs in the visible region of the electromagnetic spectrum. In this event, the complexes are colored.

CTC's have not been extensively investigated as potential chromophores in kraft lignin, despite the fact kraft lignin is known to contain suitable electron donating and accepting moieties within its polymeric matrix.

#### LITERATURE SURVEY

##### Review of Chromophoric Structures in Kraft Lignin

Early research into the so-called "kraft color" was concerned with the source of the reddish-brown color of kraft pulps. Through the 1920's and 30's

sources of kraft color were proposed<sup>8</sup> including tannins and phlobaphenes, along with the condensation products between tannins and alkali-labile carbohydrates; sulfur dyes; lignin and its reaction products; and carbohydrate degradation products. By 1948 Pigman and Csellak<sup>8</sup> were among the first to pinpoint lignin and its degradation products as responsible for the bulk of the color found in kraft pulps.

Subsequent research has centered on identifying the individual chemical structures or groupings of structures which are responsible for this color. Although some of these structures may be incorporated into the lignin macromolecule during the original lignification in the tree, many are known to result from various degradation and condensation reactions the lignin participates in during the kraft pulping process.

The work discussed in the following review is based on the results obtained from isolated kraft lignin or from lignin model compound studies. Only chromophoric structures capable of contributing to the visible absorption spectrum of kraft lignin are considered.

#### Electronic Absorption Spectroscopy

Electronic absorption spectroscopy provides a useful instrumental method for examining chromophoric or light absorbing structures. The electronic absorption spectrum obtained for one kraft lignin is given in Fig. 1. Several features of this spectrum which are characteristic for the majority of kraft lignins, may be pointed out. These include the phenolic maximum at 280 nm, a shoulder which occurs near 340 nm, and a gradually decreasing absorption above 400 nm. The smooth nature of the curve throughout the visible range may represent the action of several different chromophore systems, including the tails of absorption bands occurring in the near UV spectral region.

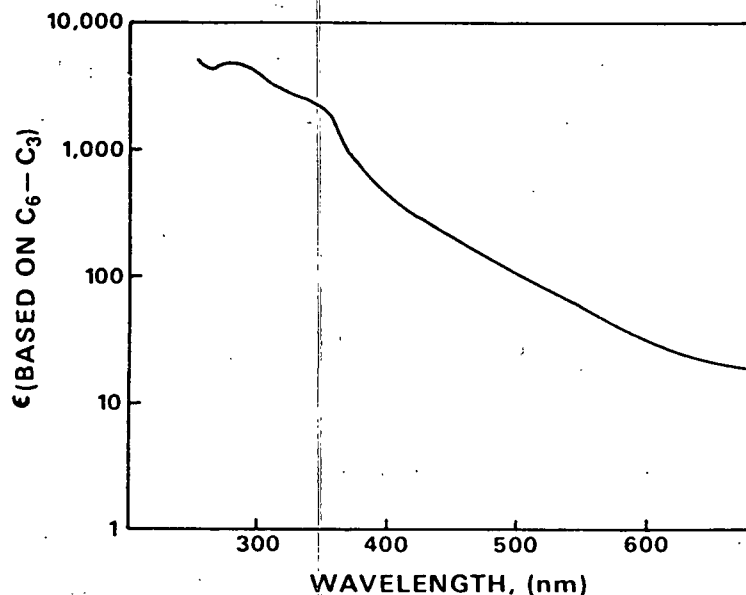


Figure 1. Electronic absorption spectrum for kraft lignin (Indulin AT).<sup>9</sup>

Several investigators have attempted to resolve the electronic absorption spectrum of kraft lignin into its component bands.<sup>10,11</sup> Norrström<sup>11</sup> modeled the lignin spectrum by the use of thirteen overlapping Gaussian bands. He divided these bands into four general groups, categorized by their response to changes in pH. However, no further characterization of these individual bands has appeared in the literature.

#### Transition Metal Complexes

Various transition metals are found in kraft lignin, iron usually being the most abundant. The metals may be present in the original wood source or may become associated with the lignin from contact with various process waters or machinery. These metals are able to form complexes with certain structures in the lignin molecule,<sup>9,12,13</sup> most notably, phenols and catechols. These complexes should be considered as potentially important contributors to the

color of kraft lignin, since they absorb light in the visible region of the spectrum.

Metal-lignin complexes have been studied by the use of model compounds. Polcin and Rapson<sup>14</sup> determined the absorption spectra of various metal ions with catechol and flavone-type structures. From these spectra, they were able to conclude iron complexes gave longer wavelength absorptions than other metal complexes, including manganese, copper, and aluminum ones. Furthermore, ferric ions ( $\text{Fe}^{3+}$ ) were found to be the most effective in color formation, whereas ferrous ions ( $\text{Fe}^{2+}$ ) had little or no effect on color. Imsgard et al.<sup>12</sup> and Marton et al.<sup>15</sup> determined the absorption spectra of various lignin model catechols and phenols with ferric ions. In general, these spectra showed the complexes had absorption maxima between 550 and 590 nm, with molar absorptivities ranging up to 2000 lit/mol-cm.

Several researchers have complexed ferric ions with kraft lignin and have observed subsequent increases in its absorption spectrum, centered at 560 nm.<sup>9,12</sup> The magnitude of this increase, together with the known molar absorptivities of model catechol complexes, were then used to estimate the catechol content of the lignin. According to these calculations, kraft lignin contains 6-7 catechol structures per 100 C<sub>9</sub> units.

Another approach has been to remove metal ions from kraft lignin using chelating agents, and then to examine the resultant absorption spectra for decreases in absorbance. Nakano and coworkers<sup>16,17</sup> found iron was the only significant metal present in kraft lignin, with respect to a contribution toward its color. Removal of the iron by EDTA chelation resulted in a decrease in absorption of the kraft lignin spectrum, centered around 500 nm. The percentage decrease in

the absorbance of the lignin was found to be about 5% at 450 nm, approximately 14% at 500 nm, and reached a maximum of about 20% at 700 nm.

#### Conjugated Unsaturated Systems

Kraft lignin contains various unsaturated functional groups, including carbonyls and carbon-carbon double bonds. Individually, these functional groups absorb light in the ultraviolet (UV) portion of the spectrum. Absorption bands appearing between 300 and 350 nm are typical for lignin model compounds which contain carbonyls or carbon-carbon double bonds.<sup>18</sup> Based on model compounds the shoulder appearing at 340 nm in the kraft lignin spectrum has been attributed to stilbene structures.<sup>9</sup> While these individual structures do not contribute to the visible absorbance of kraft lignin, conjugation with other unsaturated structures could lead to extension of the absorption bands into the visible region of the spectrum.

Both *o,p'* and *p,p'*-dihydroxystilbene structures have been shown to form from model compounds under kraft pulping conditions.<sup>9,19</sup> *p,p'*-Dihydroxystilbenes have also been isolated from kraft cooking liquors.<sup>20</sup> *o,p'*-Dihydroxystilbenes are formed from phenylcoumaran-type structures via quinonemethide intermediates as shown in Fig. 2. Figure 3 shows the similar formation of *p,p'*-dihydroxystilbenes from 1,2-diarylpropane-1,3-diol structures.

The dihydroxystilbenes absorb only in the UV portion of the spectrum, but they are readily oxidized to red-colored stilbenequinones upon standing in air.<sup>19,21,22</sup> Various metal ions including  $\text{Fe}^{3+}$  and  $\text{Cu}^{2+}$  catalyze this oxidation.<sup>19</sup> Quinonemethides, which are known oxidizing agents,<sup>9,21</sup> could perform this oxidation in kraft pulping liquors.

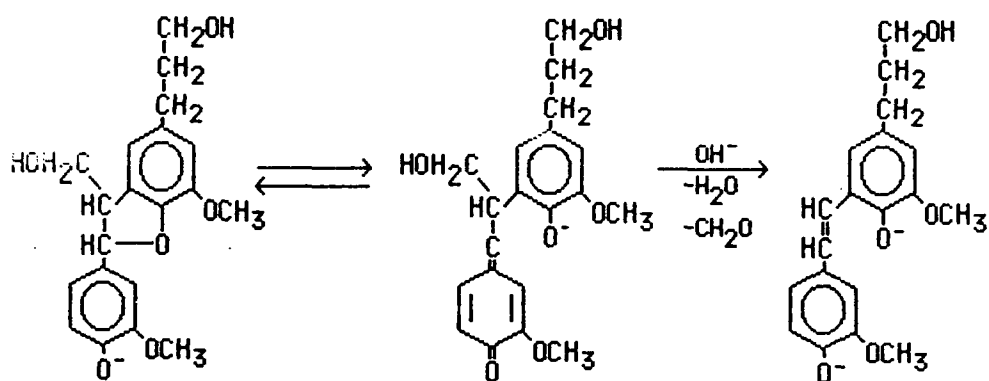


Figure 2. Formation of *o,p'*-dihydroxystilbenes.

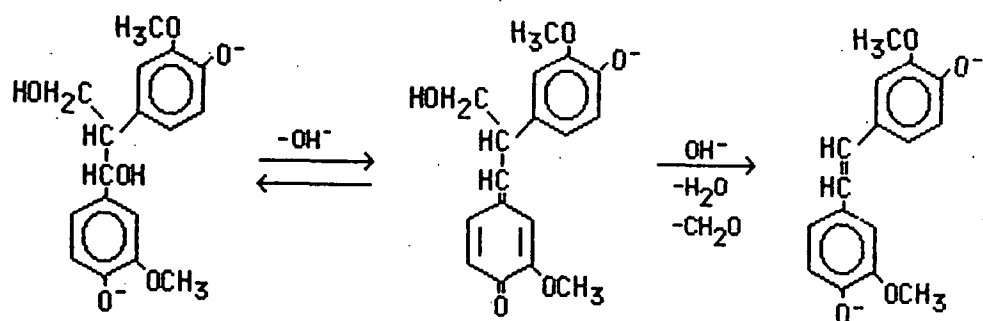


Figure 3. Formation of *p,p'*-dihydroxystilbenes.

From ionization difference spectroscopy,  $\Delta\epsilon_1$ , Falkehag *et al.*<sup>9</sup> estimated there were 0.07 stilbene structures per C<sub>9</sub> unit present in kraft lignin. Similarly the specific amount of *p,p'*-dihydroxystilbene structures was estimated to be 0.005 structures per C<sub>9</sub> unit using a technique employing peroxide oxidation of the lignin in the presence of Cu<sup>2+</sup>.

Butadiene structures have also been isolated from model compounds subjected to kraft pulping conditions. Gierer<sup>19</sup> has found 1,4-bis-(*p*-hydroxyphenyl)-buta-1,3-diene in the reaction mixture which resulted from the kraft pulping of phenolic pinosresinol structures (see Fig. 4). On oxidation these structural types are expected to yield highly conjugated quinonoid chromophores.

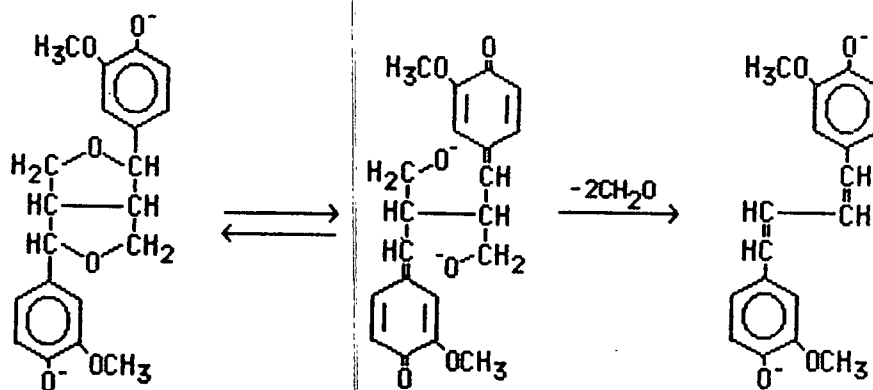


Figure 4. Formation of butadiene structures.

Finally, there is the possibility of two or more chromophores joined together by conjugation to form extended conjugated systems. Such extended systems are also expected to have absorptions in the visible range of the spectrum. In the tentative formulation for kraft lignin given by Marton,<sup>23</sup> shown in Fig. 5, units 6, 8, 9, and 10 form such an extended conjugated system.

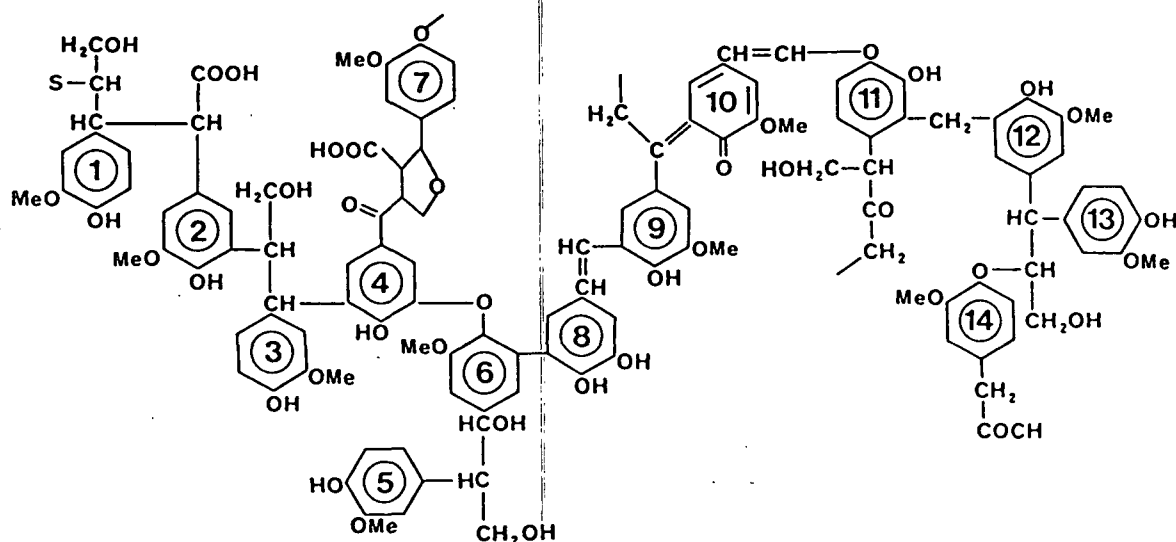


Figure 5. Tentative structural features in a segment of pine kraft lignin, according to Marton.<sup>23</sup>



## Quinones

Quinones are cyclic conjugated diketones which have two absorption bands occurring in the visible region. Quinoidal structures might form in lignin during the original lignification process in the tree.<sup>12</sup> Oxygen or hydroxyl radicals are capable of adding to phenoxyl radicals of guaiacyl and syringyl derivatives. Such additions would lead to demethoxylation of the guaiacyl and syringyl derivatives and subsequent formation of ortho-quinone structures.

Pew and Connors<sup>24</sup> found that simple lignin phenylpropanoid models underwent phenol dehydrogenation reactions analogous to those taking place during lignin biosynthesis to yield phenyl-para-benzoquinones. Harkin and Obst<sup>25</sup> showed the enzymatic phenol oxidation of 2,4,6-trimethoxyphenol caused the elimination of a methoxy group, leading to a mixture of products containing mostly the para-quinone, 2,6-dimethoxy-1,4-benzoquinone and a small amount of the ortho-quinone, 3,5-dimethoxy-1,2-benzoquinone. In the authors' opinion, similar reactions with guaiacyl and syringyl structures during lignin formation would introduce quinonoid structures into the lignin macromolecule.

Although these "original" quinone types are significant contributors to the coloration of woods, they are not as important when considering the coloration of chemical pulps. Of much more importance for kraft pulps is the formation of a substantial number of quinone precursors during the pulping process. These quinone precursors, specifically dihydroxybenzenes or catechols, are formed by demethylation of lignin structures during pulping. Under kraft pulping conditions, hydrosulfide and methyl mercaptan anions are able to demethylate guaiacyl or syringyl units in lignin to produce the corresponding catechols. This process is illustrated in Fig. 6. Although these catechols are not colored themselves, they are easily oxidized to red-colored ortho- or methoxy-ortho-benzoquinones.

The oxidation can take place in a manner similar to that described for the dihydroxystilbenes.

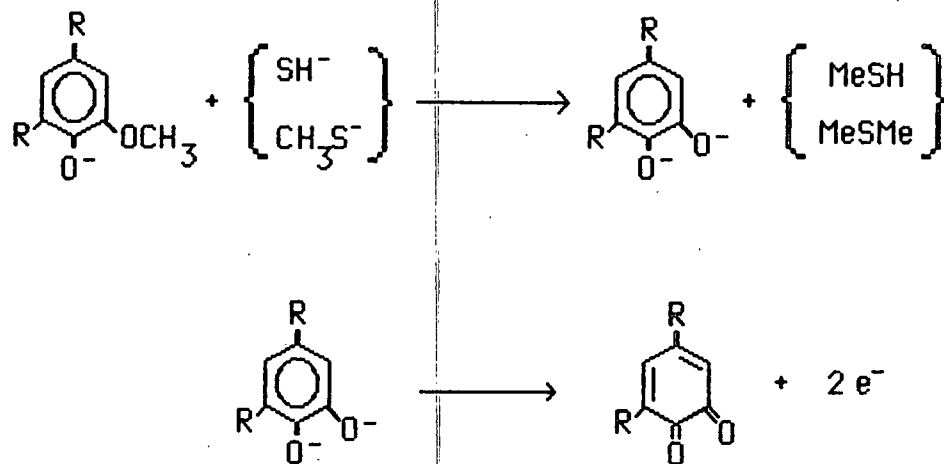


Figure 6. Formation of catechols and their oxidation to ortho-quinones (R = H or OCH<sub>3</sub>).

Although quinones clearly play a major role in the observed color of kraft lignin, determination of the magnitude of this contribution has been hampered by a lack of direct analytical or instrumental methods for the detection of quinones. Contributing to this problem is the inherently unstable nature of many quinones and the likelihood the quinones are present in kraft lignin in relatively small quantities.

The concentration of quinoidal structures in kraft lignin has been estimated from comparison of spectra obtained before and after treatment of the lignin with a reducing agent, such as sodium borohydride or sodium hydrosulfite. The magnitude of the decrease in absorbance of the lignin spectrum caused by this treatment can then be related to the quantity of quinones present, making use of average absorption frequencies and molar absorptivities from model ortho-quinones. ortho-Quinone models are used, since they will be the predominant

quinone type in kraft lignin. This method assumes spectral properties of isolated model quinones are comparable to quinone structures incorporated within the lignin macromolecule. Using this approach, Iiyama and Nakano<sup>26</sup> estimated softwood kraft lignin contained 0.03 to 0.04 ortho-quinone structures per C<sub>9</sub> unit. This number of quinones accounted for 40-45% of the lignin's absorbance in the visible region of the spectrum.

#### Other Chromophores

Quinonemethides. Quinonemethides are important intermediates, both during lignin biosynthesis and in pulping reactions. They may play a part in contributing to the color of kraft lignin in one of two ways. First, the role of quinonemethides as possible oxidizing agents for other color precursors (dihydroxystilbenes and catechols) has already been mentioned. Secondly, as Harkin<sup>27</sup> pointed out, resonance stabilized quinonemethides resulting from the dehydrogenation of dihydroxy-diphenylmethane structures are yellow-colored chromophores in their own right and could be responsible for some of the color of kraft lignin.

Free Radicals. In 1960 Rex<sup>28</sup> first demonstrated the existence of stable free radicals in lignin preparations. Several years later Steelink and coworkers<sup>29</sup> found kraft lignin, as well as other chemically or biologically modified lignins, had increased radical contents compared to native lignins. Steelink and coworkers also showed various derivatization procedures dramatically altered the free radical content of kraft lignin. This led to the novel proposal of the presence of quinhydrone-type structures in kraft lignin. These structures are complexes between a quinone and its corresponding hydroquinone. This concept

will be discussed in more detail in the section entitled "Indications for CTC's in Kraft Lignin".

Steelink<sup>30</sup> was also able to show syringol derivatives, which possessed an  $\alpha$ -carbonyl group, could be oxidized to remarkably stable radicals in solution. These radical solutions were purple in color and had several strong absorbance bands in the visible region of the spectrum.

### Charge-Transfer Complexes (CTC's)

Charge-transfer complexes are molecular complexes formed by the weak interaction between electron donors and electron acceptors. An electron donor may be defined as a molecule possessing a relatively high localized electron density. Conversely, an electron acceptor is relatively deficient in electrons. Charge-transfer complexes are also termed electron donor-acceptor complexes.

The discussion which follows will consider CTC's in some detail. Topics of particular interest to this thesis include the influences of substituent groups, solvent, and pressure on CT interactions.

### Theoretical Treatment

Charge-transfer complexes exist in two states: a ground state and an excited state. In the ground state, the two molecules composing the complex undergo the normal physical forces expected between two molecules which are in close proximity to each other. These forces include London dispersion forces and any electrostatic interactions, such as between dipole moments. In addition to these normal forces, a small amount of charge is transferred from the donor to the acceptor. This contributes some additional binding energy to the complex.<sup>31</sup>

The excited state of the complex occurs when the ground state complex absorbs a photon of light having the appropriate frequency. In the excited state, the electron which had only been slightly shifted toward the acceptor in the ground state is almost totally transferred.<sup>31</sup> Depending on the structural features of both the donor and acceptor, the wavelength of light absorbed may be in the visible range of the electromagnetic spectrum. In many cases, therefore, CTC's are colored substances.

Mulliken<sup>32</sup> was responsible for the development of what has been the most successful theoretical treatment of CTC's. He described the ground state of the complex by the wavefunction,  $\psi_N$ , which is the hybrid of two wavefunctions,  $\psi(A,D)$  and  $\psi(A^-D^+)$ . The wavefunction  $\psi(A,D)$  is termed the no-bond function and represents the wavefunction of the two molecules in close proximity to each other but with no charge-transfer between them.  $\psi(A,D)$  can include, however, the normal electrical interactions between molecules. Consequently, the ground state wavefunction for a weak complex can be described as:

$$\psi_N = a\psi(A,D) + b\psi(A^-D^+) \quad \text{where } a \gg b \quad (1)$$

Furthermore, the wavefunction  $\psi(A^-D^+)$  is called the dative function and represents the wavefunction of the two molecules held together by total transfer of an electron from the donor, D, to the acceptor, A. The excited state of the complex can then be described by:

$$\psi_E = b^*\psi(A^-D^+) - a^*\psi(A,D) \quad \text{where } b^* \gg a^* \quad (2)$$

#### Classifications of CTC's

CTC's may conveniently be classified according to the types of orbitals in the donor and acceptor molecules which are undergoing the interaction. Donor

and acceptor molecules may each be divided into three classes,<sup>33</sup> as shown in Table 1. The  $\nu$  acceptors refer to metal atoms possessing a low-lying vacant valency-orbital. Hypothetically, there are nine possible types of complexes. However in practice, the  $n$ -donors do not form complexes with metal ions but form covalent bonds instead.<sup>34</sup>

Table 1. CTC donor and acceptor types.

Donor Type	Examples
$\sigma$	R-X, cyclopropane
$n$	R <sub>2</sub> O, R <sub>3</sub> N, pyridine, dioxane
$\pi$	Aromatic and unsaturated hydrocarbons, especially if containing electron releasing substituents (hexamethylbenzene, phenols)
Acceptor Type	Examples
$\nu$	Ag <sup>+</sup> , certain organometallics
$\sigma$	I <sub>2</sub> , Br <sub>2</sub> , ICl
$\pi$	Aromatic and unsaturated hydrocarbons, especially if containing electron withdrawing substituents (TCNE, halogenated quinones)

Complexes involving  $\pi$ -donors with  $\pi$ -acceptors appear to present the most obvious candidates for CTC's in kraft lignin. Both  $\pi$ -donating and  $\pi$ -accepting structures are present in kraft lignin. Good examples of these structures are phenols and quinones, respectively.

#### Structural Considerations

CTC's can exist as intermolecular complexes, where the interaction takes place between two molecules, or as intramolecular complexes, where both the

donor and acceptor moieties are contained within one molecule. For charge-transfer interactions to occur, the donor and acceptor components must be close enough for their differences in electron density to be felt. For unrestrained complexes, distances between the components of 3.0-3.4 Å, or slightly less than the Van der Waals distance, are common.<sup>31</sup>

Most CTC's exist in a 1:1 stoichiometric ratio of donor to acceptor. For some  $\pi$ - $\pi$  types of complexes, there is evidence for the existence of higher order complexes in equilibrium with the 1:1 complexes.<sup>35</sup> For the 2:1 complex involving two donors,  $D_2A$ , support has been found for the D-A-D form rather than the D-D-A form. The crystal structures of phenol-benzoquinone complexes have been found to have both 1:1 and 2:1 stoichiometries.<sup>36</sup>

Many aromatic, crystalline CTC's, involving  $\pi$  donors and acceptors, are found to be composed of infinite chains of alternate donor and acceptor molecules in which the donor-acceptor distance is slightly less than the Van der Waals distance.<sup>36</sup> Additionally, the aromatic  $\pi$ - $\pi$  complexes are found to occur in staggered sandwich forms in which the plane of the donor is parallel to the plane of the acceptor. Ideally, the donor and acceptor molecules are staggered by one-half their widths in order for their orbital overlaps to be maximized. Direct superposition of an aromatic donor over an aromatic acceptor results in negative parts of one wavefunction overlapping positive portions of the other wavefunction, giving a net overlap of zero.<sup>31</sup>

The occurrence of a charge-transfer interaction usually requires some amount of overlap between the molecular orbitals of the donor and acceptor. Normally, the interaction is between the highest occupied molecular orbital (HOMO) of the donor with the lowest unoccupied molecular orbital (LUMO) of the acceptor. This

overlap principle is certainly true for intermolecular complexes. However, for intramolecular complexes, examples are also known of indirect, through-bond interactions, besides the direct, through-space interactions.<sup>37,38</sup>

The amount of orbital overlap between the donor and acceptor plays a critical role in the magnitude of the charge-transfer interaction observed. Constraints resulting from steric hindrances are major factors in this regard. For example, the binding energies for the CTC's between phenol and hydroquinone with para-benzoquinone were found to be larger than those for anisol and hydroquinone dimethyl ether with para-benzoquinone.<sup>39</sup> This was attributed to the steric influence of the methyl groups. For highly substituted molecules, steric hindrance may well prevent the close approach necessary in order for charge-transfer interactions to take place.

Differences in orbital overlap between donors and acceptors, caused by steric constraints, have been studied in intramolecular CTC's. Synthesis of intramolecular CTC's, which vary in their magnitudes of orbital overlap, has been an active area of research. Intramolecular complexes including para- and meta-cyclophane quinhydrones (Staab and coworkers,<sup>40-42</sup> and Tashiro and coworkers,<sup>43,44</sup> respectively), naphthalenophane quinhydrones,<sup>37,45</sup> oligooxa-paracyclophane quinhydrones,<sup>46</sup> cyclophane-ortho-quinones,<sup>47</sup> and substituted biphenyls<sup>48</sup> have been investigated. The results from these investigations clearly show the overlap between the donor and acceptor orbitals has a large influence on both the frequency and intensity of charge-transfer absorptions.

Other forces, which also influence the orientation of the donor and acceptor to each other, will likewise affect the magnitude of the charge-transfer interaction. Included among these other forces are solvation effects on the



individual donors and acceptors and hydrogen bonding between donors and acceptors. Large differences are observed in the magnitude of charge-transfer for quinoxaline-type complexes in solution and in the solid-state.<sup>49,50</sup> These differences are attributed to hydrogen bonding of the complexes in the solid state.

### Electronic Spectra

Electronic absorption or ultraviolet-visible spectroscopy is widely used for the study of CTC's, since charge-transfer interactions involve the transfer of an electron from a ground to an excited state. In fact, the observance of an extraneous absorption band in spectra of iodine dissolved in aromatic hydrocarbons by Benesi and Hildebrand<sup>51</sup> in 1949 led, several years later, to Mulliken's<sup>32</sup> valence bond treatment for complex formation between electron donors and acceptors. This, in turn, has led to the broad developments in the field to the present day.

In general, the spectrum of a CTC retains the individual absorption bands of its donor and acceptor components, possibly in a somewhat modified form. In addition, however, there are one or more absorption bands due to the complex as a whole. In cases where more than one CT band is present, the multiplicity may be caused by electron donation from more than one energy level in the donor, from acceptance at more than one energy level in the acceptor, from differences in interaction energies, or from combinations of all of these.<sup>36</sup> In all cases, these CT absorption bands are unique to the complex and characteristic for it.

Charge-transfer absorptions are usually intense, broad, and featureless. Molar absorptivities may be as high as 50,000 but as low as 500 or less.<sup>31</sup> Charge-transfer bands are frequently asymmetrical, being broader on the high frequency side.<sup>31</sup> For complexes having multiple CT bands, the individual CT

bands may overlap, making the spectrum appear as a single band with an abnormally large half-width.<sup>31</sup> Sometimes the CT band may be hidden or obscured by the absorption bands of the individual donors and acceptors.

The absorption bands of intramolecular CTC's decrease linearly with concentration or, in other words, obey the Beer-Lambert law. For intermolecular complexes, however, the concentration of the complex and, therefore, its absorbance is dependent upon its equilibrium constant.<sup>36,52</sup> Accordingly, compliance with the Beer-Lambert law by a CT band serves as evidence for an intramolecular interaction.

#### Factors Influencing CT Absorption Bands

A number of factors can influence the frequency and/or the intensity of charge-transfer absorption bands. These are discussed below.

Substituents. The CT transition energy ( $E_{CT}$ ) is a function of the ionization potential of the donor and the electron affinity of the acceptor. Both the ionization potential and electron affinity are, in turn, a function of the substituents attached to the respective donor and acceptor. Several quantitative relationships relating the frequency of the CT absorption maximum ( $\nu_{CT}$ ) to the ionization potential of the donor ( $I_D$ ) and the electron affinity of the acceptor ( $E_A$ ) have been proposed. A simple linear equation is given by Eq. (3) below.<sup>53</sup>

$$E_{CT} = h\nu_{CT} = I_D - E_A - W \quad (3)$$

In this equation,  $h$  is Planck's constant and  $W$  is the dissociation energy of the CT excited state.

A more detailed consideration has led to the following parabolic equation, relating the frequency of CT absorption to the ionization potential of the donor:<sup>36,53</sup>

$$h\nu_{CT} = I_D - C_1 + \frac{C_2}{(I_D - C_1)} \quad (4)$$

Equation (4) is used for a series of complexes involving different donors but having a common acceptor species. In this equation,  $C_1$  and  $C_2$  are constants for a given acceptor.

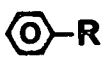
A parabolic relationship has also been used to describe the energy dependence of the CT band to the electron affinity of the acceptor species.<sup>36</sup> This relationship is given in Eq. (5).

$$h\nu_{CT} = -E_A - g_1 + \frac{g_2}{(-E_A + C_1)} \quad (5)$$

Here,  $g_1$  and  $g_2$  are constants for a given acceptor. In many cases, the observed data can just as readily be correlated with a linear relationship.

Substituent groups alter the electronic properties of a molecule. Electron releasing substituents increase the donor properties but decrease the accepting properties of a given molecule; electron withdrawing substituents act in the opposite manner. For example, para-benzoquinone is, itself, a relatively weak electron acceptor, but introduction of halogen substituents greatly enhances its acceptor strength. Table 2 below lists a number of substituent groups and some of their properties, if attached to benzene.<sup>31</sup> In summary, the position of the maximum CT absorbance shifts to higher frequencies (shorter wavelengths) with increasing ionization potential of the donor. Likewise, decreasing electron affinity of the acceptor also results in shifts of the CT maximum to higher frequencies.

Table 2. Some properties of substituted benzene.

Group R	Dipole Moment (Debyes)	Direction of Dipole 	Ionization Potential, eV
OH	1.6		8.5
NH <sub>2</sub>	1.5	←----- +	7.7
OCH <sub>3</sub>	1.2		8.2
CH <sub>3</sub>	0.3		8.8
H	0.0		9.2
Cl	1.6		9.1
CHO	2.8	+ ----->	9.5
SO <sub>3</sub> H	3.8		—
NO <sub>2</sub>	3.9		9.9

The effect of substituent groups on the intensity of CT maxima is not as easily explained as the effect on frequency. One would expect the molar absorptivity of the complex to increase with increasing donor or acceptor character of the individual components of the complex. In fact, just the opposite behavior is observed.<sup>54</sup> This behavior may be caused by what is termed contact charge-transfer (collisional CT interactions as opposed to longer lasting ones). Other causes may include changing mixtures of orientation isomers and deviations from ideality in solution.<sup>54</sup>

Solvent. The ground and excited states of CTC's usually have different dipole moments.<sup>55</sup> Due to this difference in dipole moments, different polarity solvents have an appreciable effect on the position of the CT absorption band. Solvent effects may be summarized in the following manner.<sup>56</sup> As the solvent polarity increases a blue shift of the CT band is observed if the ground state

of the complex is ionic while the excited state is not ionic; a red shift of the CT band is observed when the ground state is not ionic and the excited state is ionic; blue or red shifts are observed when both the ground and excited states are ionic.

For weak CTC's between uncharged component species, the effect of solvent polarity on the position of the CT band is relatively small.<sup>36</sup> However, as expected, slight red shifts of the CT band maxima are observed with increasing dielectric constant or refractive index of the solvent.<sup>31,55</sup> For strong CTC's, solvents with high dielectric constants may actually dissociate the complex into its component ions.<sup>31</sup> In this case, the CT band is replaced by the absorption bands of the individual ions.

Although it is possible to predict changes in CT band frequencies using solvent polarity parameters, in many cases the relationships break down due to specific interactions between the solute and solvent. These specific interactions become more prevalent as solvent polarity increases and as hydrogen bonding occurs.<sup>55</sup> Anomalous solvent shifts can occur for solvents which act as electron donors themselves. For example, aromatic and olefinic hydrocarbons may act as  $\pi$ -donors; alcohols, ethers, amines, carboxamides, nitriles, ketones, sulfoxides, and N and P-oxides may act as n-donors; while alkyl halides may act as  $\sigma$ -donors.<sup>33</sup>

The study of CTC's in both the gas and liquid states has shown the effect of solvent to be a combination of two factors: dielectric effects related to the different dipole moments of the ground and excited states and solvent cage or internal compression effects.<sup>57,58</sup> Solvent internal compression effects are

analogous to those seen for external pressures and may explain some of the anomalous solvent shifts which have been observed.

Solvents may also affect the intensity of the CT band. The general trends observed for shifts in position of the CT band with solvent are also true for intensities of CT bands. As the complex becomes increasingly dissociated from changes in solvent, the intensity of the CT band will decrease. Again, specific interactions between the solute and solvent may cause anomalous results. Molar absorptivity values may be used to make comparisons between CT band intensities, since the band widths are mostly independent of changes in the medium.<sup>55</sup>

Temperature. Charge-transfer interactions are greatly enhanced at low temperatures or in frozen solutions. On the other hand, these interactions are diminished at high temperatures. The CT electronic absorption band also mimics these trends with temperature. Increased molecular movement due to increased temperatures hinders interactions between molecules. As the temperature decreases, thermal motion decreases and results in less inhibition of charge transfer.

Pressure. The sensitivity of CTC's to external pressure is in accord with Mulliken's<sup>32</sup> original theory. According to Mulliken's theory, the stability of CTC's and the energy of the CT absorption are sensitive to changes in the orbital overlap of the molecular orbitals of the donor and acceptor. Any perturbation of this overlap, for example, by hydrostatic pressure will produce changes in the magnitude of charge transfer. Mulliken predicted that weak  $\pi$ - $\pi$  complexes, where the initial orbital overlap is relatively small, would be particularly sensitive to pressure. For a small enough initial overlap between the two molecules, the overlap must increase exponentially as the molecules are squeezed together.

Subsequent experiments, in which CTC's have been subjected to high external pressures, have proven Mulliken's original predictions correct. These results can be found in the work of Ham,<sup>59</sup> Stephens and Drickamer,<sup>60</sup> Gott and Maisch,<sup>61</sup> Offen and coworkers (in a series of papers),<sup>62-66</sup> and Ewald.<sup>67</sup>

Offen<sup>68</sup> has summarized the general trends observed for pressure effects on weak CTC's. In short, CT absorption maxima shift to longer wavelengths, while the intensities of CT bands increase with increasing pressure. At increased pressures, bulk solvent properties, such as density, refractive index, and dielectric constant increase, thus making the solvent appear more polar. This increased polarity of the solvent accounts for the long wavelength shift of CT band maxima. Increases in CT band intensities are a result of the increased orbital overlap between donors and acceptors in the compressed solvents.

Solution studies of complexes under pressure have ordinarily been recorded in the range between one and six thousand atmospheres. Significant differences in spectra of CTC's are observed in this pressure regime, whereas pressures up to 50,000 atmospheres are required to bring about significant compression of normal chemical bonds.<sup>69</sup>

#### Association Constants

The strength or stability of a CTC is given by its association constant,  $K$ . The association constant may be obtained by Eq. (6),

$$K = \frac{[(D:A)]}{[D_0 - (D:A)][A_0 - (D:A)]} \quad (6)$$

where  $D_0$  and  $A_0$  are the initial concentrations of donor and acceptor before interaction, and  $(D:A)$  is the concentration of the complex. The association

constant may be determined from ultraviolet-visible spectra. In order to do this, the molar absorptivity of the complex is needed and may be obtained from Eq. (7),

$$\epsilon_{CT} = \frac{\log (I_0/I)}{l[(D:A)]} \quad (7)$$

where  $\epsilon_{CT}$  is the molar absorptivity of the CT band,  $l$  is the cell path length, and  $\log (I_0/I)$  is the absorbance. This equation is correct only when A and D do not absorb in the region of the CT transition.

Equations (6) and (7) may be combined to give the Benesi-Hildebrand equation, [Eq. (8)].

$$\frac{[A]l}{\log (I_0/I)} = \left( \frac{1}{K\epsilon_{CT}} \right) \left( \frac{1}{[D]} \right) + \left( \frac{1}{\epsilon_{CT}} \right) \quad (8)$$

Experimentally, the donor concentration is varied while keeping the acceptor concentration constant. The values of  $[A]l/[\log (I_0/I)]$  are then plotted against the values of  $1/[D]$ . The slope of the resulting line has a value of  $1/K\epsilon_{CT}$  and an intercept of  $1/\epsilon_{CT}$ .

A number of variations to the Benesi-Hildebrand equation and corrections to it are in the literature.<sup>31,36</sup> Many of these correct for solvent interactions.

#### Thermodynamic Parameters

The interactions of donors and acceptors in solution are normally accompanied by only small changes in enthalpies and entropies. For weak,  $\pi-\pi$  complexes, the enthalpy of dissociation,  $\Delta H^\circ$ , is usually between 0 and 5 kcal/mole.<sup>33</sup>



The thermodynamic constants are commonly obtained by investigating the effects temperature changes have on the spectrometrically determined equilibrium constants.<sup>31,53</sup> The enthalpy of dissociation can then be determined from Eq. (9).

$$\frac{\ln K_{T_2}}{\ln K_{T_1}} = \frac{-\Delta H^\circ}{R} \left( \frac{1}{T_2} - \frac{1}{T_1} \right) \quad (9)$$

The standard free energy,  $\Delta G^\circ$ , and entropy,  $\Delta S^\circ$ , may be obtained from Eq. (10) and (11), respectively.

$$\Delta G^\circ = -RT \ln K \quad (10)$$

$$\Delta G^\circ = \Delta H^\circ - \Delta TS^\circ \quad (11)$$

In general,  $\Delta H^\circ$  and  $\Delta S^\circ$  become more negative as the equilibrium constant for complex formation increases.<sup>53</sup> In this regard, the individual donor and acceptor molecules are less free to move about as the bond between them becomes stronger.

#### Selected Examples of CTC's

Kraft lignin is primarily aromatic in character. The aromatic rings of lignin are predominantly substituted with electron releasing groups (OH, OCH<sub>3</sub>) and, therefore, should make good electron donors. Kraft lignin also contains other functional groups which are known electron acceptors, most notably quinones. CTC's between phenols and quinones, especially of the quinhydrone type, are well known in the literature. Some examples of these complexes are given in Table 3, below. Also included in the table is an interesting complex between cinnamic acid derivatives. The complexes listed at the end of the table are intramolecular ones.

Table 3. CTC Examples.

Complex	$\lambda_{\text{max}}$ , nm	$\epsilon_{\text{max}}$	Solvent	Citation
Quinhydrone	440 $\pm$ 2 558	890	Several solid	(70,71) (60)
1,4-Benzoquinone with phenol	315	1200	C <sub>6</sub> H <sub>12</sub>	(70)
1,4-Benzoquinone with 1,4-dimethoxybenzene	413	370	C <sub>6</sub> H <sub>12</sub>	(70)
Methoxy-1,4-benzoquinone with hexamethylbenzene	397		CCl <sub>4</sub>	(36)
Methoxy-1,4-benzoquinone with hydroquinone	526		Solid	(50)
3,4-Dimethoxycinnamic acid with 2,4-dinitrocinnamic acid	460		Solid	(72)
<u>ortho</u> -Anisyl-1,4-benzoquinone	400	1200	EtOH	(73)
<u>para</u> -Anisyl-1,4-benzoquinone	430	4000	EtOH	(73)
[2.2] <u>Para</u> -cyclophane-4,5-quinone	480	870	CHCl <sub>3</sub>	(47)
[3.3] <u>Para</u> -cyclophane-5,6-quinone	520	930	CHCl <sub>3</sub>	(47)
<u>pseudo-geminal</u> [2.2] <u>Para</u> cyclophane quinhydrone	495	1600	MeOH	(40)
<u>pseudo-ortho</u> [2.2] <u>Paracyclophane</u> quinhydrone	515 375	170 790	MeOH	(40)

#### Indication for CTC's in Kraft Lignin

Besides the fact that kraft lignin contains structural moieties which are known to form CTC's in other environments, additional circumstantial evidence comes from a lack of detectable chromophores which could be responsible for kraft lignin's color. Kratzl and coworkers<sup>22</sup> investigated the reductive acetylation of kraft lignin, which reduces quinones and removes them as chromophores. Neither proton NMR, nor carbon-hydrogen elemental data revealed any difference

between the reductively acetylated lignin and a normally acetylated lignin, within the experimental error. These results were obtained even though the reductively acetylated lignin was lighter in color and had a substantially less intense visible absorption spectrum than the normally acetylated lignin.

The presence of CTC's in kraft lignin may help explain these observations, since CTC's could have a "reinforcing" effect on the quinone chromophores. Quinones in kraft lignin may be playing a dual role; they are colored substances by themselves, but additional color may be created by their participation as acceptor moieties in CTC's. This may explain why such a large color reduction could only be attributed to so few chromophores.

Apart from speculation, there has been one report published which indicated the possible presence of CTC structures in kraft lignin. Electron paramagnetic resonance data were used by Steelink<sup>29</sup> to postulate the existence of a semiquinone radical structure in kraft lignin, coexistent with a diamagnetic quinhydrone moiety. Quinhydrones, as just illustrated, are known CTC's. A portion of Steelink's data are given in Table 4 below.

Table 4. Free Radical Content of Lignin Derivatives<sup>29</sup> [(spins/g) x 10<sup>17</sup>].

	Untreated	Na salt	Acidified Salt	NaBH <sub>4</sub> Reduced	Na Salt of NaBH <sub>4</sub> Reduced
Kraft yellow pine	3.0	100-300	3.0	1.3	22

The untreated, yellow pine kraft lignin was found to have a spin content of  $3.0 \times 10^{17}$  spins/g, which increased one-hundred fold upon basification. This increased radical content was reversible, and upon acidification the initial spin content was again obtained. This type of behavior, wherein a large and

reversible change in spin content is caused by pH alone, is also characteristic of quinhydrone-type systems and therefore led to Steelink's proposal. Figure 7 shows the type of quinhydrone system envisioned by Steelink.

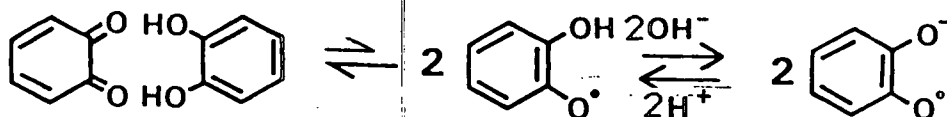


Figure 7. Possible quinhydrone-type system in kraft lignin.<sup>29</sup>

As further evidence for this type of structure, quinone structures in the lignin were removed by sodium borohydride reduction. In this case, basification of the reduced lignin did not produce the same large increase in the free radical content.

#### THESIS OBJECTIVES

The thesis objectives were, first, to determine if charge-transfer complexes are present in kraft lignin and, second, if CTC's are present, to determine their contribution to the color of kraft lignin. In accomplishing the second goal an evaluation will be made of other chromophore types in kraft lignin. Included in this evaluation will be transition metal complexes, extended conjugated systems, and quinones.

By satisfying these objectives, we hope to provide a more fundamental understanding of the chromophores responsible for color in kraft lignin. This understanding may lead to new insights into the problems of pulp bleaching and lignin utilization touched on in the perspective section earlier.

## EXPERIMENTAL APPROACH

In broad form, the approach taken to achieve the thesis objectives is given below. The experimental approach can be divided into two parts, paralleling the thesis objectives. Since these objectives involved investigating the color of kraft lignin, the majority of the work was done using an isolated kraft lignin. Work with model compounds was performed where appropriate or useful.

An isolated kraft lignin was chosen for investigation instead of a residual kraft lignin for a number of reasons. First, the isolation procedure was much less complicated than one needed to obtain a residual kraft lignin. Secondly, practically all previous investigations with respect to color have employed isolated kraft lignins, and therefore the results obtained in this study could be compared to these previous results. Finally, recent studies of residual kraft lignin have shown that in essence residual kraft lignin is very similar to isolated kraft lignin.<sup>3-7</sup> The major points of difference between the two are that residual kraft lignin has a higher molecular weight, probably has covalent linkages to carbohydrates, and has been degraded to a lesser extent than isolated kraft lignin. With regard to the last point, the same functional groups have been found in both residual and isolated kraft lignins. However, the content of these groups is less in the residual lignin. It would, therefore, appear that residual and isolated kraft lignins should contain the same types of chromophore structures. However, the isolated kraft lignin probably contains more of these structures.

### Determination of CTC's in Kraft Lignin

The first step in this determination involved identifying the most likely type of CTC in kraft lignin. In other words, which functional groups in kraft

lignin are acting as electron donors and which groups are acting as electron acceptors? From the evidence available, the most likely type of CTC in kraft lignin probably involves an interaction between a phenol and a quinone. Using this as a working hypothesis, the following approach was planned to identify these possible CTC's.

The electronic absorption spectrum of kraft lignin is very complex, indicating a number of different chromophores probably present in relatively small quantities. If CTC's are indeed present in kraft lignin, their content will probably be small and their effect difficult to determine. Therefore, a material rich in these proposed CTC's will be extremely helpful. Having such a modified kraft lignin available should lead to easier identification of the CTC, and the modified lignin will serve as a useful comparison to the original kraft lignin. Knowledge gained from CTC's in the modified kraft lignin will then be used in helping to identify possible CTC's in the original kraft lignin.

The first objective in obtaining this modified kraft lignin will be to eliminate as many of the other known chromophores as possible. This will simplify the resulting lignin spectrum, and hopefully lead to eventual isolation of the introduced CTC. Elimination of these other chromophores will include reduction of carbonyl groups, hydrogenation of double bonds, and removal of metal ions from the lignin. Information gained from these procedures can later be used to evaluate the contributions of different chromophore types to the overall color of kraft lignin.

Next, the lignin will be modified in order to enhance the formation of CTC's. Kraft lignin contains a relative abundance of free phenolic groups (approximately 60 per 100 C<sub>9</sub> units<sup>74</sup>), but a relative scarcity of quinone groups

(estimated at about 4 per 100 C<sub>9</sub> units<sup>26</sup>). Therefore, in order to increase the amount of CT complexation in the lignin, additional quinone groups will be introduced into the kraft lignin matrix. During modifications of the original lignin, a concern will be to keep side reactions to a minimum in order for a useful comparison between the original and the modified lignin to be obtained.

Measurements for CTC's in the modified and original kraft lignins will be conducted using electronic absorption spectroscopy. This will be done in association with environmental factors which influence the amount of charge-transfer complexation taking place. These environmental factors will include solvent, pressure, and substituent effects. Comparisons will then be made between the modified and the original lignins.

#### Evaluation of the Contribution to Color of Various Chromophores

The evaluation of the contribution of various chromophores to color will simply involve the methodical removal of these chromophores from kraft lignin and the determination of their individual effects on the kraft lignin spectrum. Difference spectroscopy should be possible to use to great advantage in this regard. Extended conjugated systems in lignin will be studied by sodium borohydride reduction and diimide hydrogenation of carbonyls and carbon-carbon double bonds, respectively. Transition metal complexes will be investigated by EDTA chelation and removal of these metals. The contribution of quinones and the separation of their individual contribution from that caused by their participation in charge-transfer complexes will be determined by carbon-14 labeling of the quinones.

## MATERIALS AND METHODS

### LIGNIN STARTING MATERIAL

#### Isolation

Kraft lignin was isolated from the black liquor resulting from a kraft cook of loblolly pine chips. Cooking conditions were as follows: effective alkali, 16%; sulfidity, 27.5%; time to final temperature, 90 minutes; time at final temperature (173°C), 90 minutes. The kappa number of the pulp was determined by TAPPI Standard Method T 236 to be 39.4.

The black liquor from the cook was retained and had the properties listed in Table 5. The density of the black liquor was determined gravimetrically. The ash content was determined as sulfated ash, according to TAPPI Standard Method T 625. The solids content was determined by the method given by McDonald.<sup>75</sup> The lignin content of the liquor was determined gravimetrically, after electro-dialysis (see below) of the water-washed precipitated lignin.

Table 5. Black liquor analyses.

Density	1.12 g/mL
Ash content	36.40% <sup>a</sup>
Solids content	20.50%
Lignin content	5.75%

---

<sup>a</sup>Of the solids, as NaOH.

The kraft lignin was isolated from the black liquor by acid precipitation as shown in Fig. 8. In this isolation procedure, a quantity of liquor was acidified by dropwise addition of 6N H<sub>2</sub>SO<sub>4</sub>, with stirring, until the pH of the liquor had dropped to 2-3. The acidified liquor was then degassed by spinning on a rotary



## Isolation of Kraft Lignin

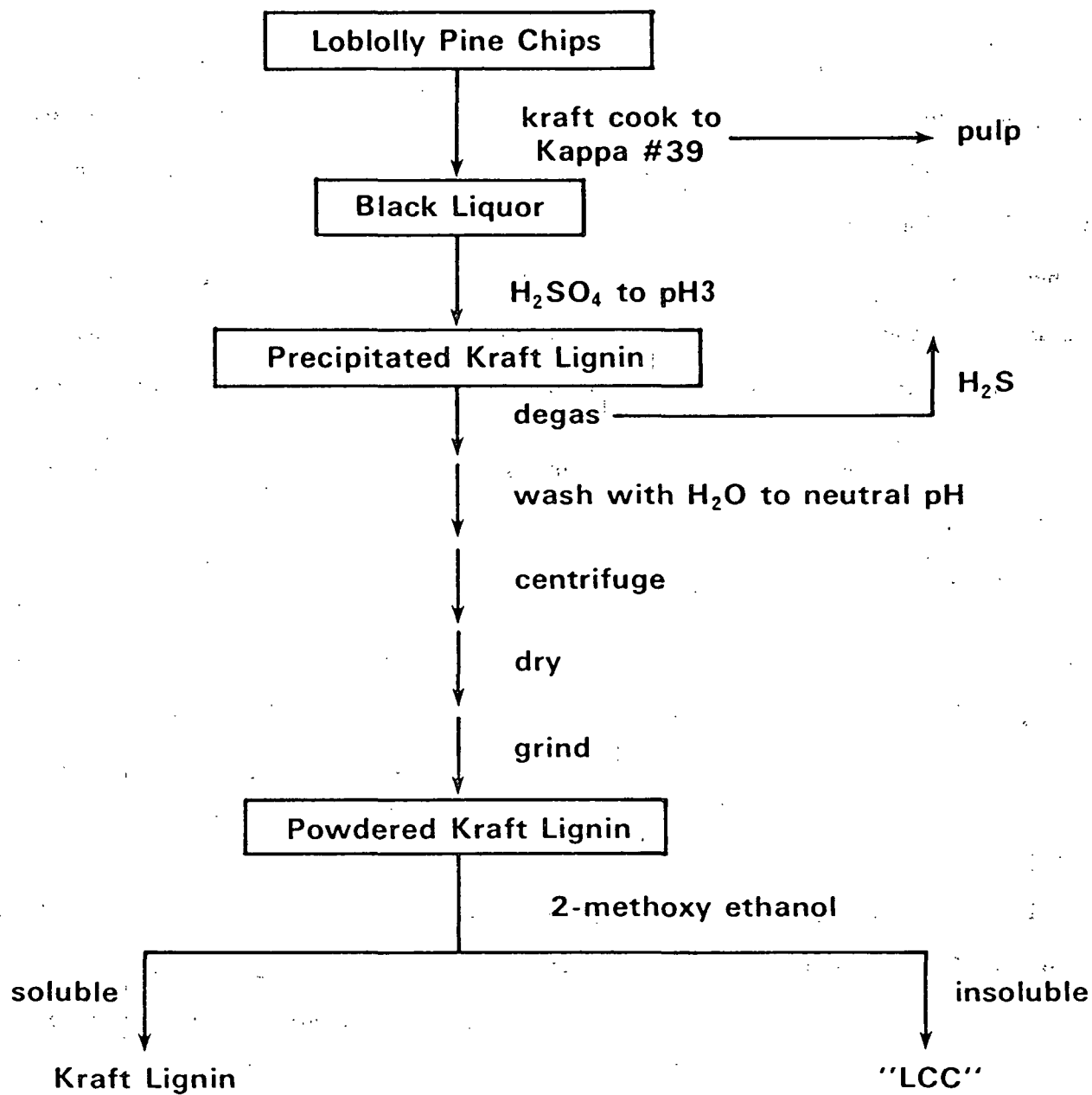


Figure 8. Isolation of kraft lignin.

evaporator at room temperature and under vacuum for two hours. The removed  $\text{H}_2\text{S}$  gas was bubbled through a gas washing bottle filled with an alkaline solution of  $\text{Zn}(\text{OH})_2$  (zincate solution).

The lignin precipitate in this degassed suspension was concentrated by centrifugation. The supernatant was discarded and the lignin was repeatedly washed with distilled water until the wash water attained a pH of approximately 6. After decanting away the wash water, the lignin was transferred to evaporating dishes which were placed inside vacuum desiccators. Initial drying of the lignin was accomplished in the desiccators over KOH and silica gel. Final drying was completed in an oven at 35-40°C.

The dried product was ground to a uniform powder using a Pyrex mortar and pestle. The powdered kraft lignin was stored in amber glass bottles at room temperature. For long term storage, a nitrogen atmosphere was placed over the lignin.

In some experiments an industrially obtained kraft lignin was used. This lignin was an Indulin AT, obtained from Westvaco, North Charleston, South Carolina.

#### Carbohydrate Removal

The kraft lignin, isolated by acid precipitation, contained a significant quantity of carbohydrate material. These carbohydrates accounted for 6.7% of the total material isolated. The majority of the carbohydrates present were fragments of xylans, as shown in Table 6. A major portion of these carbohydrates was removed based on their insolubility in 2-methoxyethanol.

Experimentally, the powdered lignin material was dissolved in an excess of 2-methoxyethanol (Mallinckrodt AR). The insoluble material was then removed by

successive filtration. The filtration was performed through 40-60  $\mu$ , followed by 10-15  $\mu$  glass fritted funnels. The 2-methoxyethanol fraction, or soluble portion, was retained and transferred to a round bottom flask. The 2-methoxyethanol was then removed on a rotary evaporator at 45-50°C. The lignin material, which remained in the flask, was dried over  $P_2O_5$  in a vacuum desiccator. The thoroughly dried lignin was loosened and removed from the flask with distilled water, collected by suction filtration, and redried over KOH and  $P_2O_5$ . The dried lignin was then ground to a uniform powder.

The 2-methoxyethanol-treated lignin had a total carbohydrate content of 1.3%. Values for the individual carbohydrates in the treated lignin are given in Table 6.

Table 6. Carbohydrate analyses of kraft lignins.

Carbohydrate	Before Removal		After Removal	
	% of Total Sample	% of Total Carbohydrate	% of Total Sample	% of Total Carbohydrates
Arabinose	0.5	7.5	0.2	15.4
Xylose	4.0	59.7	0.6	46.2
Mannose	0.2	3.0	0.1	7.7
Galactose	0.7	10.5	0.2	15.4
Glucose	1.3	19.4	0.2	15.4

The material which was insoluble in 2-methoxyethanol had the following make-up: 47.2% ash, 32.6% carbohydrates, and 16.3% Klason lignin. The carbohydrates which were present had the composition given in Table 7. The concentrations of the individual carbohydrates as a percentage of the total carbohydrate content are clearly similar in the lignin before carbohydrate removal and in the 2-methoxyethanol insoluble material.

Table 7. Carbohydrate analysis of 2-methoxyethanol insoluble material.

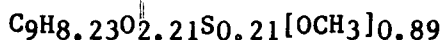
Carbohydrate	% of Total Sample	% of Total Carbohydrate
Arabinose	2.3	7.1
Xylose	21.4	65.7
Mannose	1.2	3.7
Galactose	3.3	10.1
Glucose	4.4	13.4

Carbohydrate analyses of kraft lignin and lignin-carbohydrate material were performed using the method of Borchardt and Piper.<sup>76</sup> Acid insoluble, or Klason lignin determinations were made after the primary and secondary hydrolysis in this procedure. Some experimental difficulties were encountered in accurately determining the carbohydrate content of lignin materials by the alditol acetate method. These difficulties have been accounted for in Table 6. Details of the problems encountered are given in Appendix I.

#### LIGNIN ANALYSES

##### Elemental, Methoxyl, and Ash Analyses

The ash content, elemental composition, and methoxyl content of various lignins were determined at the Microanalytical Laboratory of the University of Vienna, Waehringerstrasse 38, A-1090 Vienna, Austria. These values for the isolated kraft lignin are given in Table 8. They were obtained after removal of the excess carbohydrate material from the lignin. From these values, the average composition for a C<sub>9</sub> unit in the lignin was calculated to be



Accordingly, the unit molecular weight for the isolated kraft lignin was calculated to be 186 g/mole.

Table 8. Kraft lignin analyses.<sup>a</sup>

% Carbon	63.46
% Hydrogen	5.87
% Oxygen	26.49 <sup>b</sup>
% Sulfur	3.53
% Methoxyl	14.74
% Ash	0.66

<sup>a</sup>Average of two separate samples.

<sup>b</sup>By difference.

#### Phenolic Hydroxyl Content

The phenolic hydroxyl content of the lignin was determined by the aminolysis of an acetylated sample of the lignin, following the procedure given by Månsson.<sup>74</sup> In general, 20-25 mg of acetylated kraft lignin was dissolved in 0.5 mL of dioxane (Aldrich, Gold Label 99+%). The aminolysis was started by the addition of 0.5 mL of pyrrolidine (Aldrich) which contained a known amount of propionylpyrrolidine (0.1 mmol) as an internal standard.

Five minutes after the pyrrolidine addition, regular (approximately every 13 min) 2  $\mu$ L injections of the reaction mixture were made directly into a Hewlett Packard 5890 gas chromatograph. GC conditions were as follows:

Column: 6 ft x 2 mm ID, OV-17 on 80/100 mesh Supelcoport

Column Temperature: 100°C, isothermal

Injector Temperature: 220°C

Detector Temperature: 250°C

Carrier Gas Flow Rate: 20 cc/min He

Calibrating against the internal standard, the amount of acetylpiperrolidine produced by the aminolysis was determined versus the time of reaction. Extrapolation of this kinetic curve back to zero time gave a phenolic hydroxyl content of 57.9/100 Cg units in the lignin.

### Catechol Content

The method used by Falkehag, et al.<sup>9</sup> was employed as a basis for this procedure. In determining the catechol content, 5 mL of a 0.1M solution of lignin dissolved in DMSO was pipetted into a 100 mL volumetric flask. Also pipetted into the flask were 20 mL of 0.1M Na<sub>2</sub>HPO<sub>4</sub> buffer solution,<sup>77</sup> 5 mL of 0.005M Na<sub>2</sub>SO<sub>3</sub>, and 5 mL of a solution containing 0.005M FeSO<sub>4</sub> and 0.0125M sodium potassium tartrate. The flask was then filled to volume with distilled water. A reference solution was prepared in the same manner as the sample solution, except it contained no ferrous sulfate. All sample solutions had a pH between 8.1 and 8.5. The catechol content of the lignin sample was estimated at 4.6/100 Cg units from the maximum in the visible absorption curve found for the sample vs. the reference solutions.

### Instrumental Methods

#### Electronic Absorption Spectroscopy

Electronic absorption spectra of various lignins were recorded on a Perkin-Elmer 320 Spectrophotometer. The spectrophotometer had a wavelength accuracy of  $\pm 0.2$  nm and a wavelength reproducibility of  $\pm 0.1$  nm. The photometric accuracy of the instrument was  $\pm 0.002$  AU at 0.5 AU. The spectrophotometer was interfaced with an Apple III computer for data storage and manipulation. Lignin concentrations in the visible region of the spectrum were usually on the order of 7.5 mg/25 mL of solvent. For ultraviolet (UV) spectra, the concentrations of the visible solutions were diluted by a factor of twenty. In most cases, the

solvents used were spectroscopic grade DMF (Baker) and 2-methoxyethanol (Burdick and Jackson). For periodate oxidized lignins, solutions were kept in the dark, and spectra were recorded within an hour after dissolution of the sample. An UV-visible absorption spectrum of the isolated kraft lignin is shown in Fig. 9.

Ionized lignin spectra were obtained by direct scanning of an alkaline solution of the lignin placed in the sample cell vs. a neutral solution of the lignin placed in the reference cell. Alternately, the individual ionized and neutral lignin spectra were stored in the computer and then subtracted.

#### Infrared Spectroscopy

Infrared spectra of lignin samples were recorded using a Nicolet 7199C Fourier Transform Infrared Spectrometer. Lignin samples were formed into KBr pellets and recorded in the transmission mode of operation. A spectrum of the isolated kraft lignin is given in Fig. 10.

#### Nuclear Magnetic Resonance (NMR) Spectroscopy

$^1\text{H}$  and  $^{13}\text{C}$  NMR spectra of various lignin samples were recorded on a JEOL FX100 Fourier Transform NMR Spectrometer. TMS was used as a reference in all samples. Experimental addition of paramagnetic metal ions to a kraft lignin model compound [1-(4-hydroxy-3-methoxyphenyl)-ethanol] had a negligible effect on its spectrum. Therefore, paramagnetic metals which are found in kraft lignin were also expected to have a negligible effect on the lignin spectrum.

Proton Spectra. For  $^1\text{H}$  NMR spectra, approximately 30 mg of acetylated or reductively acetylated lignin was dissolved in 0.5 mL of  $\text{CDCl}_3$ . Spectra were taken at room temperature using  $45^\circ$  pulses, five seconds apart. Integration of proton types was performed over the following ranges ( $\delta$ ): aromatic, 8.00-6.25; methoxyl, 3.95-3.55; aromatic acetoxyl, 2.50-2.15; aliphatic acetoxyl, 2.15-1.75.

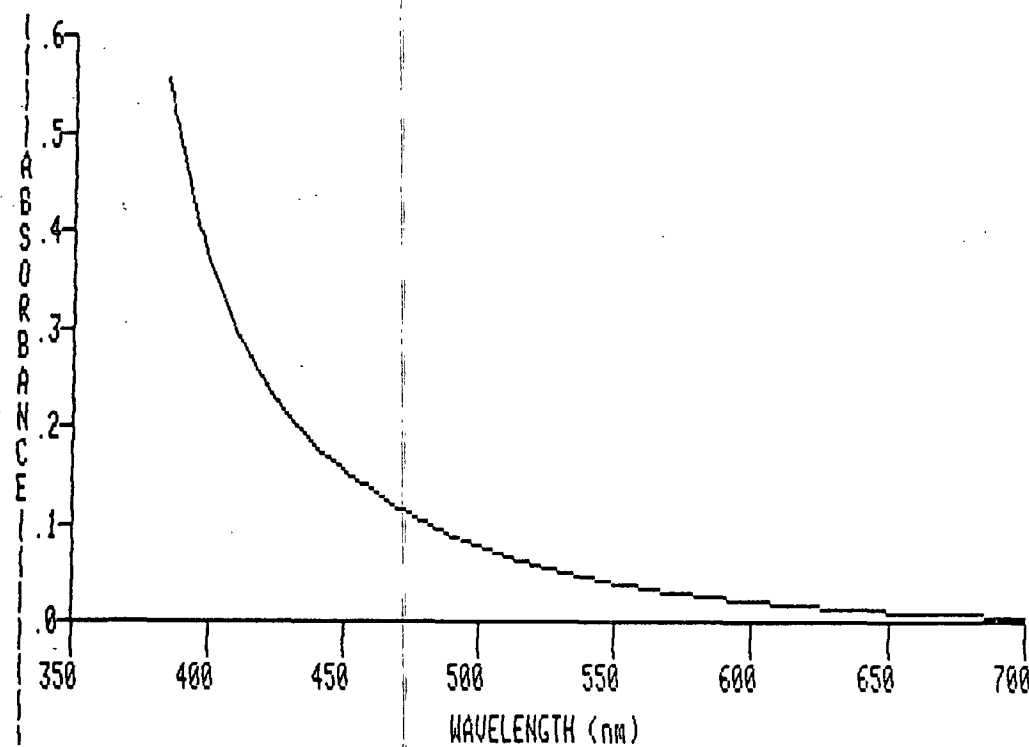
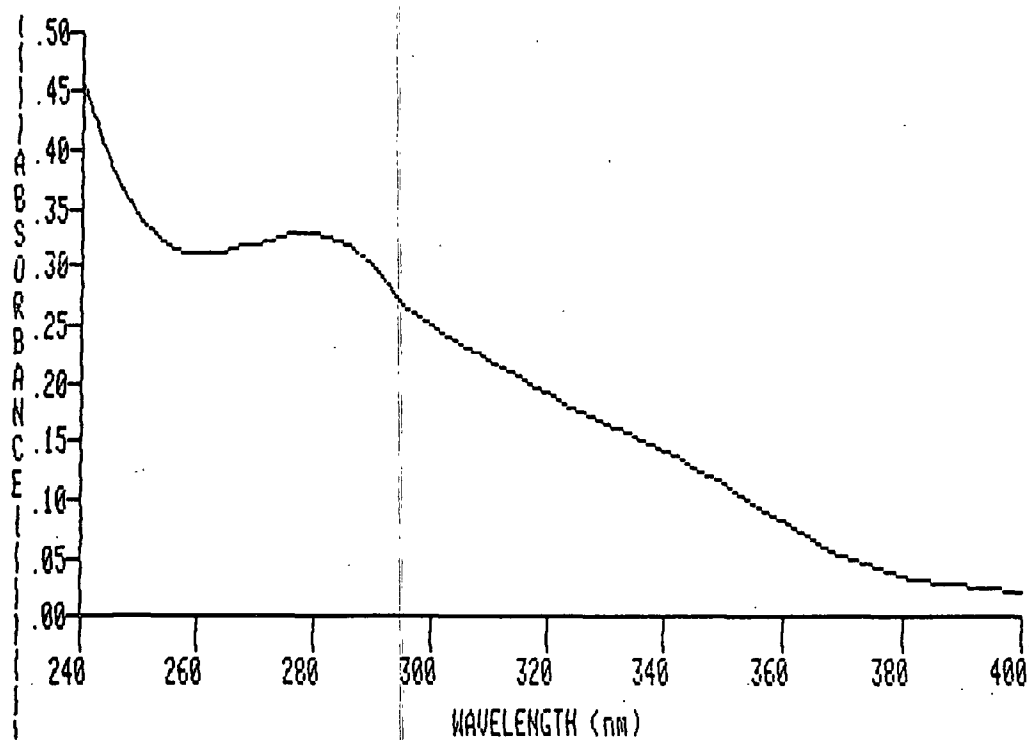


Figure 9. UV-visible absorption spectrum of isolated kraft lignin; solvent, 2-methoxyethanol; visible concentration, 25.6 mg/100 mL; UV concentration, 1/20th of visible.



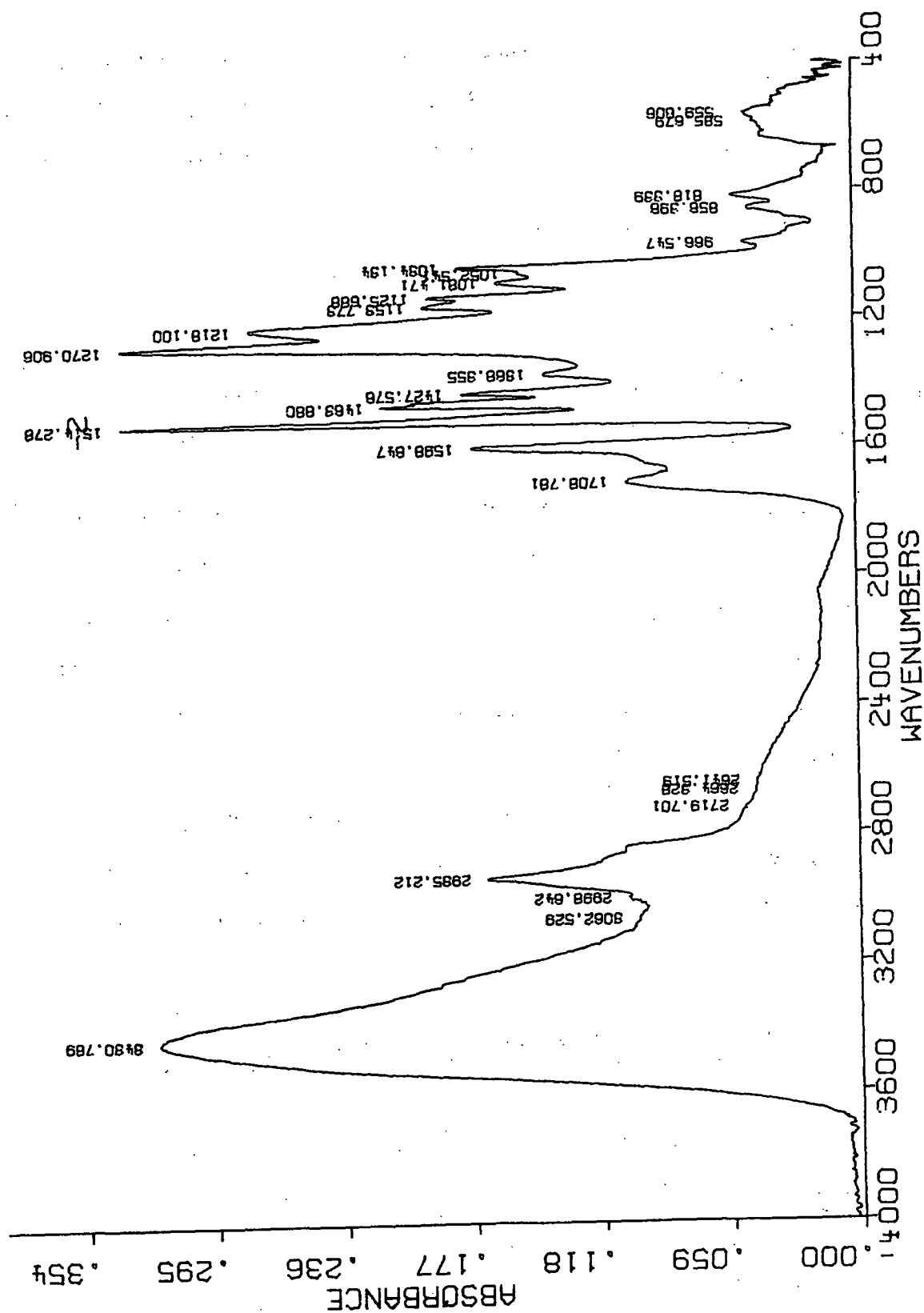


Figure 10. FTIR spectrum of isolated kraft lignin.

A  $^1\text{H}$  NMR spectrum of the isolated and then acetylated lignin is given in Fig.

11. The relative quantities of the different proton types shown in Table 9 were calculated from the areas under the peaks found in Fig. 11 and the methoxyl content of the acetylated lignin. In Table 9, the aromatic acetoxyl and the aliphatic acetoxyl types represent phenolic and aliphatic hydroxyl groups, respectively.

Table 9. Proton analysis.

Proton Type	Moles/1000 g lignin
Methoxyl	3.38
Aromatic acetoxyl	2.74
Aliphatic acetoxyl	3.56

Carbon-13 Spectra.  $^{13}\text{C}$  spectra of nonderivatized kraft lignin were obtained in  $\text{DMSO-d}_6$  solution (300 mg/mL), using a 10 mm tube. For the spectrum shown in Fig. 12, 259,584 scans were accumulated, using  $80^\circ$  pulses, one second apart. The temperature of the sample was maintained at  $100^\circ\text{C}$  in order to lower the viscosity of the solution. Spectra of acetylated or reductively acetylated kraft lignins were obtained in  $\text{CDCl}_3$  solution (200-300 mg/0.5-0.6 mL), using a 5 mm tube. For a spectrum of non- $^{13}\text{C}$  enriched lignin, 234,024 scans were accumulated using  $70^\circ$  pulses, one second apart. The temperature of the sample was  $52^\circ\text{C}$ . For  $^{13}\text{C}$  enriched samples, 60,000 to 65,000 scans were collected.

#### Metal Analysis

The contents of the transition metals, Cr, Mn, Fe, Co, Ni, and Cu, in kraft lignins were determined at VHG Labs, Inc., 140 Hampstead St., Methuen, MA 01844, using inductively coupled plasma emission spectroscopy. The levels of these transition metals in the isolated lignin are given in Table 19 of the "Results and Discussion" section.

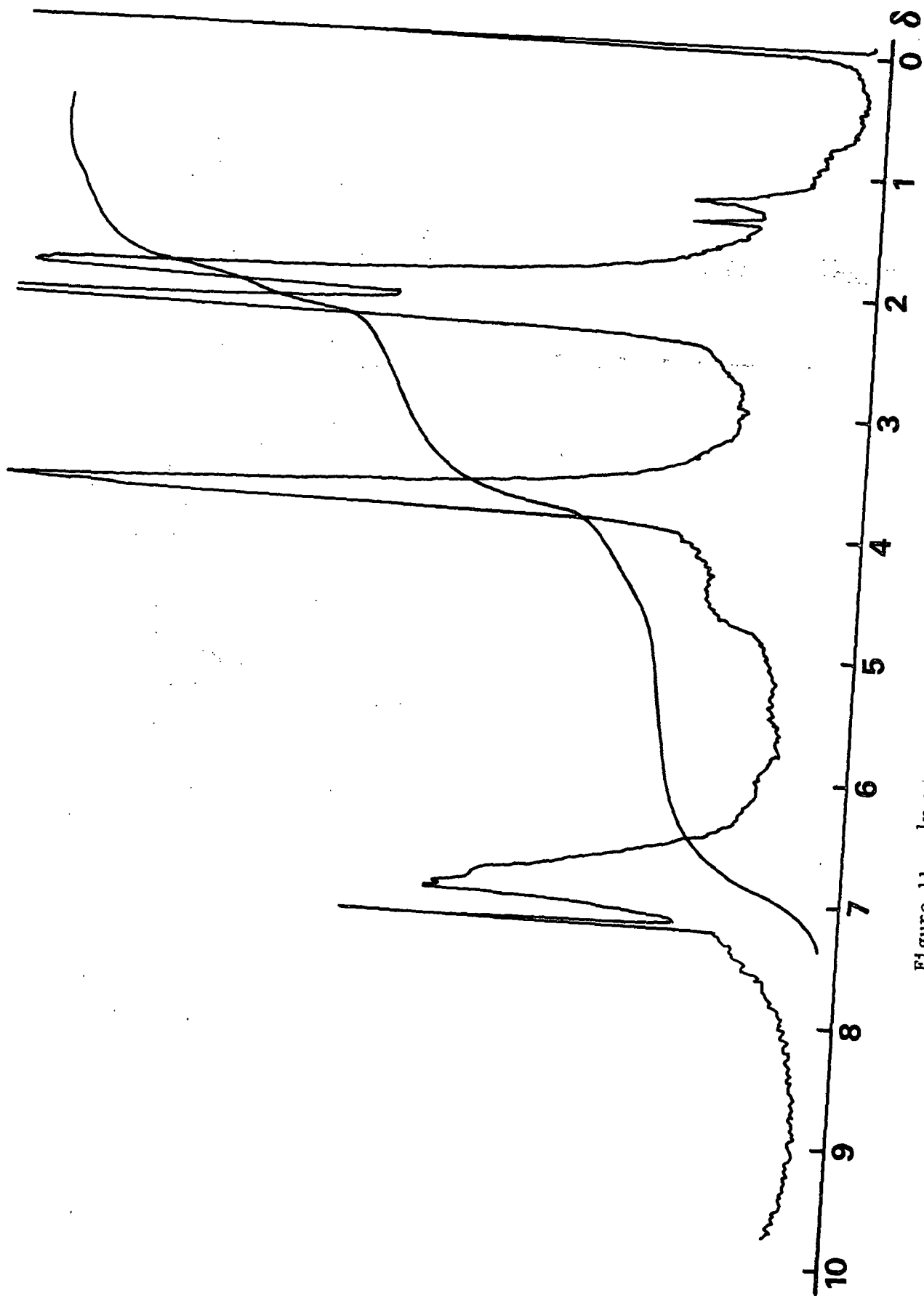


Figure 11.  $^1\text{H}$  NMR spectrum of acetylated kraft lignin.

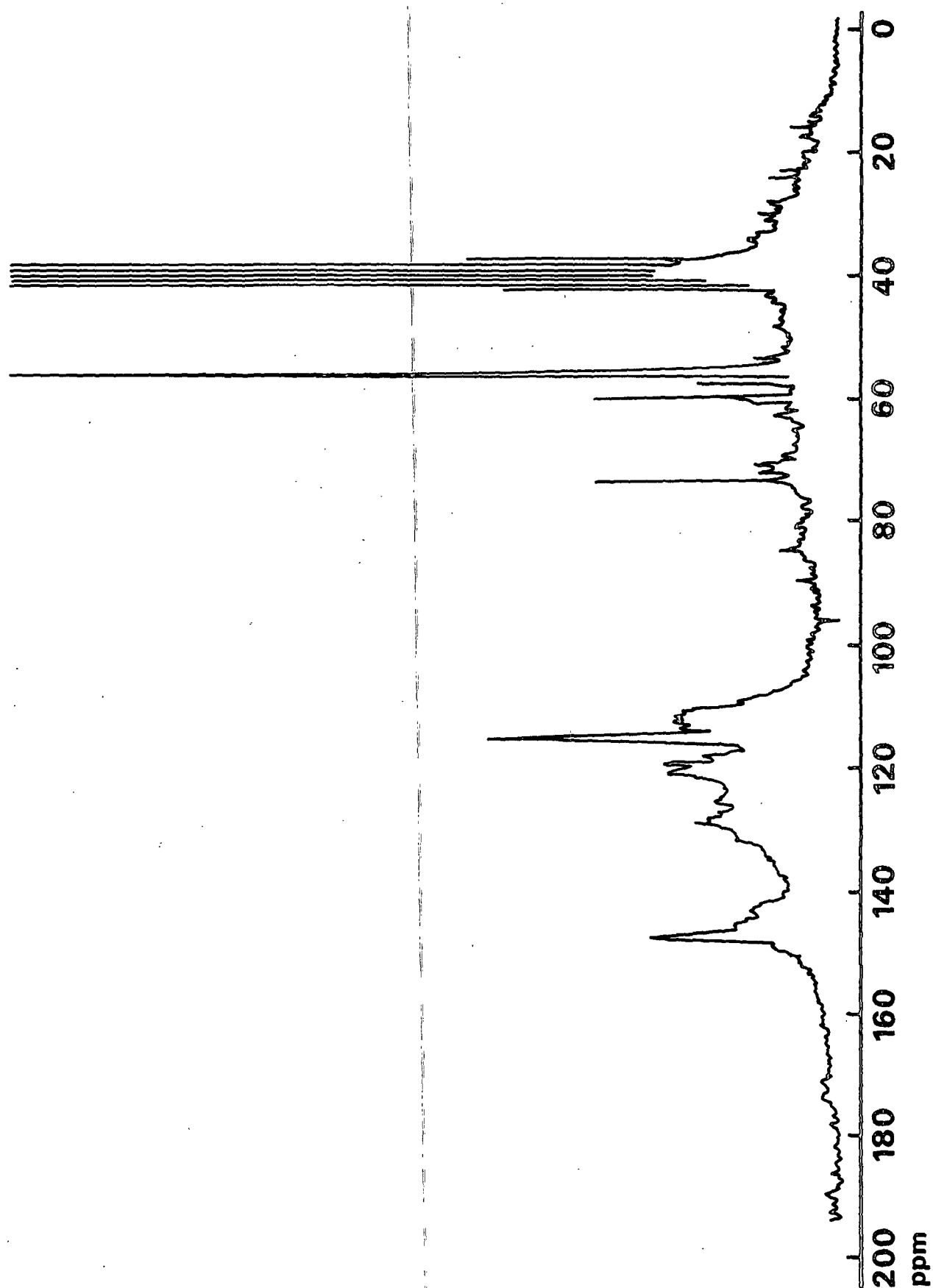


Figure 12.  $^{13}\text{C}$  NMR spectrum of isolated kraft lignin.

## COMPOUNDS AND SYNTHESIS

2-Methoxy-4-methyl phenol and 3,5-di-tert-butyl-1,2-benzoquinone were purchased from Eastman Kodak Company and Aldrich Chemical Company, respectively. 4-Methylcatechol and 2-methoxyhydroquinone were purchased from Pfaltz and Bauer, Inc. 1-(4-Hydroxy-3-methoxyphenyl)-ethanol was obtained from D. R. Dimmel. Catechol and hydroquinone were provided by W. F. W. Lonsky. The following compounds were synthesized:

### Acetylated Models

The procedure for the isolation of the acetylated models varied according to whether the acetylated product was a liquid or solid. The compounds 1,4-diacetoxybenzene, 1,2-diacetoxybenzene, 1,2-diacetoxy-4-methylbenzene, and 1,4-diacetoxy-2-methoxybenzene were isolated as solids according to the following general procedure.

Approximately 11 mmol of the appropriate model phenol was dissolved in 10-15 mL of dry pyridine. Acetic anhydride, in a quantity one-half the amount of pyridine present, was then added to the reaction flask. Approximately 0.25 g of zinc dust was added to the solutions when the starting phenol was a hydroquinone. The solution was stirred overnight at room temperature. The following morning, the reaction mixture was hydrolyzed over crushed ice. During this time, the ice mixture was stirred occasionally until the ice melted. The acetate which precipitated was collected by suction filtration. The precipitate was washed with cold distilled water, followed by cold 0.01N HCl, and cold distilled water again. It was then dried over P<sub>2</sub>O<sub>5</sub> in a vacuum desiccator.

1,4-diacetoxybenzene: Yield, 92% m.p. 120-121°C, literature 123-124°C.<sup>78</sup>

<sup>1</sup>H NMR (CDCl<sub>3</sub>) δ 2.27(s, 6, Ar-OCO-CH<sub>3</sub>); 7.04(s, 4, Ar-H). <sup>13</sup>C NMR (CDCl<sub>3</sub>) 21.0 ppm (Ar-OCO-CH<sub>3</sub>); 122.1 ppm (C-2); 147.7 ppm (C-1); 168.8 ppm (C=O).

1,2-diacetoxybenzene: m.p. 62°C; literature value, 64-65°C.<sup>79</sup> <sup>1</sup>H NMR

(CDCl<sub>3</sub>) δ 2.26(s, 6, Ar-OCO-CH<sub>3</sub>); 7.16(m, 4, Ar-H). <sup>13</sup>C NMR (CDCl<sub>3</sub>) 20.4 ppm (Ar-OCO-CH<sub>3</sub>); 123.2 ppm (C-3,6); 126.3 ppm (C-4,5); 142.0 ppm (C-1,2); 167.7 ppm (C=O).

1,2-diacetoxy-4-methylbenzene: Yield, 76.6% m.p. 57-59°C; literature

value, 57-58°C.<sup>80</sup> <sup>1</sup>H NMR (CDCl<sub>3</sub>) δ 2.27(s, 6, Ar-OCO-CH<sub>3</sub>); 2.33(s, 3, Ar-CH<sub>3</sub>); 7.01(center)(broad d, 3, Ar-H). <sup>13</sup>C NMR (CDCl<sub>3</sub>) 20.5 ppm (Ar-OCO-CH<sub>3</sub>); 20.8 ppm (Ar-CH<sub>3</sub>); 122.7 ppm (C-6); 123.6 ppm (C-3); 126.8 ppm (C-5); 136.4 ppm (C-4); 139.5 ppm (C-1); 141.4 ppm (C-2); 167.9 ppm and 168.0 ppm (C=O's).

1,4-diacetoxy-2-methoxybenzene: m.p. 93-95°C; literature value, 93-94°C.<sup>81</sup>

<sup>1</sup>H NMR (CDCl<sub>3</sub>) δ 2.28 and 2.30(s's, 3 and 3, Ar-OCO-CH<sub>3</sub>); 3.80(s, 3, Ar-OCH<sub>3</sub>); 6.80(center)(m, 3, Ar-H). <sup>13</sup>C NMR (CDCl<sub>3</sub>) 20.5 ppm (Ar-OCO-CH<sub>3</sub>, ortho to OMe); 20.9 ppm (Ar-OCO-CH<sub>3</sub>, meta to OMe); 55.8 ppm (Ar-OCH<sub>3</sub>); 106.3 ppm (C-3); 113.0 ppm (C-5); 122.6 ppm (C-6); 137.0 ppm (C-1); 148.7 ppm (C-4); 151.2 ppm (C-2); 168.4 ppm (C=O on C-1); 168.8 ppm (C=O on C-4).

1-Acetoxy-2-methoxy-4-methylbenzene and 1-(4-acetoxy-3-methoxyphenyl)-ethyl acetate were isolated as liquids in a similar manner to that given by Ludwig *et al.*<sup>82</sup> For example, 2-methoxy-4-methylphenol (7.24 mmol) was dissolved in 5 mL of dry pyridine and placed in a 15 mL round bottom flask. Next, 2.5 mL of acetic anhydride was added, and the flask was stoppered. This solution was allowed to stand overnight at room temperature, with stirring.

The following morning, the reaction solution was hydrolyzed over crushed ice and stirred occasionally until the ice melted. This mixture was then extracted with 2 x 40 mL of diethyl ether. The combined ether extracts were washed with 40 mL of 0.06N HCl, 40 mL of distilled water, 40 mL of saturated NaHCO<sub>3</sub> solution, and finally 40 mL of distilled water again. The ether layer was then dried over anhydrous, powdered Na<sub>2</sub>SO<sub>4</sub>. The ether was decanted and removed on a rotary evaporator. This left the product acetate as a liquid, which was dried over KOH and P<sub>2</sub>O<sub>5</sub> until all traces of residual pyridine were removed.

1-acetoxy-2-methoxy-4-methylbenzene: <sup>1</sup>H NMR (CDCl<sub>3</sub>) δ 2.28(s, 3, Ar-OCO-CH<sub>3</sub>); 2.33(s, 3, Ar-CH<sub>3</sub>); 3.80(s, 3, Ar-OCH<sub>3</sub>); 6.77(center)(m, 3, Ar-H). <sup>13</sup>C NMR (CDCl<sub>3</sub>) 20.4 ppm (Ar-OCO-CH<sub>3</sub>); 21.3 ppm (Ar-CH<sub>3</sub>); 55.5 ppm (Ar-OCH<sub>3</sub>); 113.0 ppm (C-3); 120.8 ppm (C-5); 122.1 ppm (C-6); 136.4 ppm (C-1); 137.3 ppm (C-4); 150.4 ppm (C-2); 168.6 ppm (C=O).

1-(4-acetoxy-3-methoxyphenyl)-ethyl acetate: <sup>1</sup>H NMR (CDCl<sub>3</sub>) δ 1.53(d, 3, Ar-CHOAc-CH<sub>3</sub>); 2.07(s, 3, Ar-CHOCOCH<sub>3</sub>); 2.30(s, 3, Ar-OCO-CH<sub>3</sub>); 3.83(s, 3, Ar-OCH<sub>3</sub>); 5.868(g, 1, Ar-CHOAc-CH<sub>3</sub>); 6.96(center)(m, 3, Ar-H). <sup>13</sup>C NMR (CDCl<sub>3</sub>) 20.4 ppm (Ar-OCO-CH<sub>3</sub>); 21.1 ppm (Ar-CHOAc-CH<sub>3</sub>); 22.1 ppm (Ar-CHOCOCH<sub>3</sub>-CH<sub>3</sub>); 55.6 ppm (Ar-OCH<sub>3</sub>); 71.7 ppm (Ar-CHOAc-CH<sub>3</sub>); 110.3 ppm (C-2); 118.0 ppm (C-6); 122.4 ppm (C-5); 139.0 ppm (C-1); 140.3 ppm (C-4); 150.7 ppm (C-3); 168.4 ppm (Ar-OCO-CH<sub>3</sub>); 169.6 ppm (Ar-CHOCOCH<sub>3</sub>-CH<sub>3</sub>).

#### meta-Nitrobenzene Sulfonyl Hydrazide

meta-Nitrobenzenesulfonyl hydrazide was synthesized from the corresponding sulfonyl chloride as suggested by Cremlyn.<sup>83</sup> The sulfonyl chloride, in turn, was synthesized from the sodium salt of meta-nitrobenzenesulfonic acid.<sup>84,85</sup>

In a typical synthesis, 6 g of dry meta-nitrobenzenesulfonic acid sodium salt (Eastman Kodak Co.) was combined with 15 g of  $\text{PCl}_5$  in a 100 mL round bottom flask. The  $\text{PCl}_5$  was weighed out under nitrogen. The round bottom flask was equipped with a reflux condenser attached to a  $\text{CaCl}_2$  tube. The reaction mixture was heated at  $150^\circ\text{C}$  in a glycerol bath for 30 minutes. After this time, it was cooled to room temperature, and then 100 mL of benzene was added.

The benzene mixture was stirred thoroughly while being warmed in an  $80^\circ\text{C}$  water bath. After extraction of the sulfonyl chloride into the benzene, the solids were filtered off using a dry, fluted filter paper. The benzene filtrate was then washed successively with 2 x 75 followed by 1 x 35 mL of distilled water. Removal of the benzene on a rotary evaporator left a brown colored oil. The oil crystallized after drying over silica gel in a vacuum desiccator. The melting point for the crude material was  $58\text{--}64^\circ\text{C}$ ; literature value,  $64^\circ\text{C}$ .<sup>86</sup> The yield of the material was 81%.

IR (mull)  $\text{cm}^{-1}$     3100(arom C-H); 1600(arom C=C);  
1540(aryl  $\text{NO}_2$ ); 1360 and 1180(sulfonyl chloride S=O)

The crude sulfonyl chloride was used without any further cleanup to produce the sulfonyl hydrazide. Crude sulfonyl chloride (1.95 g) was dissolved in 30 mL of dioxane and placed in a 50 mL round bottom flask. The flask was equipped with an air condenser attached to a  $\text{CaCl}_2$  tube. While stirring, 1 g of hydrazine monohydrate was added to the dioxane solution. This produced an immediate precipitate. The solution was then stirred continuously overnight and kept at room temperature. Workup of the reaction mixture involved, first, removal of the precipitated material (hydrazine monohydrochloride) by filtration. The dioxane filtrate was transferred to a clean 50 mL round bottom flask and the dioxane removed on a rotary evaporator. This left a yellow oil which later



crystallized. This crystallized material was recrystallized from 95% EtOH, yielding yellow prisms; m.p. 125-127°C; literature value, 130°C.<sup>87</sup>

IR (mull)  $\text{cm}^{-1}$  3350, 3260, and 3200(1° and 2° N-H);  
3100(arom C-H); 1600(arom C=C); 1520(aryl NO<sub>2</sub>); 1350 and  
1165(sulfonyl hydrazide S=O)

<sup>1</sup>H NMR (acetone d<sub>6</sub>)  $\delta$  3.00(broad s, 2, Ar-SO<sub>2</sub>-NH-NH<sub>2</sub>);  
8.27(center)(m, 4, Ar-H); 9.26(broad s, 1,  
Ar-SO<sub>2</sub>-NH-NH<sub>2</sub>)

MS (DIP) m/e % 217(0.5, M<sup>+</sup>); 187(2.9); 170(5.0); 153(53.9);  
141(3.0); 123(100.0); 107(2.2); 92(10.0); 76(79.4); 65(16.6);  
50(44.9).

#### 1-Propionyl-Pyrrolidine

1-Propionyl-pyrrolidine was synthesized from pyrrolidine and propionyl chloride in the following manner. Propionyl chloride (10 mL), in 10 mL of CH<sub>2</sub>Cl<sub>2</sub>, was added slowly from a dropping funnel to 11.5 mL of pyrrolidine, in 20 mL of CH<sub>2</sub>Cl<sub>2</sub>. During this addition, the reaction flask was kept immersed in a cold water bath and stirred by a magnetic stir bar. Following addition of the propionyl chloride, the reaction mixture was transferred to a 250 mL separatory funnel, where it was washed with 2 x 50 mL of a saturated NaHCO<sub>3</sub> solution (organic phase pH 6 after washing). The organic phase was then dried over anhydrous, powdered Na<sub>2</sub>SO<sub>4</sub>. After drying, the CH<sub>2</sub>Cl<sub>2</sub> was evaporated leaving a clear liquid. Thin layer chromatography indicated the liquid was pure, and it gave the following confirming NMR analysis:

<sup>1</sup>H NMR (acetone d<sub>6</sub>)  $\delta$  1.02(t, 3, C<sub>4</sub>H<sub>8</sub>N-CO-CH<sub>2</sub>CH<sub>3</sub>);  
1.86[m, 4, (CH<sub>2</sub>)<sub>2</sub>-(CH<sub>2</sub>)<sub>2</sub>-N-CO-CH<sub>2</sub>CH<sub>3</sub>];

2.23(q, 2,  $C_4H_8N-CO-CH_2CH_3$ );

3.36(m, 4,  $(CH_2)_2-(CH_2)_2-N-CO-CH_2CH_3$ ).

## LIGNIN PREPARATIONS

### Acetylation

For each acetylation, the lignin sample was dissolved in an appropriate amount of dry pyridine and placed in a round bottom flask. Acetic anhydride was then added to the flask in a quantity one-half the amount by volume of the pyridine added. This reaction mixture was allowed to stand or was stirred, overnight (16 hrs or more).

Following this time, the reaction mixture was poured over crushed ice. Any nondissolved solids were filtered before this. The crushed ice mixture was stirred occasionally until the ice completely melted. The acetylated lignin which precipitated was then collected by suction filtration. The lignin was washed with cold distilled water, followed by cold dilute HCl (0.01N), followed by cold distilled water again. The isolated lignin was dried in a vacuum desiccator over KOH and  $P_2O_5$ .

### Reductive Acetylation

For each reductive acetylation, the lignin sample was dissolved in an appropriate quantity of dry pyridine and placed in a round bottom flask equipped with a reflux condenser connected to a  $CaCl_2$  tube. Zinc dust (20-30% by weight of lignin) was then added to the lignin solution. Finally, acetic anhydride (one-half the amount by volume of pyridine) was added to the reaction flask. At this time, the flask was placed in a 100°C glycerol bath for one hour with stirring.

At the end of one hour, the flask was removed from the glycerol bath and allowed to cool to room temperature. Any remaining Zn dust was removed from the

reaction solution by suction filtration. The collected Zn was washed with several mL of a 1:1 mixture of acetic acid and pyridine. The combined filtrates were then poured over crushed ice. The crushed ice mixture was stirred occasionally until the ice melted. The acetylated lignin which precipitated was recovered by suction filtration. The isolated lignin was washed with ice cold 0.01N HCl, followed by ice cold distilled water. The recovered lignin was dried over KOH and P<sub>2</sub>O<sub>5</sub> in a vacuum desiccator.

#### Sodium Borohydride Reduction

For small scale reductions conducted in a spectrophotometer cell Marton's<sup>88</sup> procedure was used as a guide. In one such reduction, a solution containing 10 mg of kraft lignin dissolved in 50 mL of 2-methoxyethanol/95% EtOH (2:3) was prepared. Also prepared was a 0.05M NaBH<sub>4</sub> in 0.03N NaOH solution. Two mL of the lignin solution and 1 mL of the borohydride solution were pipetted into a quartz spectrophotometer cell. A reference cell was prepared in the same manner but did not contain any lignin.

Both cells were sealed with Teflon stoppers and kept in the dark. The progress of the reaction was monitored spectrophotometrically in the wavelength range from 260 to 400 nm. Spectra were taken periodically - hourly at the start of the reduction and daily thereafter. The reduction was considered complete when no further decrease in the absorbance spectrum of the lignin was observed. This occurred after one week. Sodium borohydride is relatively stable for this period of time in alkaline solutions.<sup>89</sup> Borohydride reduction of a "quinone lignin" was conducted in a similar manner, except DMF/H<sub>2</sub>O (2:1) was used as the solvent.

In order to obtain isolated, NaBH<sub>4</sub> reduced kraft lignin, the reduction was performed on a much larger scale. In one reduction, 29 g of kraft lignin was

dissolved in 547 mL of 2-methoxyethanol (Mallinckrodt AR). This solution was transferred to a 2000 mL, 3-neck, round bottom flask equipped with a gas inlet tube and a magnetic stir bar. Also added to the flask was 547 mL of 95% EtOH and finally 18.26 g of  $\text{NaBH}_4$  dissolved in 551 mL of 1N NaOH. After addition of the  $\text{NaBH}_4$ , the flask was purged with nitrogen and wrapped in aluminum foil to exclude light. The reaction mixture was kept at room temperature and stirred constantly.

The reduction was again monitored spectrophotometrically by the withdrawal of sample aliquots at the start of, and at various times throughout the course of the reaction. For each aliquot, 0.1 mL of solution was pipetted from the reaction flask and diluted with 10 mL of 2-methoxyethanol/95% EtOH (1:1). One mL of this solution was then diluted again with 9 mL of 2-methoxyethanol/95% EtOH (1:1). This twice diluted aliquot was then used for UV measurements. A reference solution was prepared by dissolving 0.25 g of  $\text{NaBH}_4$  in 7.55 mL of 1N NaOH and 15 mL of 2-methoxyethanol/95% EtOH (1:1). Aliquots (0.1 mL) of the reference solution were diluted as above for measurement purposes. One week was again required for the reduction to go to completion.

After the reduction was complete, the reaction solution was neutralized (pH 7) by the dropwise addition of 1N HCl. During this neutralization, the lignin solution was constantly stirred and kept cool using a cold water bath. The solvents were evaporated using a rotary evaporator (35-40°C). The wet lignin which remained was washed three times with distilled water and collected by centrifugation after each washing. The washed lignin was then air dried and subsequently ground to a uniform powder. Yield of reduced lignin was greater than 95%.

#### Diimide Reduction

Diimide ( $\text{N}_2\text{H}_2$ ) hydrogenations were performed on kraft lignin and on  $\text{NaBH}_4$  reduced kraft lignin. In each case, the procedure was similar. An example of a

large scale hydrogenation of  $\text{NaBH}_4$  reduced kraft lignin is given by the following.  $\text{NaBH}_4$  reduced kraft lignin (20.46 g) was dissolved in 700 mL of 2-methoxyethanol (Mallinckrodt AR), in a 2000 mL, 3-neck, round bottom flask. The flask was equipped with a gas inlet tube, a 250 mL dropping funnel, and a magnetic stir bar. The flask containing the 2-methoxyethanol lignin solution was placed in a 75°C oil bath and allowed to equilibrate. The pH of the lignin solution was adjusted to slightly basic (pH 8) by the addition of 10% KOH.

Next, 12.32 g of meta-nitrobenzenesulfonyl hydrazide dissolved in 100 mL of 2-methoxyethanol was placed in the dropping funnel. The hydrazide solution was slowly added to the lignin solution over a period of approximately 30 minutes. After approximately 15 minutes, hydrogen gas evolution was evident. After completion of the hydrazide addition, the dropping funnel was replaced with an air condenser connected to a  $\text{CaCl}_2$  tube. A slight stream of nitrogen was left flowing over the lignin solution.

After 4 and 8 hours, new charges of meta-nitrobenzenesulfonyl hydrazide (12.32 g in 100 mL 2-methoxyethanol) were again slowly added to the reaction mixture through the dropping funnel. Throughout the course of the reaction, the pH of the lignin solution was kept slightly alkaline by the addition of 10% KOH.

At the end of 12 hours, the reaction flask was removed from the oil bath and its contents cooled to room temperature. For ease of handling, the hydrogenated lignin was recovered from the reaction solution in three portions. Each 330 mL portion was transferred to a 2000 mL beaker, and the beaker was placed in an ice bath. The lignin solution was then acidified (pH 2-3) by the dropwise addition of 1N HCl. The hydrogenated lignin was precipitated by the addition of 800 mL of distilled water and collected by centrifugation. The supernatant was decanted

and the lignin washed twice with distilled water and collected again, each time by centrifugation. The isolated, hydrogenated kraft lignin was then air dried and ground to a uniform powder. Yield of hydrogenated lignin was 73.8%.

In earlier hydrogenations, where the necessary reaction conditions for complete hydrogenation were being delineated, aliquots of the reaction mixture were taken at various times for analysis. The lignin samples in these aliquots were isolated by acidification and addition of distilled water, as above. They were collected by suction filtration, washed until neutral with distilled water, and dried over  $\text{CaCl}_2$  and silica gel. Each lignin sample was then swirled with 3 x 40 mL of diethyl ether, and dried again over  $\text{CaCl}_2$  and silica gel. The lignin samples were finally analyzed by UV spectroscopy for decreases in absorbance.

#### Metal Ion Removal

Metal ions were removed from kraft lignin using a technique which combined EDTA chelation with electrodialysis of the lignin. In one such procedure, 0.78 g of kraft lignin was dissolved in the minimum amount of 2-methoxyethanol needed to give complete dissolution. This lignin solution was poured into 150 mL of 0.05M EDTA, resulting in the lignin precipitating in a swollen, accessible form. The precipitated lignin mixture was centrifuged, and the supernatant, including the 2-methoxyethanol, was decanted. The lignin was then redispersed in an additional 120 mL of 0.05M EDTA.

This lignin dispersion was loaded into the central compartment of an electrodialysis cell (see Fig. 13). The lignin in the sample was retained in the central compartment by two cellulose acetate membranes having a 50 angstrom pore size (Sartorius Filters, Inc.; Hayward, CA; filter No. SM11739). Impurities in the lignin sample, including EDTA-chelated metals, were electrodialyzed through

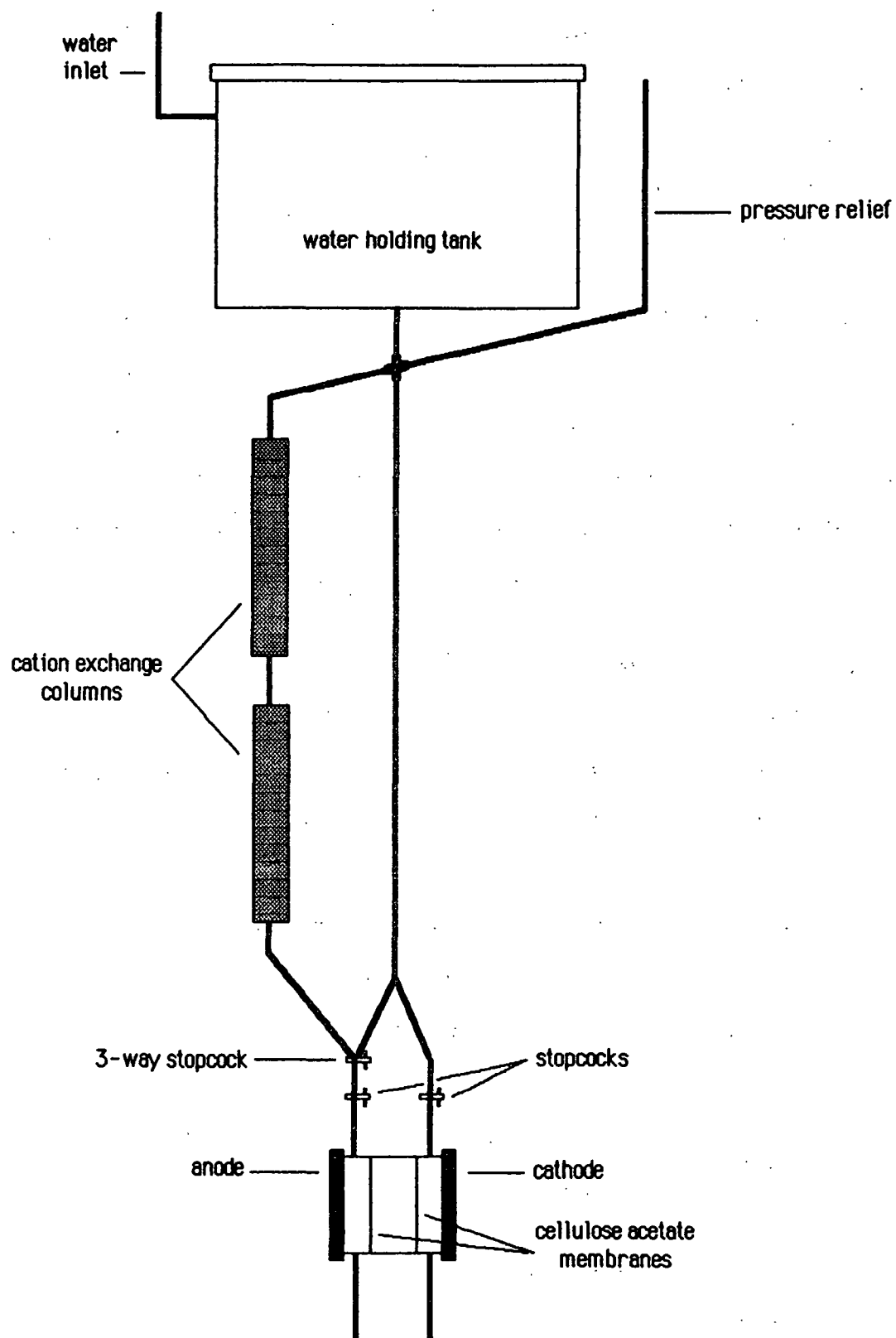


Figure 13. Electrodialysis cell with water supply.

the membranes and carried out of the cell by the water flowing through the two outside compartments. The water used to flush the outer compartments of the cell was distilled and deionized. In addition, two cation exchange columns (Metex Ionxchanger Model 1; Illinois Water Treatment Co.; Rockford, Ill.) were placed in series in the water line flushing the anodic side of the cell.

A voltage of 40-50 V was applied across the cell during the dialysis. The electrical system for the electrodialysis unit is diagrammed in Fig. 14. The electrodialysis was continued for a period of six days. At this time, the current measured across the cell had decreased to a constant value of 3.65 mA, at an applied voltage of 40 V. The lignin-water suspension was then removed from the electrodialysis cell and the lignin was recovered by freeze-drying.

In some cases, including the run described above, a large excess of EDTA was employed. In the course of recovering the lignin after dialysis, white rectangular crystals were observed clinging to the inside of the membrane located on the anodic side of the cell. The crystals were also found interspersed with the lignin. These crystals behaved similarly to the tetrprotic form of EDTA. They were separated from the lignin based on their insolubility in 90% acetic acid. After dissolution of the lignin in the acid, the solid crystals were collected by centrifugation. The supernatant, containing the lignin, was then poured into distilled, deionized water in order to precipitate the lignin. The lignin was collected by centrifugation, washed to a neutral pH, and then dried over  $P_2O_5$  and KOH in a vacuum desiccator.

In one experiment aimed at increasing the color of the lignin, ferric ions were readded to the EDTA-chelated, electrodialyzed kraft lignin. One mL of an aqueous  $FeCl_3 \cdot 6H_2O$  solution (14.8 mg/1000 mL) was added to 7.5 mg of lignin



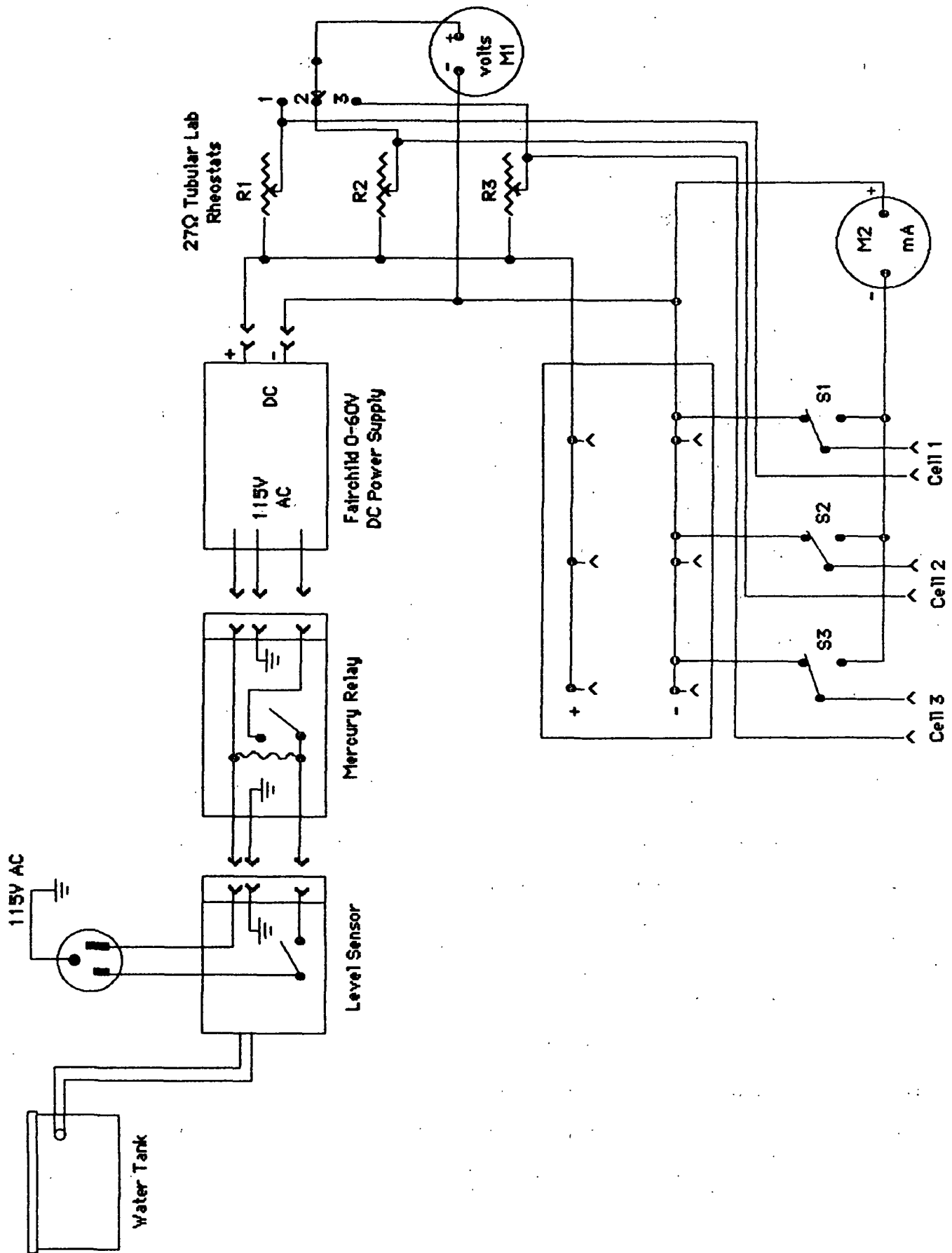


Figure 14. Electrical system for electroanalysis cell.

dissolved in 2-methoxyethanol. Total volume of the combined solutions was 25 mL. The concentration of iron to lignin was calculated to be 400 ppm.

#### Periodate Oxidation

The procedure for periodate oxidation of kraft lignin was dependent upon the method used to halt the oxidation. Three different techniques were used to quench the reaction:

##### Lead Nitrate Addition

In a typical oxidation, 0.56 g of kraft lignin was dissolved in 50 mL of 2-methoxyethanol (Mallinckrodt AR) and placed in a 125 mL Erlenmeyer flask. Added to this solution was 0.59 g (2.8 mmol) of  $\text{NaIO}_4$  dissolved in 20 mL of distilled water. The reaction mixture was allowed to stand at approximately 4°C from 30 minutes up to 12 hours with occasional swirling. At the end of the allowed time, the reaction was terminated by the addition of 0.89 g (2.8 mmol) of  $\text{Pb}(\text{NO}_3)_2$ , which was dissolved in 5 mL of distilled water.

After several minutes, the lead iodate and periodate precipitates were removed by repeated filtrations. The lignin was isolated by the evaporation of the solvents on a rotary evaporator (40-50°C). The flask containing the lignin residue was dried over  $\text{P}_2\text{O}_5$  and KOH in a vacuum desiccator. The dried residue was removed from the flask by slurrying with water and subsequent filtration. The lignin was then redried.

##### Sulfur Dioxide Addition

In a typical oxidation, 0.56 g of kraft lignin was dissolved in 60 mL of 90% acetic acid and placed in a 125 mL Erlenmeyer flask. This solution was cooled to 0-2°C and placed in an ice bath. Next, 20 mL of 0.14M  $\text{NaIO}_4$  in 60% acetic acid, also cooled to 0-2°C, was added to the flask. The combined solutions were

stirred with a magnetic stir bar and allowed to react for 2 minutes. During this time, the color of the solution, originally dark brown, became violet tinged. After 2 minutes had passed,  $\text{SO}_2$  was bubbled through the solution. The solution again turned brown in color.

The reaction solution was then poured into 400 mL of cold distilled water, precipitating the lignin. The lignin precipitate was collected by centrifugation followed by suction filtration. It was washed with distilled water and then dried over  $\text{P}_2\text{O}_5$  and KOH in a vacuum desiccator.

For some oxidations, a mixture of 2-methoxyethanol or dioxane and AcOH was used as the solvent. In one experiment using 90% AcOH as the solvent, the amount of added  $\text{NaIO}_4$  was doubled.

#### Ethylene Glycol Addition

In a typical oxidation, 0.56 g of kraft lignin was dissolved in 60 mL of 90% AcOH and placed in a 125 mL Erlenmeyer flask. This solution was cooled to  $0-2^\circ\text{C}$  and placed in an ice bath. Next, 20 mL of cold ( $0-2^\circ\text{C}$ )  $0.14\text{M}$   $\text{NaIO}_4$  in 60% AcOH was added to the flask. The combined solutions were stirred magnetically and allowed to react for 2 minutes. After this time, 20 mL of cold ethylene glycol was added to the solution and stirring was continued for an additional 2 minutes.

At this point, the reaction solution was poured into 400 mL of cold distilled water. The lignin which precipitated was concentrated by centrifugation and collected by suction filtration. It was washed with cold distilled water and then dried over  $\text{P}_2\text{O}_5$  and KOH in a vacuum desiccator.

In other oxidations, the reaction time was varied from 0 minutes (no  $\text{NaIO}_4$  addition) up to 4 minutes.

## HIGH PRESSURE SPECTROSCOPY

High pressure electronic spectra of various lignin samples were recorded at the Department of Chemistry of the University of California at Santa Barbara in the laboratories of Dr. Henry W. Offen.

### Apparatus

The high pressure optical cell, window assembly, and sample capsule have been described previously.<sup>90</sup> In brief, the pressure cell was machined to size from a 6.4 cm bar of "Berylco 25", a Be-Cu alloy. The pressure fluid was admitted through the top of this cylindrical cell. The cell was fitted with four ports which were 90° apart and perpendicular to the cylinder axis. Three of these seated sapphire windows while the sample was loaded via the fourth port.

The window material was composed of oriented Linde synthetic sapphire, ground optically flat parallel and perpendicular to the cylinder axis. The windows were held in place by a series of spacers, gaskets, and O-rings and finally by a threaded Be-Cu plug.

The cylindrical quartz sample capsule was made from 4.21 mm ID precision bore tubing and matching discs fused with a microtorch. The sample solution within the quartz capsule was isolated from the pressure-transmitting fluid by a movable piston.

Absorption spectra were recorded on a Cary Model 14 spectrophotometer. The sample compartment of the Cary 14 had been previously modified in order to accommodate the high pressure cell. In addition to the direct readout from the strip chart recorder of the Cary 14, the spectrophotometric data were digitized by a Quasitronics, Inc. Q3024 Computer Interface and fed to an Apple III computer. A

slide wire assembly was used to feed the analog data from the Cary 14 to the A/D converter, since there was no suitable DC output on the spectrophotometer. Analog data were transmitted to a contact which traversed the slide wire via a mechanical linkage from the pen drive mechanism.

The slide wire mounted to the front of the Cary 14 was supplied with a constant +5V. The position of the contact along the slide wire resulted in a voltage reading directly proportional to the absorbance of the sample. Spectral data were stored in the computer therefore as wavelength versus voltage values but were then easily converted to wavelength versus absorbance values. This transformation was accomplished from knowledge of the the linear response and full scale values for the slide wire. These values were recorded daily and proved to be constant throughout the series of high pressure spectra which were obtained.

#### Sample Preparation

All lignin samples were recorded as solution spectra in either DMF or 2-methoxy-ethanol (Aldrich, Gold Label, spectrophotometric grade). Lignin concentrations ranged from 9.7-10.2 mg/25 mL of solvent. Lignin solutions were prepared just prior to measurement, and were kept in the dark.

#### Procedure for High Pressure Run

Lignin solutions were loaded into the cylindrical quartz sample capsule, taking care to exclude air bubbles. The pressure cell was filled with spectro-quality hexane, and the sample capsule was inserted through the sample port of the cell. The sample port was then sealed. Next, the pressure cell was connected to a barrel intensifier, also filled with hexane. All connections were made through Aminco tubing, fittings, and valves. A hand-operated Enerpac oil

pump was used to pressurize the system. Pressure values were measured directly by a Heise 47054 gage. When the desired pressure was reached, the proper valves were closed, and the cell was detached from the barrel intensifier. The pressure cell was then mounted into the sample compartment of the Cary 14.

In a typical pressure experiment, absorption spectra were recorded of the lignin sample in the pressure sequence: atmospheric, 100 MPa, 200 MPa, 300 MPa, and return to atmospheric. Spectra were recorded after the return to atmospheric pressure in order to check for irreversible pressure effects. For some samples, 50 and 150 MPa pressure spectra were also recorded. Duplicate pressure runs were made for each lignin sample, using a fresh lignin sample for the duplicate run.

#### LABELING TECHNIQUES FOR KRAFT LIGNIN

Quinone groups in kraft lignin were tagged as both  $^{13}\text{C}$  and  $^{14}\text{C}$  labeled acetates by reductive acetylation procedures:

##### Carbon-13

In one labeling experiment, twice acetylated kraft lignin (0.515 g) was dissolved in 2.5 mL of dry pyridine and placed in a 10 mL round bottom flask. Added to this solution was 1.25 mL of  $^{13}\text{C}$ -labeled  $(\text{CH}_3^*\text{CO})_2\text{O}$  (11.2% enriched). The  $^{13}\text{C}$  enriched acetic anhydride was prepared from 0.5 g of 90%  $(\text{CH}_3^*\text{CO})_2\text{O}$  (Stohler Isotope Chemicals, Waltham, MA) which was diluted with 3.25 mL of unlabeled acetic anhydride.

One-half of the lignin solution was then pipetted into a 5 mL round bottom flask. Zinc dust (0.052 g) was added to the solution remaining in the 10 mL flask. To the solution in the 5 mL flask, a trace of zinc acetate was added. Both flasks were fitted with reflux condensers connected to  $\text{CaCl}_2$  tubes. They

were then placed in 100°C glycerol baths. The flasks were kept in the glycerol baths for 1 hour, with occasional stirring.

At the end of 1 hour, the flasks were removed from the glycerol baths and cooled to room temperature. The Zn dust which remained in the 10 mL flask was removed by filtration. The recovered Zn was then washed with 1 mL of dry pyridine/AcOH (1:1). The combined filtrates were poured over crushed ice, and the lignin which precipitated was collected by filtration. The recovered lignin was washed with cold 0.01N HCl followed by cold distilled water. It was then dried over P<sub>2</sub>O<sub>5</sub> and KOH in a vacuum desiccator. The contents of the 5 mL flask were poured directly over crushed ice, and the precipitated lignin was recovered as just described.

In another labeling experiment, 0.261 g of a twice acetylated, periodate oxidized lignin was dissolved in 5 mL of dry pyridine and placed in a 10 mL round bottom flask. Added to this solution was 2.5 mL of <sup>13</sup>C-labeled (CH<sub>3</sub><sup>\*</sup>CO)<sub>2</sub>O (11.2% enriched). Also added to the lignin solution was 0.159 g of Zn dust. The reductive acetylation was then carried out using the same conditions and isolation procedures as given above.

#### Carbon-14

For <sup>14</sup>C labeling of quinones in lignin, <sup>14</sup>C-labeled (CH<sub>3</sub><sup>\*</sup>CO)<sub>2</sub>O (liquid under vacuum; specific activity, 20 mCi/mmol) was purchased from Amersham Corp., Arlington Heights, Illinois. The [1-<sup>14</sup>C] acetic anhydride was diluted with 50 mL of unlabeled acetic anhydride, according to the procedure given by "Method B" in the Amersham publication "Guide for users of labelled compounds."<sup>91</sup> The final specific activity of the acetic anhydride was calculated to be 4.72 x 10<sup>-4</sup> mCi/mmol or 1.75 x 10<sup>4</sup> Bq/mmol. This value was checked experimentally by adding

50  $\mu$ L of the radioactive  $\text{Ac}_2\text{O}$  to 10 mL of scintillation cocktail (see below) in a glass counting vial and determining the sample's activity. Duplicate determinations yielded a value for the specific activity of  $1.62 \times 10^4$  Bq/mmol. This experimentally determined value was used in all subsequent calculations.

A typical radioactive labeling experiment is described by the following. Twice acetylated kraft lignin (50.9 mg) was dissolved in 2 mL of dry pyridine and placed in a 5 mL round bottom flask. Added to this solution was 16.7 mg of Zn dust and 1 mL [ $1\text{-}^{14}\text{C}$ ] acetic anhydride. The flask was equipped with a magnetic stir bar and with a reflux condenser connected to a  $\text{CaCl}_2$  tube. It was lowered into a  $100^\circ\text{C}$  glycerol bath for one hour.

Following this time, the flask was removed from the glycerol bath and cooled to room temperature. The contents of the flask were then suction filtered through a glass fritted microfilter (3C), and the filtrate was collected in a test tube. The filter was washed with 1 mL of dry pyridine/ $\text{AcOH}$  (1:1), and the combined filtrates were hydrolyzed over crushed ice. The ice mixture was stirred occasionally until the ice melted. At this time, the lignin which precipitated was collected by suction filtration through a Buchner funnel ( $\sim 1$  cm diameter). The recovered lignin was washed with cold distilled water, followed by  $0.01\text{N}$   $\text{HCl}$  and distilled water again. It was then dried over  $\text{P}_2\text{O}_5$  and  $\text{KOH}$  in a vacuum desiccator. Yield of the dried product was 44.2 mg.

Some acetylations with [ $1\text{-}^{14}\text{C}$ ] acetic anhydride were done under "blank conditions". For these acetylations, no Zn dust was added to the reaction mixture.

The activity of all radioactive lignin samples was analyzed by liquid scintillation counting. A Beckman LS 3801 Liquid Scintillation System was employed.



The radioactive lignin samples (40-50 mg) were dissolved in 10 mL of scintillation cocktail and placed in glass counting vials. The scintillation cocktail was prepared from 100 g of naphthalene (Aldrich, Gold Label, Scintillation grade, 99+%) and 5 g of 2,5-diphenyloxazole (scintillation grade), both dissolved in 1 liter of dioxane (Baker AR). Before counting, the lignin samples were left in the dark (several days) until the natural luminescence of the lignin had decayed. Each sample was counted at least three separate times; recorded values were at the 95% confidence level and within 1% of the mean.

Efficiencies for the various lignin samples were determined by the internal standard method.<sup>92</sup> After finding the cpm values of the individual sample vials, 100 L of [1-<sup>14</sup>C]-n-hexadecane standard (Amersham; dpm = 87200), was added to the vials. The count rate of the sample plus the internal standard was then determined. The efficiency of the sample was calculated from the equation:

$$\text{Efficiency} = \frac{C_2 - C_1}{C_{IS}} \quad (12)$$

Where,

$C_2$  = count rate of sample + internal standard

$C_1$  = count rate of sample

$C_{IS}$  = count rate of internal standard

## RESULTS AND DISCUSSION

### LIGNIN MATERIALS

#### Kraft Lignin

As detailed in the "Materials and Methods" section, the elemental composition and methoxyl content of the isolated kraft lignin were typical for a softwood kraft lignin. In addition, the instrumental analyses for this lignin, including infrared, ultraviolet-visible, and proton and carbon-13 nuclear magnetic resonance spectroscopy (Fig. 9-12), gave representative spectra. Reviews of infrared,<sup>93</sup> ultraviolet-visible,<sup>18</sup> and proton NMR<sup>94</sup> spectra of lignins, including kraft lignin have been published previously. Recent reports concerning carbon-13 NMR spectra of kraft lignin have also been published.<sup>95,96</sup> Individual aspects of these spectra will be discussed as needed.

#### Periodate Oxidized Kraft Lignin

Some of the isolated kraft lignin was modified in order to increase the likelihood of CT interactions. This modification involved increasing the quinone content of the lignin. Increased numbers of quinones were incorporated into the lignin by a periodate oxidation technique.

Periodate oxidation appears to have been first used, in connection with lignin chemistry, as a method to isolate lignin from other plant materials.<sup>97</sup> The so called "periodate lignins" contained from 75% to nearly quantitative amounts of the lignin present in the original material. However, this lignin was in an oxidized form. Adler and Hernestam<sup>98</sup> later demonstrated that sodium meta-periodate reacted rapidly with guaiacyl-type structures in lignin, liberating methanol. Adler and coworkers<sup>99</sup> used periodate oxidation on various lignins

to estimate their concentrations of guaiacyl residues having free phenolic hydroxyl groups.

In more detail, periodate oxidation of guaiacyl structures results in their rapid oxidative demethoxylation to produce the corresponding ortho-quinones.<sup>98</sup> If excess periodate is present, the ortho-quinones may react further in a relatively slow step to yield dicarboxylic acids. These reactions are depicted in Fig. 15.

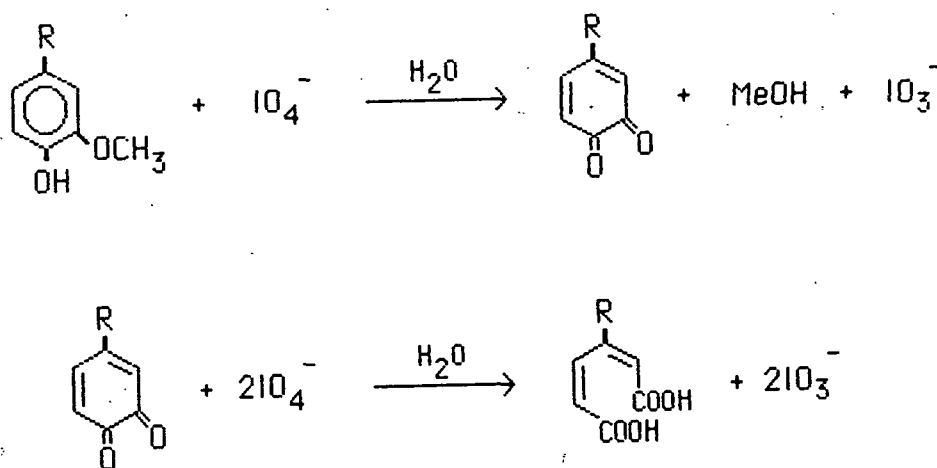


Figure 15. Oxidation of guaiacyl structures by periodate.

The mechanism of the oxidation was elucidated by using <sup>18</sup>O labeled water as the reaction medium.<sup>100</sup> The quinone which was obtained from the oxidation was found to have incorporated the label. This indicated the sequence of reactions shown in Fig. 16. The oxidation proceeds through the periodate ester, 10, which is converted directly or via the intermediate, 11, to the ortho-quinol, 12. The ortho-quinol subsequently decomposes into the ortho-quinone. Studies by Adler and coworkers in the area of periodate oxidation of phenols have been reviewed by Sklarz.<sup>101</sup>

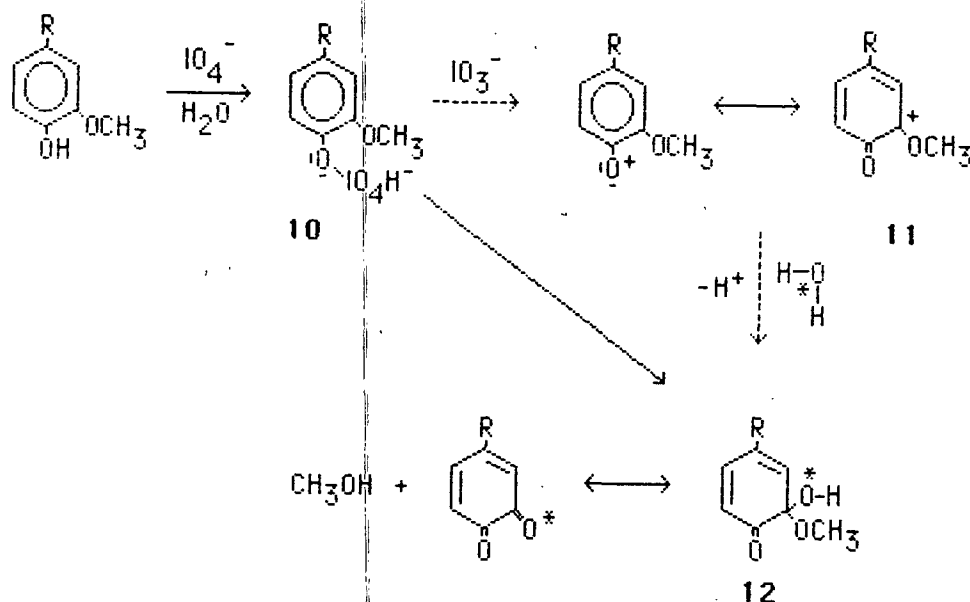


Figure 16. Mechanism of the periodate oxidation of guaiacyl structures.

Three different periodate oxidation techniques were employed in attempting to incorporate ortho-quinones into kraft lignin. The major difference between the oxidation procedures was in the method used to halt the oxidation. The three procedures included periodate oxidation with lead nitrate, sulfur dioxide, and ethylene glycol additions. Periodate oxidation of kraft lignin with ethylene glycol addition proved to be the most successful method of incorporating the ortho-quinones. The results of the periodate oxidations with lead nitrate and sulfur dioxide additions are provided in Appendix II.

#### Periodate Oxidation with Ethylene Glycol Addition

Periodate rapidly cleaves molecules containing 1,2-diol structures. Therefore, the addition of a glycol in excess to a periodate oxidation mixture should be effective in consuming the unreacted periodate and halting the oxidation. This concept was tested for the periodate oxidations of lignin using ethylene glycol. Ethylene glycol was inert to the lignin under the reaction conditions employed, and the excess glycol was easily washed away. Initial reaction

conditions employed an equimolar concentration of periodate to methoxyl groups in the lignin, a two minute reaction time, and a temperature of approximately 0°C. A large excess of ethylene glycol (one-hundred fold) was most effective in halting the oxidation.

The lignins which resulted were soluble in DMF and 2-methoxyethanol (unlike the lignins which were obtained from the periodate oxidation with lead nitrate addition, see Appendix II). The incorporation of ortho-quinone groups into the lignins was demonstrated by a number of instrumental techniques. An FTIR spectrum of a kraft lignin oxidized in this manner appears in Fig. 17. The most important feature of this spectrum is the appearance of a strong band due to ortho-quinones at approximately  $1663\text{ cm}^{-1}$ . Confirmation of this assignment comes from literature evidence concerning the position of the ortho-quinone carbonyl stretch and from disappearance of this band upon reduction of the lignin. Otting and Staiger,<sup>102</sup> in a study of ten ortho-benzoquinones, reported the carbonyl stretching band of these quinones occurred from  $1667$  to  $1656\text{ cm}^{-1}$ . Reductive acetylation of the lignin shown in Fig. 17 resulted in the spectrum given in Fig. 18. In this spectrum, the quinone carbonyl stretch has been eliminated. The absorptions appearing at  $1768.5$  and  $1746\text{ cm}^{-1}$  are due to acetate carbonyls.

The isolated periodate oxidized lignins, termed "quinone lignins", were darker in appearance than the original kraft lignin. This observation was confirmed by visible spectroscopy. A typical visible spectrum is shown by Fig. 19, where the quinone lignin spectrum is compared to the original kraft lignin spectrum. The spectra in Fig. 19 demonstrate periodate oxidation greatly increased the visible absorbance of the original lignin. The difference spectrum between these two lignins, shown in Fig. 20, clearly displays the absorbance which was

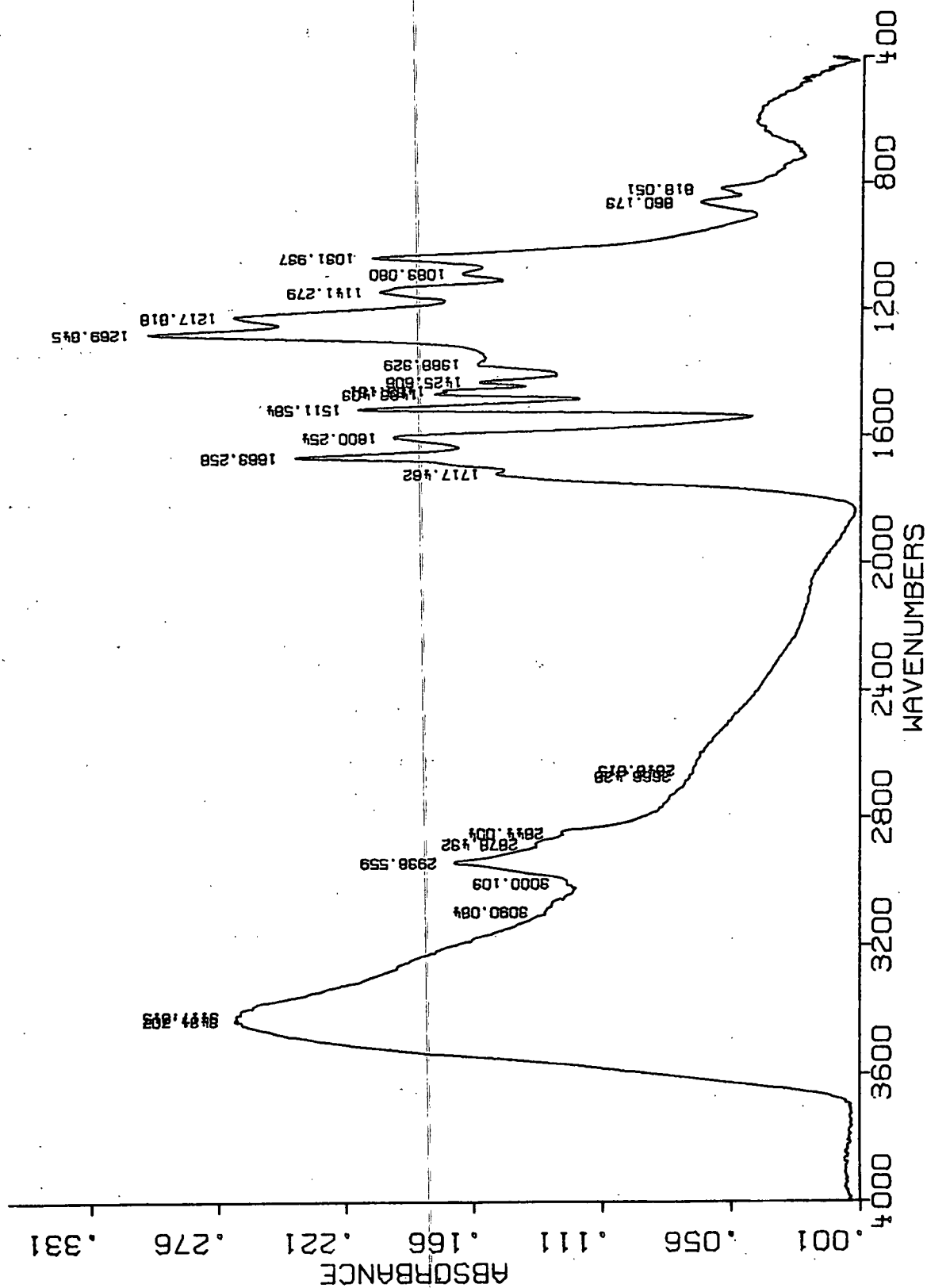


Figure 17. FTIR spectrum of periodate oxidized (two minutes) kraft lignin; ethylene glycol added to halt the oxidation.

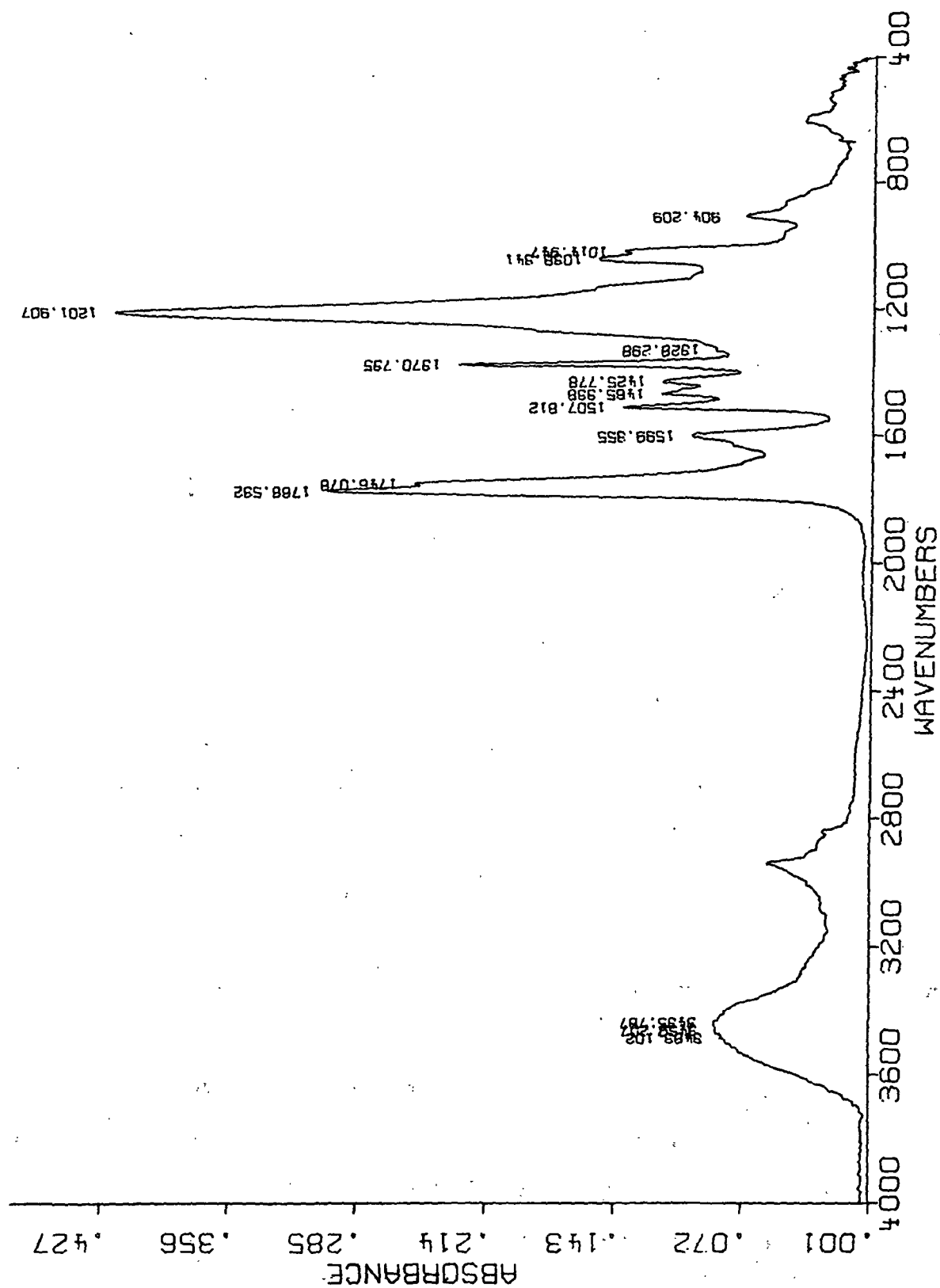


Figure 18. FTIR spectrum of reductively acetylated, periodate oxidized kraft lignin shown in Fig. 17.

added to the original lignin by its oxidation. This difference spectrum has a maximum absorbance at approximately 416 nm. The  $\pi$ - $\pi^*$  absorption band of ortho-quinones occurs in this region of the spectrum<sup>103</sup> and, so, visible absorption spectroscopy was consistent with the incorporation of ortho-quinones in these oxidized lignins.

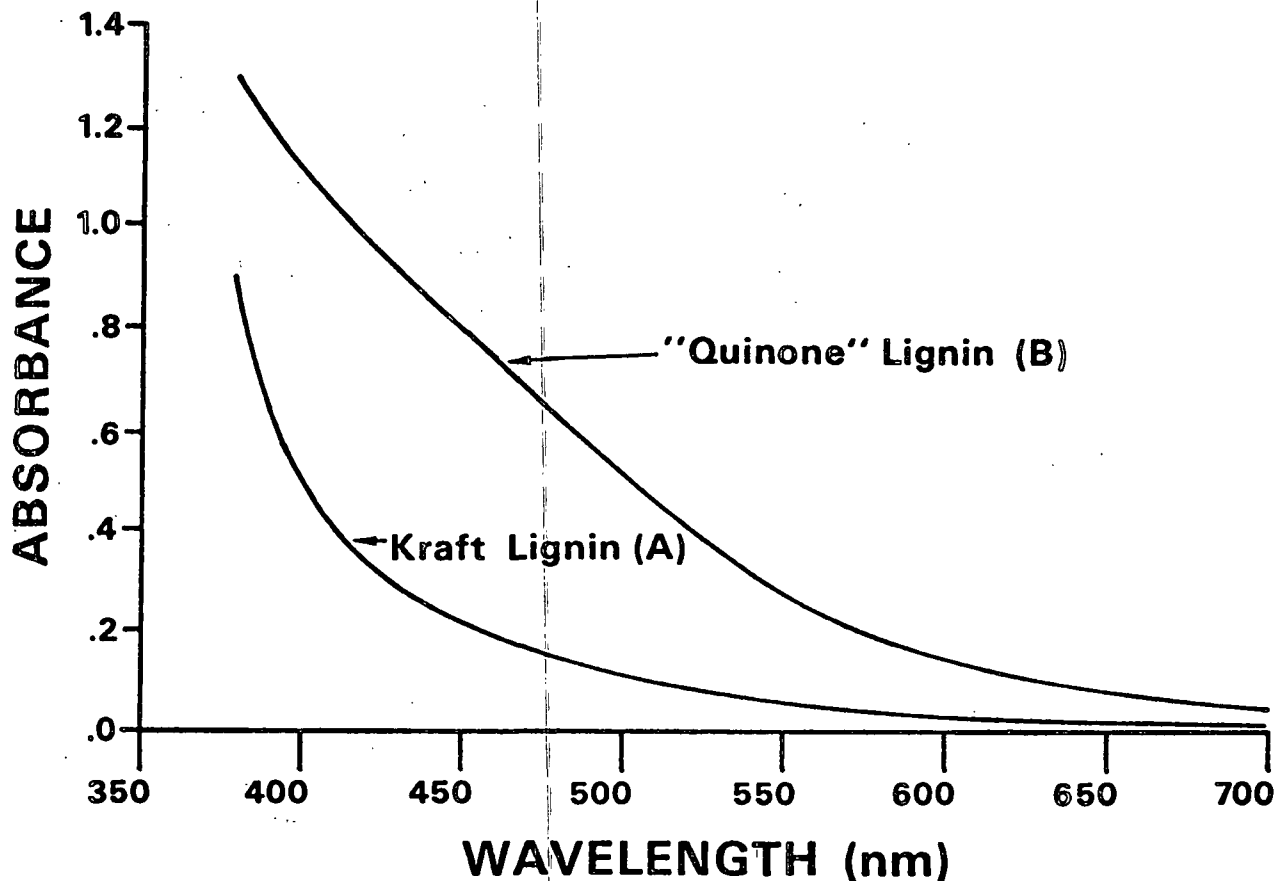


Figure 19. Visible spectra of "quinone lignin" (oxidized two minutes) and original kraft lignin.

Carbon-13 NMR spectroscopic studies of the periodate oxidized lignins was used to confirm that the introduced quinones were ortho-quinones. The presence of ortho-quinones was verified by using reductive acetylation to produce the corresponding <sup>13</sup>C-labeled catechol acetates. The carbonyl carbons of the



catechol acetates were easily observed in the  $^{13}\text{C}$  NMR spectra of the reductively acetylated quinone lignins. The distinction between ortho- and para-diacetates was made on the basis of the different carbonyl chemical shift values. The carbonyl carbons of the ortho-diacetates appeared upfield from the carbonyl carbons of para-diacetates due to steric crowding. Steric crowding of carbon atoms results in upfield shifts of those carbon atoms, compared to the similar uncrowded ones.<sup>104</sup>

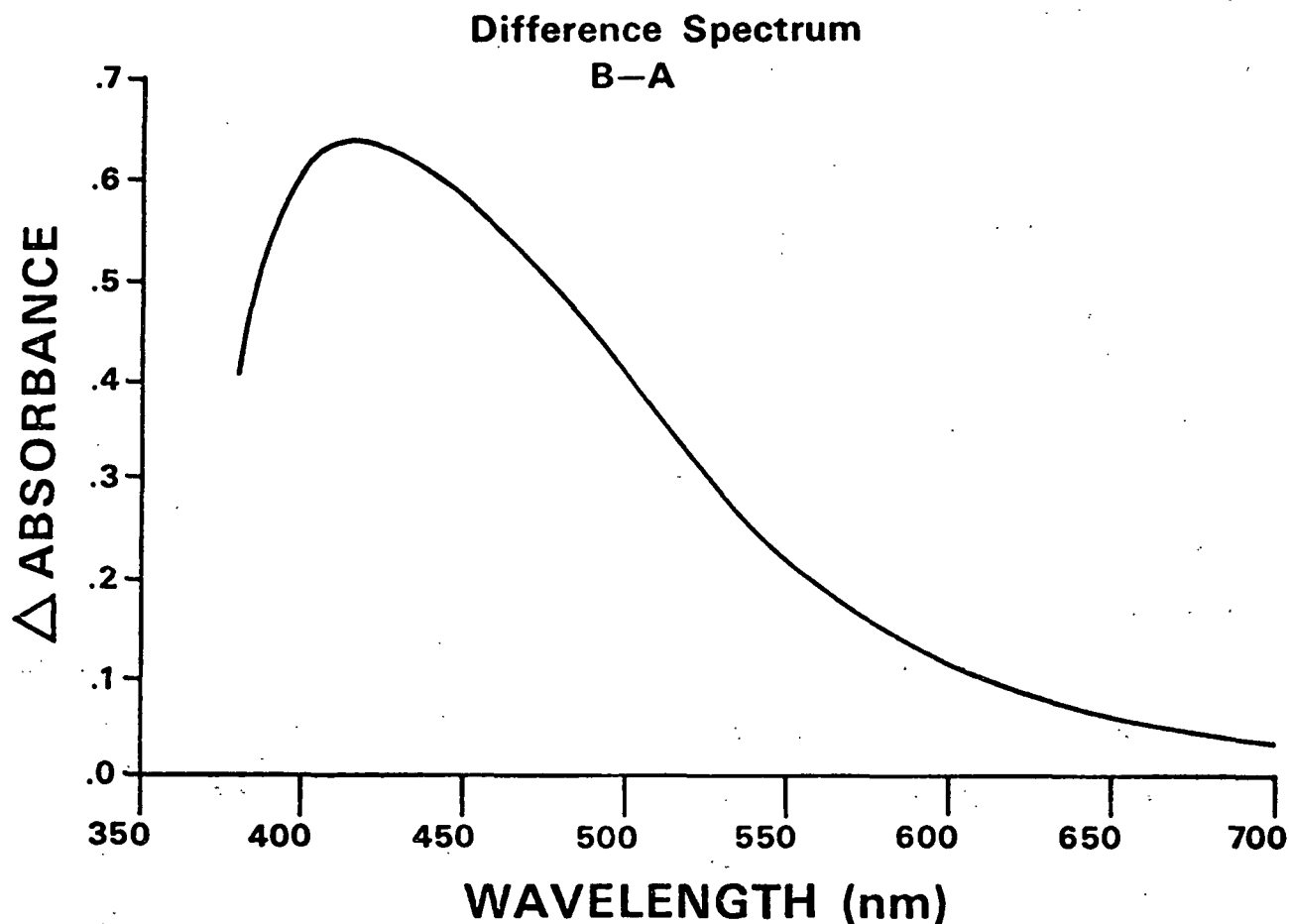


Figure 20. Difference spectrum from Fig. 19.

The steric crowding effect was demonstrated for ortho- and para-diacetoxy-benzenes through a study of model compounds. The chemical shifts for the carbonyl carbons in these model acetates are given in Table 10. As shown, the carbonyl carbons of the para-acetates generally occurred between 168.4 and 168.8 ppm. The carbonyl carbons of the ortho-acetates appeared slightly upfield from this, between 167.7 and 168.0 ppm.

Table 10. Carbonyl chemical shift values.

Substituents on Benzene Skeleton	Chemical Shift of C=O, ppm from TMS
1,4-diacetoxy-	168.75
1,4-diacetoxy-3-methoxy-	168.75 168.41
1-acetoxy-2-methoxy-4-methyl-	168.61
1-acetoxy-2-methoxy-4-ethyl- acetate-	168.37 169.58 (aliphatic)
1,2-diacetoxy-	167.74
1,2-diacetoxy-4-methyl-	167.88 167.98

The  $^{13}\text{C}$  NMR spectrum of the original kraft lignin after reductive acetylation with  $^{13}\text{C}$ -labeled acetic anhydride is shown in Fig. 21. The spectrum contains three carbonyl acetate absorptions at 169.9, 169.2, and 168.3 ppm. These absorptions correspond to acetates attached to primary, secondary, and aromatic carbon atoms, respectively.<sup>96</sup> Reductive acetylation of a periodate oxidized lignin with  $^{13}\text{C}$ -labeled acetic anhydride gave the spectrum shown in Fig. 22. For this lignin, the aromatic carbonyl acetate absorption was shifted upfield to 167.5 ppm. In Fig. 23, the carbonyl regions for these two lignins are shown on an expanded scale. The upfield shift of the aromatic acetate peak in the

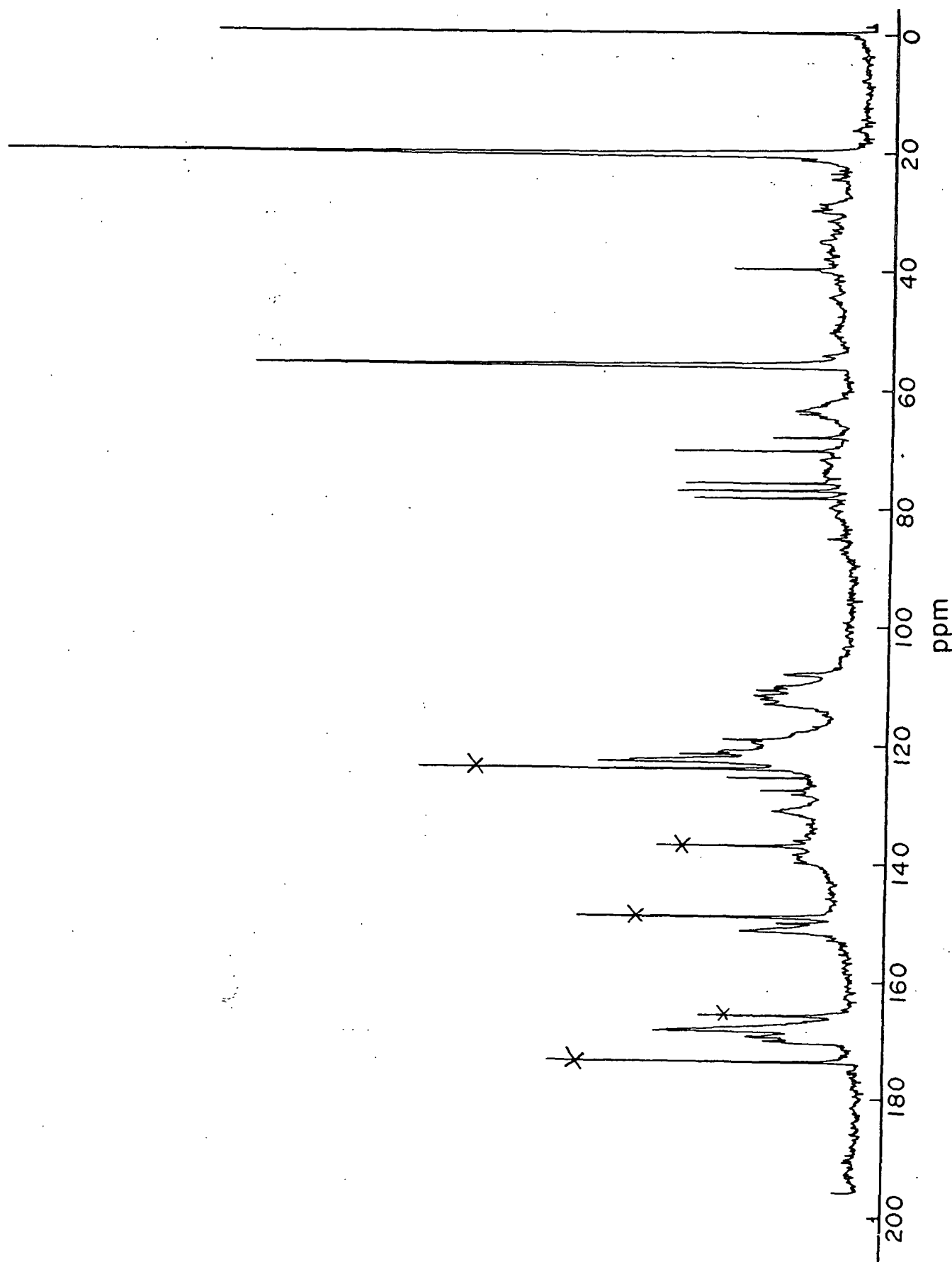


Figure 21.  $^{13}\text{C}$  NMR spectrum of kraft lignin reductively acetylated with  $^{13}\text{C}$ -labeled  $\text{Ac}_2\text{O}$ ;  $\text{CDCl}_3$  as solvent; peaks marked by an "x" are solvent residues (173.6 ppm,  $\text{HOAc}$ ; 165.9 ppm,  $\text{Ac}_2\text{O}$ ; 149.4, 135.8, and 123.6 ppm, pyridine).

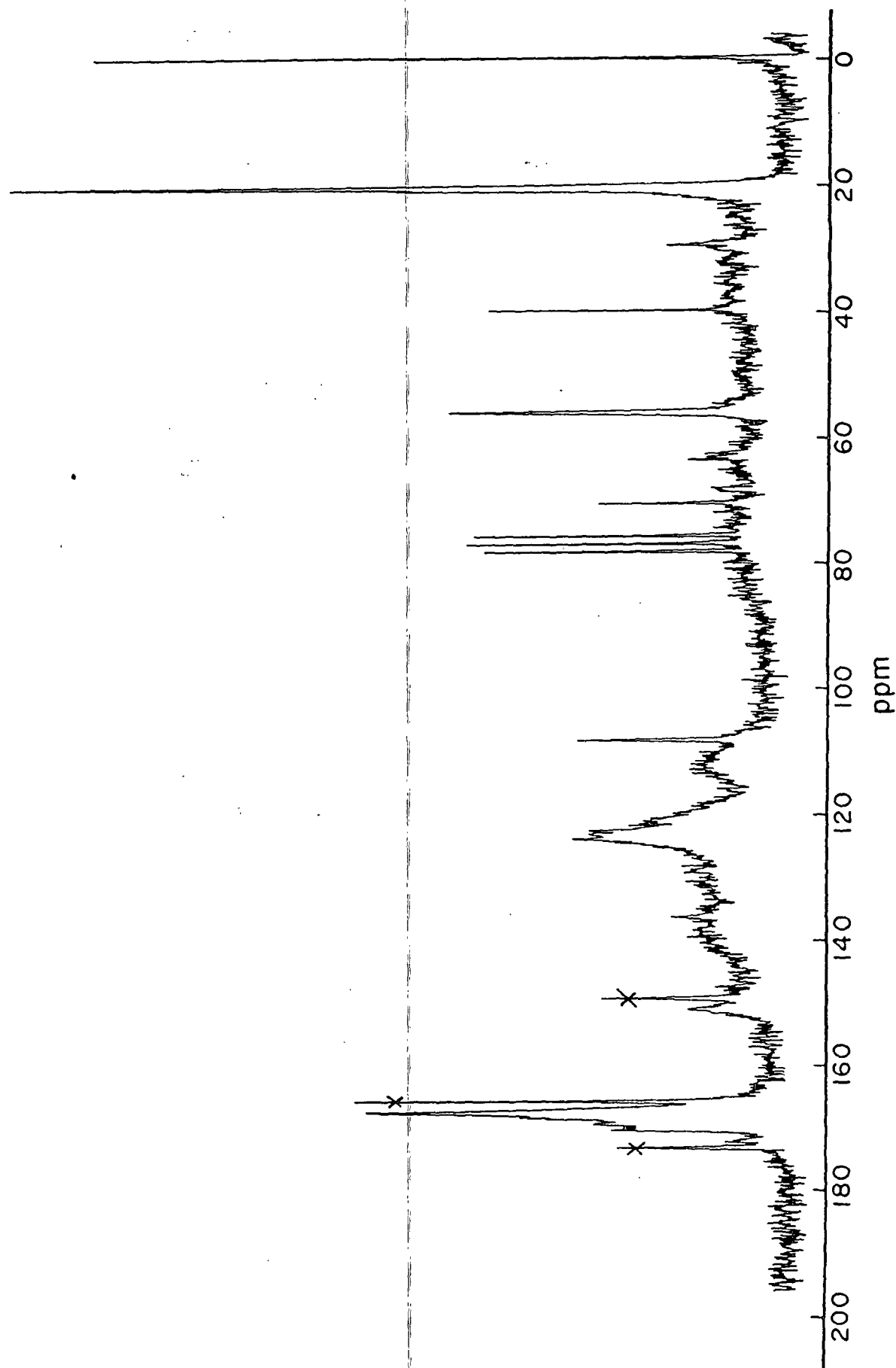


Figure 22.  $^{13}\text{C}$  NMR spectrum of periodate oxidized (2 min) kraft lignin reductively acetylated with  $^{13}\text{C}$ -labeled  $\text{Ac}_2\text{O}$ ;  $\text{CDCl}_3$  as solvent; peaks marked by an "x" are solvent residues as in Fig. 21.

periodate oxidized lignin is a reflection of its increased content of ortho-diacetate groups. These groups are present in the lignin from the reductive acetylation of ortho-quinones.

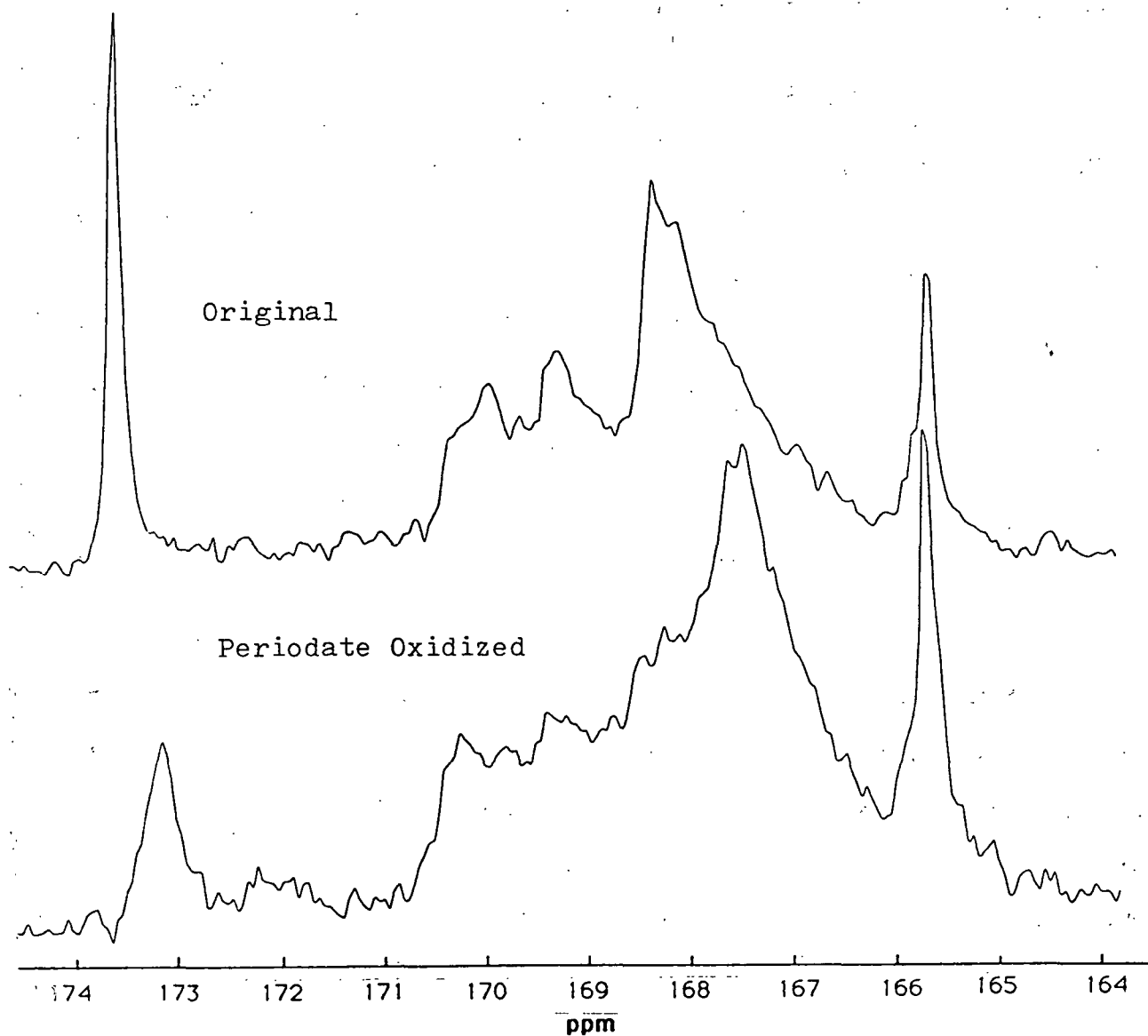


Figure 23. Enlargement of carbonyl region from Fig. 21 and 22.

Finally, periodate oxidized lignins were characterized with respect to their methoxyl loss versus the length of the oxidation. This characterization was performed by evaluation of  $^1\text{H}$  NMR spectra of the reductively acetylated,

periodate oxidized lignins. Data from these NMR evaluations along with the corresponding oxidation conditions are given in Table 11. For each oxidation the temperature was approximately 1°C.

Table 11. Reductively acetylated periodate lignins.

Sample	Reaction Conditions			<sup>1</sup> H NMR Analysis		
	Mole NaIO <sub>4</sub> Mole OCH <sub>3</sub>	Solvent, % HOAc	Time, min	OMe Arom	OAc <sub>arom</sub> Arom	OAc <sub>aliph</sub> Arom
1	0	90.0	-	0.90	0.77	0.94
2	0	90.0	-	0.84	0.71	0.89
3	1	82.5	1	0.70	0.84	0.89
4	1	82.5	1	0.66	0.86	0.88
5	1	82.5	2	0.66	0.85	0.86
6	1	82.5	2	0.60	0.81	0.79
7	1	82.5	4	0.54	0.81	0.75
8	1	82.5	4	0.56	0.89	0.82

The <sup>1</sup>H NMR data in Table 11 were obtained by evaluating the NMR integral trace over the appropriate chemical shift ranges. In order to compare the different oxidized lignins, their respective integral values were normalized by dividing by the integral value obtained for the aromatic protons in each lignin. The number of aromatic protons was not significantly affected by the oxidation treatment.

Data from Table 11 were used to plot the % demethoxylation vs. time, as shown in Fig. 24. The values for the % demethoxylation were calculated based on the reduction in the OMe/Arom ratios for the oxidized lignins compared to the control samples 1 and 2. The rate of methoxyl loss was very rapid, reaching

21.8% after one minute, and continuing on to a value of 36.8% after four minutes. A four minute reaction time was perceived as the practical limit for the oxidation, since some insoluble lignin material was encountered at this point.

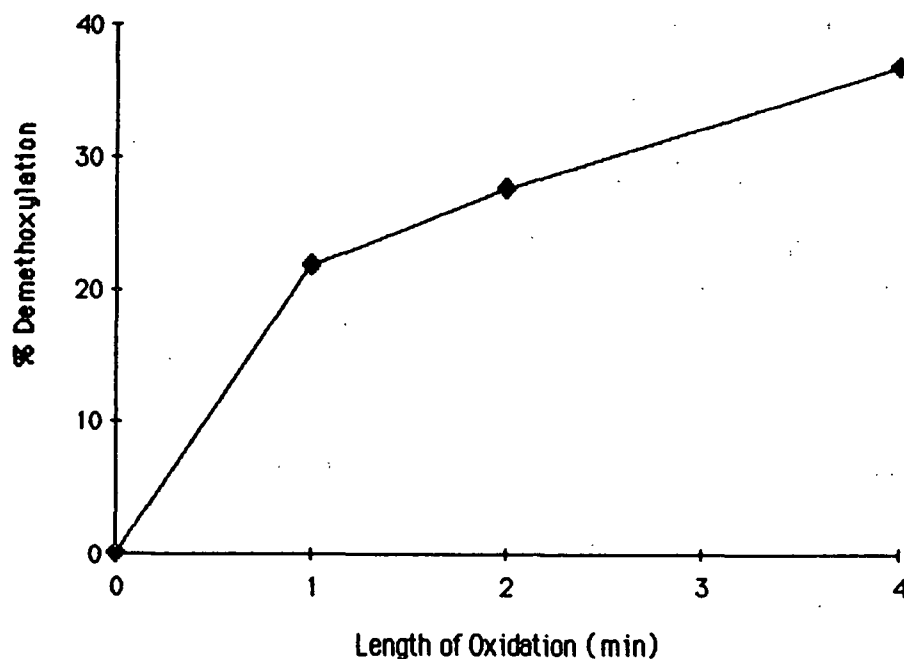


Figure 24. Methoxyl loss versus length of oxidation for periodate lignins with ethylene glycol addition.

Besides the methoxyl ratios given in Table 11, ratios for the aromatic and aliphatic acetates are also given. These ratios are indicative of the numbers of aromatic and aliphatic hydroxyls, respectively, in the lignin prior to the reductive acetylation. Since the acetylation was conducted under reducing conditions, the aromatic acetate content includes quinone groups. Compared to the control samples, the number of aromatic acetates increased after one minute of oxidation as expected (samples 3 and 4). The increased aromatic acetate content of these lignins was a reflection of their higher quinone contents. However, the aromatic acetate content remained the same at longer oxidation times (samples 5-8). Apparently the quinone content of the lignins reached an equilibrium

value; that is, the additional quinones which were formed by extending the reaction time were offset by the loss of already formed quinones due to continued oxidation and condensation reactions. Also in Table 11, the number of aliphatic acetates should remain relatively constant with oxidation; however, a decrease in this value was generally observed.

The effect of a second reductive acetylation, performed on some of these lignins, is shown in Table 12. The second acetylation brought the aliphatic acetate values up to the level observed in the control samples. Therefore, the low aliphatic acetate values noted in Table 11 were due to incomplete acetylation of the samples.

Table 12. Twice reductively acetylated periodate lignins.

Sample	Time, min	OMe/Arom	OAc <sub>arom</sub> /Arom	OAc <sub>aliph</sub> /Arom
1	1	0.61	0.86	0.97
2	2	0.61	0.88	0.93
3	4	0.53	0.84	0.97

Periodate oxidations were also performed on kraft lignins which were to be analyzed by high pressure spectroscopy. These lignins received several treatments prior to oxidation in order to remove various chromophores. In sequence, the treatments included sodium borohydride reduction, diimide hydrogenation, and removal of metals by an EDTA chelation technique. The length of oxidation and the methoxyl content in these lignins as determined by the Zeisel method are given in Table 13. Also given in the table are the % methoxyl losses in these lignins, based on a methoxyl content after metal removal of 13.28%.



The values in Table 13 reveal the oxidation of these lignins proceeded at a more rapid pace than earlier oxidations (see Fig. 24). This rapid oxidation may have been caused by the lower methoxyl content of the lignin after the chromophore-removing treatments (13.28% vs. 14.74% in the original lignin). In addition, the pretreated lignin was somewhat different in character, having been reduced and hydrogenated. Finally, the quantities of lignin oxidized were much larger. This necessitated the use of more concentrated lignin solutions due to practical experimental considerations.

Table 13. % Methoxyl loss for pretreated periodate lignins.

Length of Oxidation	OMe Content, %	% OMe loss
40 sec	9.28	30.12
2 min	8.61	35.17
4 min	8.67	34.71

#### CHARGE-TRANSFER COMPLEXES IN KRAFT LIGNIN

For the purposes of discussion, the topic of CTC's in kraft lignin is divided into three parts. These are, in the order presented: (1) CTC's in model compounds and between model compounds and kraft lignin; (2) CTC's in modified kraft lignins, where the possibility of CTC formation was increased; and (3) CTC's in the original, unmodified kraft lignin. Information gained through the study of CTC's in models and in the modified kraft lignins was used to help draw conclusions about CTC's in the original kraft lignin.

##### CTC's Between Model Compounds and Kraft Lignin

Since a scarcity of quinone groups acting as acceptor moieties in the proposed phenol-quinone CTC was expected in kraft lignin, the effect of an added

model quinone was investigated. For the initial experiments, the model quinone, 3,5-di-tert-butyl-1,2-benzoquinone, was added to 2-methoxyethanol solutions of kraft lignin. This particular quinone model was chosen, since ortho-quinones were expected to be the dominant quinone type in kraft lignin. In addition, the tertiary butyl groups provided stability. Electronic absorption spectra were recorded of these combined quinone and lignin solutions and of the individual quinone and lignin species. These spectra are shown in Fig. 25.

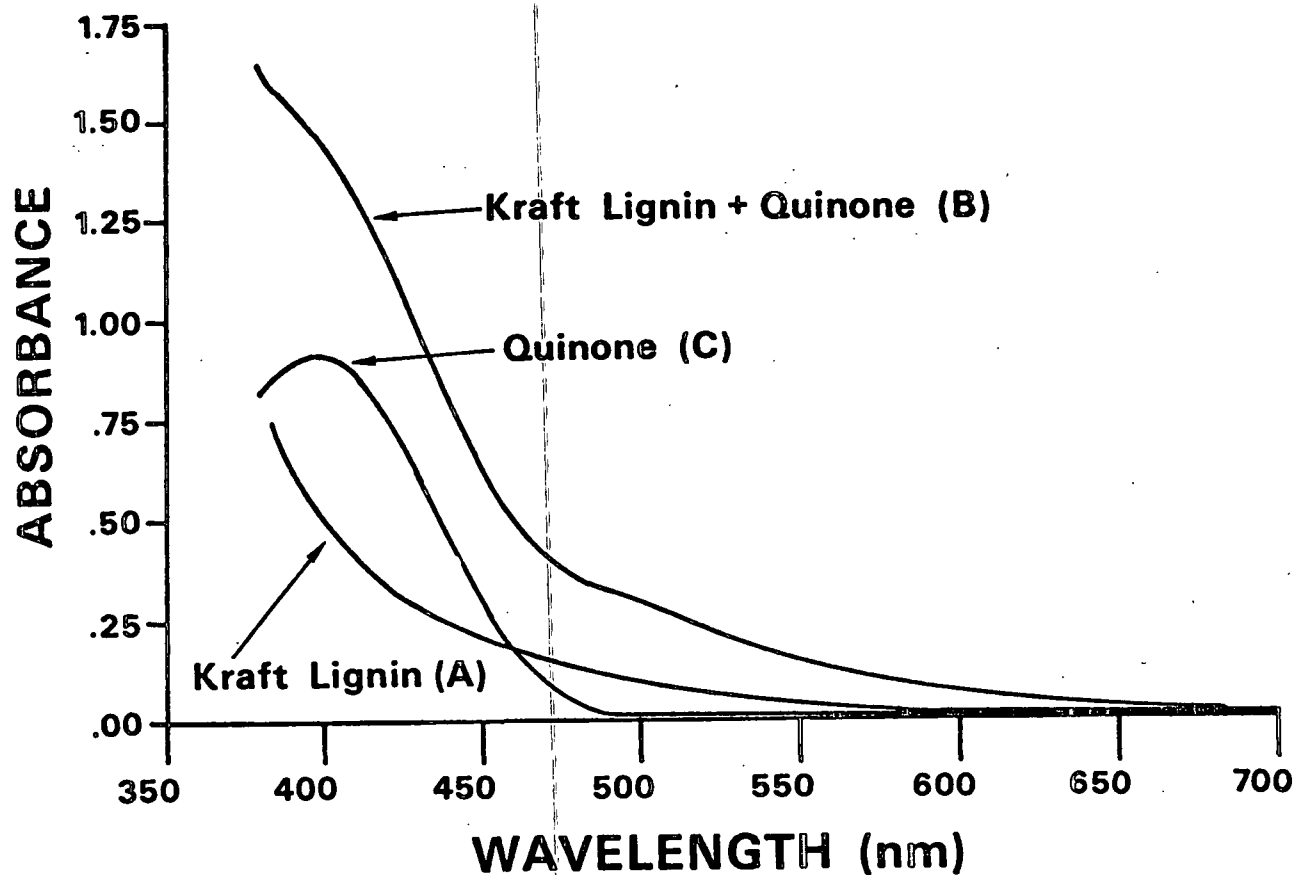


Figure 25. Visible spectra of (A) kraft lignin [ $16.3 \times 10^{-4}M$ ], (C) 3,5-di-tert-butyl-1,2-benzoquinone [ $5.00 \times 10^{-4}M$ ], and (B) kraft lignin plus quinone [same concentrations]; 2-methoxyethanol as solvent.

In Fig. 25, the kraft lignin concentration is 7.6 mg/25 mL (or  $16.3 \times 10^{-4}M$ , using the unit molecular weight of 186 g/mole), whereas the concentration of the 3,5-di-tert-butyl-1,2-benzoquinone added to it is  $5.00 \times 10^{-4}M$ . In the spectrum of the quinone added to the kraft lignin, an extra absorbance, not present in either of the individual spectra, is evident in the 500 nm and longer wavelength region. This additional absorbance signifies the occurrence of a CTC between a donating moiety in the lignin and the quinone.

The CTC band may be more clearly observed from the difference spectrum presented in Fig. 26. Figure 26 is the result of the subtraction of the individual lignin and quinone spectra, (A) and (C), respectively, from the quinone plus lignin spectrum, (B), in Fig. 25. The CTC band has a maximum absorbance located at 494 nm, with a molar absorptivity of approximately 360 lit/mol-cm.

#### Effect of Acetylating the Lignin

An interesting observation made in the course of these experiments involved the spectra obtained upon addition of the model quinone to acetylated kraft lignin solutions. After acetylation of the kraft lignin, the CT band was no longer present. This observation is shown by Fig. 27. In this figure, the concentrations of the quinone ( $5.00 \times 10^{-4}M$ ) and lignin (7.6 mg/25 mL) are the same as in Fig. 25, but the additional absorbance is no longer present. Upon subtraction of the spectra, as before, no difference was observed between the two curves.

The effect of acetylation (disruption of the model quinone-lignin CTC) may be explained by some of the factors which influence CTC's, discussed in the "Introduction". Acetylation results in the conversion of alcoholic and phenolic functionalities in lignin to their respective acetates. The derivatization of phenolic groups alters the electron density of the  $\pi$ -electron clouds above and

below the aromatic rings to which they are attached. A phenolic substituent strongly activates the ring, but an acetate substituent is only mildly activating.<sup>34</sup> The diminished electron donating capacity of these rings would, of course, affect CT interactions. Steric factors may also be important in preventing CT interactions between the acetylated kraft lignin and 3,5-di-tert-butyl-1,2-benzoquinone. The acetate group is a much bulkier substituent than the hydroxyl group, and, therefore, could prevent a close approach by the quinone group. As mentioned in the literature review of CTC's earlier, replacement of a phenolic proton by a methoxyl group resulted in weaker complexes.<sup>39</sup>

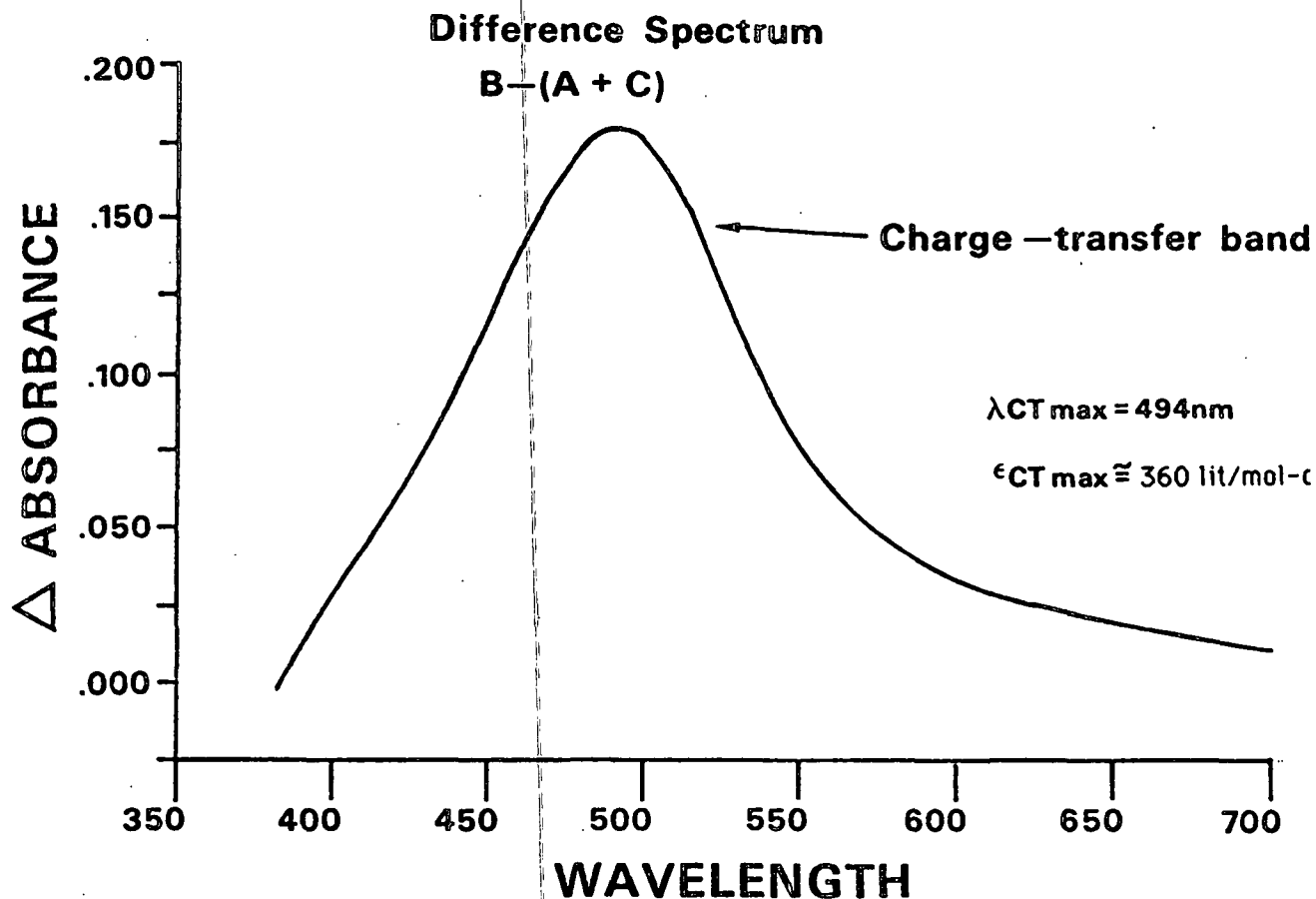


Figure 26. Difference spectrum from Fig. 25.

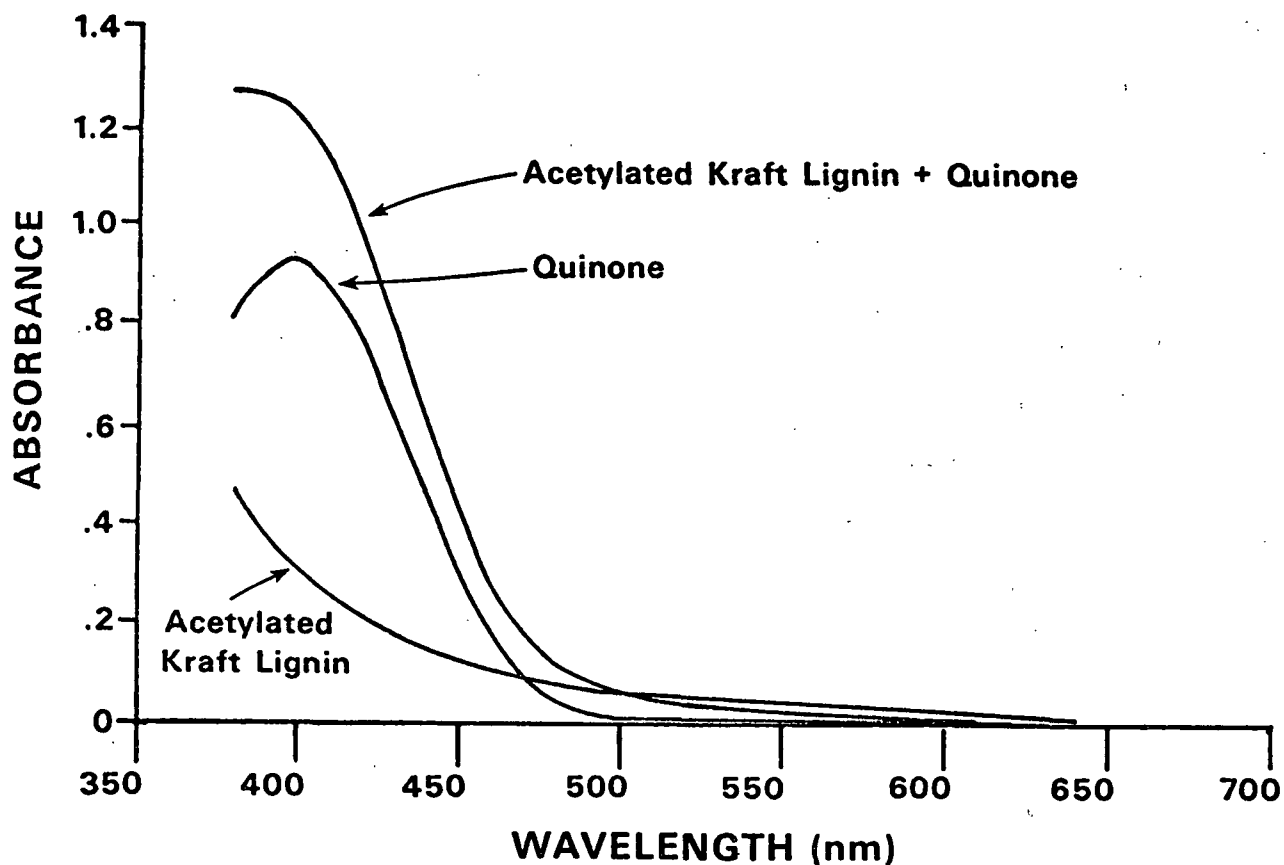


Figure 27. Visible spectra of acetylated kraft lignin (7.6 mg/25 mL), 3,5-di-tert-butyl-1,2-benzoquinone ( $5.00 \times 10^{-4}M$ ), and acetylated kraft lignin plus quinone (same concentrations); 2-methoxyethanol as solvent.

Finally, by replacing the phenoxy substituents with acetoxy ones, possibilities for hydrogen bonding are being eliminated. Hydrogen bonding may be a contributing force in attracting the two halves of the complex close enough to each other in order for CT interactions to occur.

Any of the factors mentioned above may have been the reason for the lack of a CT interaction between the model quinone and the acetylated kraft lignin. Most likely a combination of these effects resulted in the observed behavior. In any case, the results strongly suggested free phenolics were the donating moieties in kraft lignin.

### Effect of Added Quinone Concentration

In one set of experiments, the concentration of 3,5-di-tert-butyl-1,2-benzoquinone was varied, while the lignin concentration was kept constant. Under these conditions, the effect of changing the ratio of acceptor groups (quinones) to donor groups (in the lignin) was investigated. For this set of experiments the donor groups in kraft lignin were assumed to be the free phenolics. Again, the solvent was 2-methoxyethanol. The data which resulted from this investigation appear in Table 14. In the table, "phenol" refers to the free phenolic content of the lignin.

Table 14. Effect of acceptor/donor ratio on model quinone-kraft lignin CTC.

Quinone Conc., M	Phenol Conc., M <sup>a</sup>	Quinone/Phenol	$\lambda$ CT <sub>max</sub>	Abs CT <sub>max</sub>	$\epsilon$ CT <sub>max</sub> <sup>b</sup>
9.10 x 10 <sup>-5</sup>	9.32 x 10 <sup>-4</sup>	0.10	492	0.023	253
2.51 x 10 <sup>-4</sup>	9.32 x 10 <sup>-4</sup>	0.27	492	0.113	450
5.00 x 10 <sup>-4</sup>	9.44 x 10 <sup>-4</sup>	0.53	492	0.182	364
7.45 x 10 <sup>-4</sup>	9.32 x 10 <sup>-4</sup>	0.80	490	0.248	333
1.01 x 10 <sup>-3</sup>	9.32 x 10 <sup>-4</sup>	1.08	490	0.254	272
1.51 x 10 <sup>-3</sup>	9.44 x 10 <sup>-4</sup>	1.60	488	0.277	294

<sup>a</sup>Based on a unit molecular weight of 186 g/mole and a phenol content of 57.9/100 C<sub>9</sub> units.

<sup>b</sup>Calculated assuming 100% quinone complexation in 1:1 complexes, up to a quinone/phenol ratio of 1.00; for quinone/phenol ratios greater than 1.00, 100% complexation of the quinones in 1:1 complexes, up to the limit of available phenols, was assumed.

The data in Table 14 reveal the absorbance of the CTC depended on the quinone/phenol ratio. The intensity of the CTC band linearly increased at low quinone/phenol ratios but then leveled off at ratios of 0.65 and higher. This result is shown in Fig. 28. Apparently, at the higher levels of quinone addition

all good donor sites in the lignin were exhausted, and no new complexes could form. Observation of the leveling off effect at ratios lower than one was not surprising, since every phenol in the lignin cannot be expected to be a good donor. Steric restraints or participation in intramolecular complexes will render some phenolic sites poor donors. The apparent relationship between the intensity of the complex with the quinone/phenol ratio again implicates free phenolics in the lignin as the donating moiety in this quinone-lignin CTC.

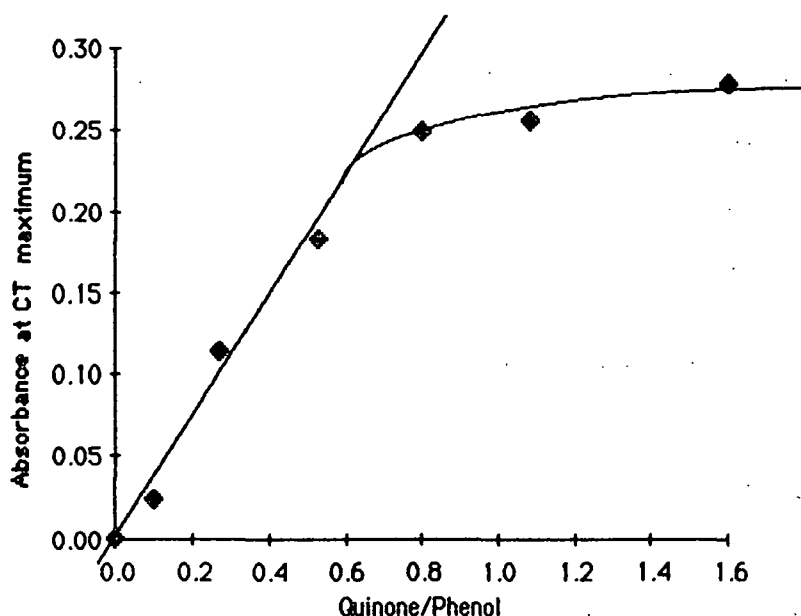


Figure 28. Effect of quinone/phenol ratio on absorbance of CTC between kraft lignin and 3,5-di-tert-butyl-1,2-benzoquinone. Phenol refers to the free phenolic content of the lignin.

Bearing in mind the assumptions made in order to calculate the molar absorptivities in Table 14 (complexation of every quinone molecule up to the limit of available phenolics), the variation in the values probably indicates the differences in the types of phenolic groups in the lignin. Depending on the immediate environment of the phenolic groups, both the molar absorptivity and the association constant of the complex may change. Not all the phenolics will be

equally good donors. Most importantly, the magnitude of the calculated values is within the range of values reported for similar types of complexes in the literature (see Tables 3 and 17).

#### Effect of Solvent

The complex between kraft lignin and 3,5-di-tert-butyl-1,2-benzoquinone was also studied in the solvent N,N-dimethylformamide (DMF). In terms of physical constants which can be used as measures of solvent polarity, DMF has both a dielectric constant and a dipole moment which are approximately twice as large as those for 2-methoxyethanol.<sup>33</sup> A spectrum was recorded of the complex at a quinone concentration of  $5.00 \times 10^{-4}$  and compared to the results obtained in 2-methoxyethanol. The quinone and lignin concentrations were the same in each case. The results are shown in Fig. 29 and summarized in Table 15.

Oppositely from the predicted behavior, 2-methoxyethanol behaved as the more polar solvent. The maximum absorbance of the complex was slightly red-shifted and less intense when employing 2-methoxyethanol as compared to DMF. However, this solvent behavior was not surprising when considering the polar nature and hydrogen bonding tendencies of the two solvents employed. Predicted solvent behavior breaks down when specific interactions between the solute and solvent are possible. For example, the CT absorption of the DMSO-I<sub>2</sub> complex occurred at a longer wavelength (288 nm) in CHCl<sub>3</sub> (dielectric constant = 5.5) than in water (CT<sub>max</sub> at 285 nm; dielectric constant = 80).<sup>105</sup>

#### CTC Between Model Phenol and Model Quinone

By the addition of a model quinone to kraft lignin solutions, two basic conclusions were reached. These were, first, that a CTC actually did form between the quinone and the lignin, and, second, that the donating moieties in



kraft lignin were free phenolic groups. These conclusions were substantiated by the observance of a CTC in the simpler system, between a model phenol and the model quinone. The model phenol used in this study was 2-methoxy-4-methyl-phenol.

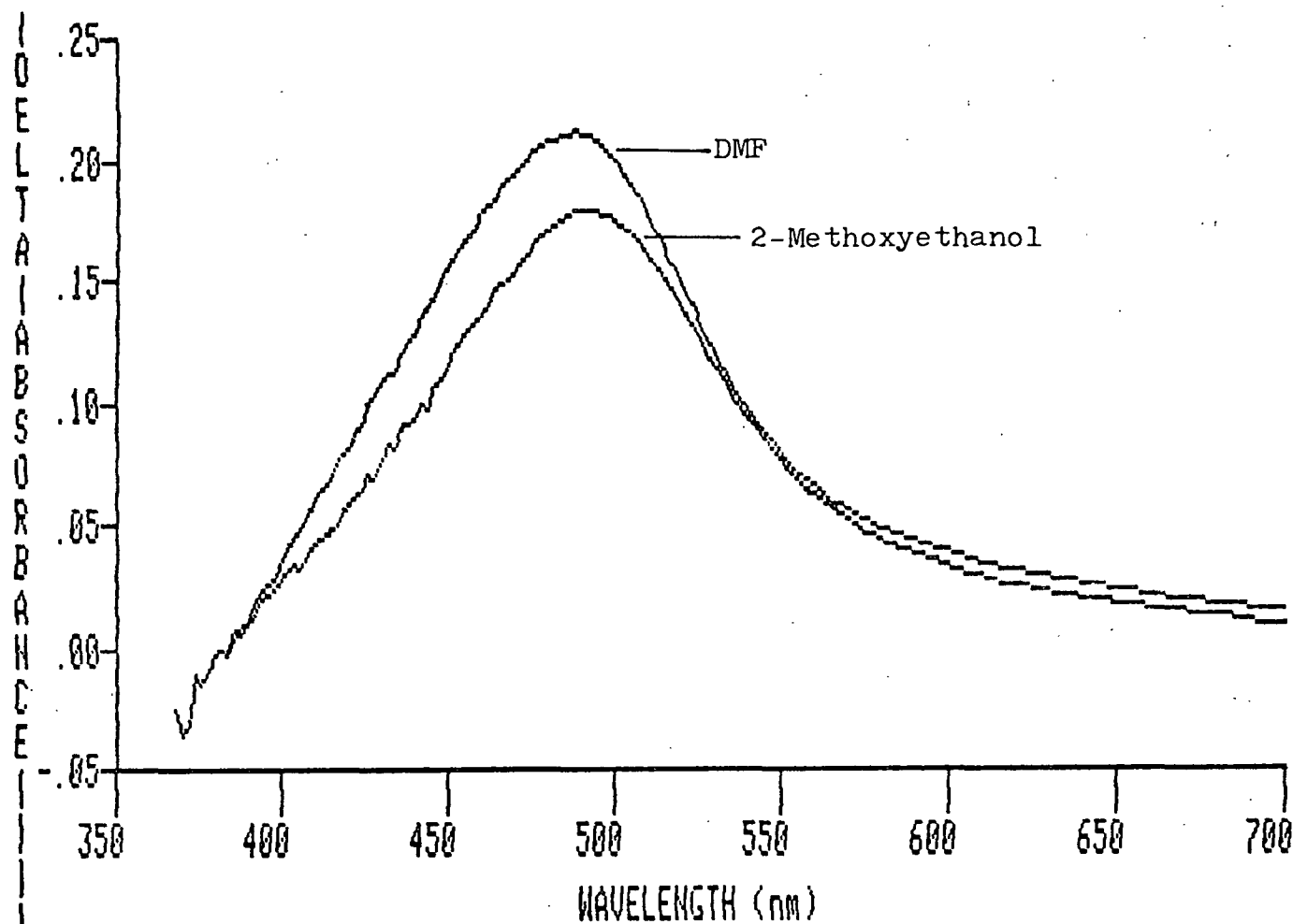


Figure 29. Effect of solvent on the difference spectrum between kraft lignin and 3,5-di-tert-butyl-1,2-benzoquinone; lignin concentration ( $1.63 \times 10^{-3}\text{M}$ ), quinone concentration ( $5.00 \times 10^{-4}\text{M}$ ).

Table 15. Effect of solvent on kraft lignin - 3,5-di-tert-butyl-1,2-benzoquinone CTC.

Solvent	$\lambda_{\text{CTmax}}$ , nm	$\text{Abs}_{\text{CTmax}}$ , AU
2-Methoxyethanol	492	0.182
DMF	488	0.213

Spectra of the phenol, quinone, and phenol plus quinone appear in Fig. 30. The solvent used in these studies was hexane, since the complex was unstable in the more polar solvents, DMF and 2-methoxyethanol. In fact, the yellow color of the quinone gradually disappeared in these solvent systems when the phenol was present, indicating a possible chemical reaction. Figure 30 reveals the spectrum of the quinone plus phenol had a slightly higher absorbance on the long wavelength side of the quinone  $\pi-\pi^*$  absorption band than the individual quinone spectrum had.

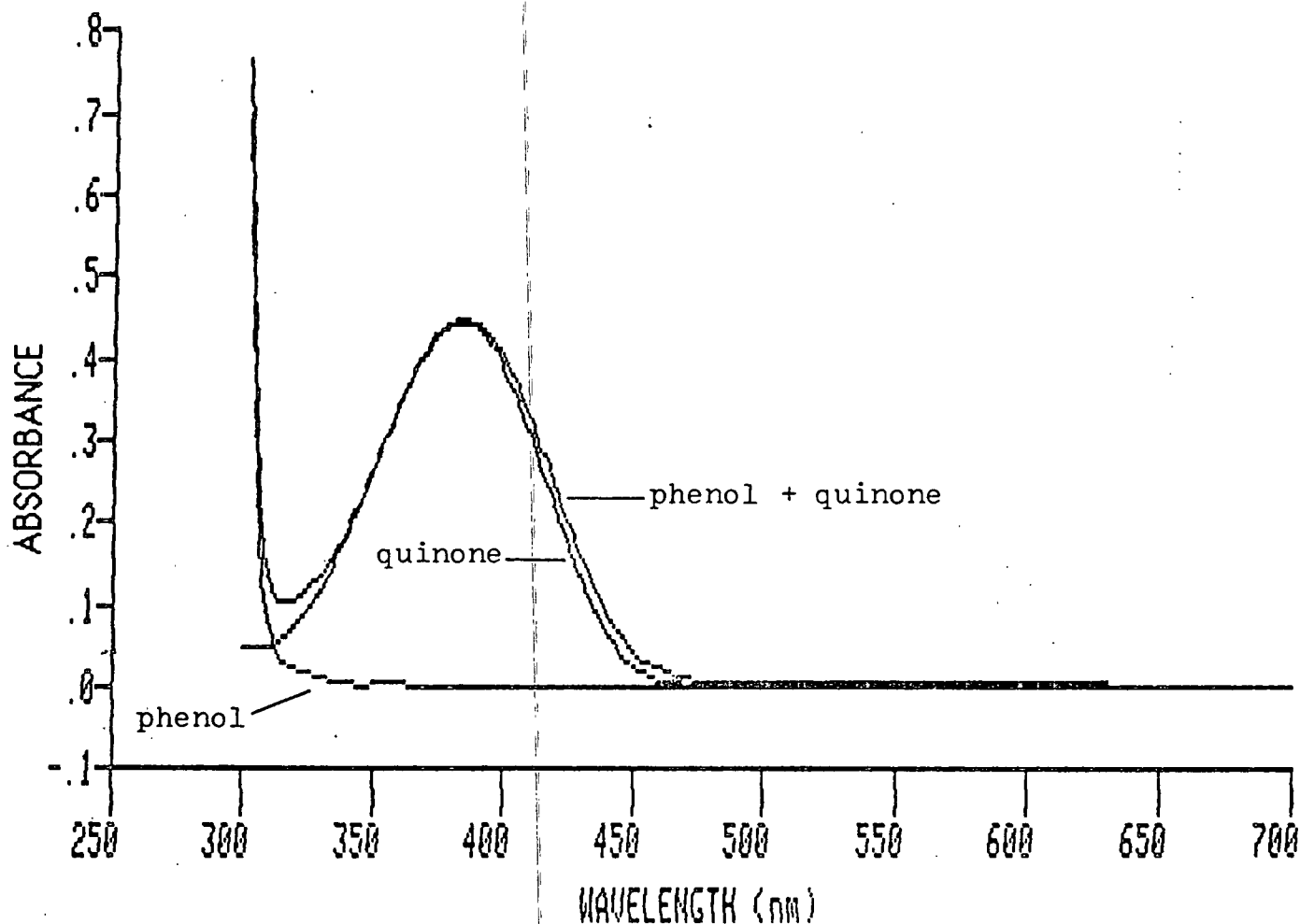


Figure 30. Visible spectra of 2-methoxy-4-methyl-phenol ( $1.77 \times 10^{-1}M$ ), 3,5-di-tert-butyl-1,2-benzoquinone ( $2.21 \times 10^{-4}M$ ), and phenol plus quinone (same concentrations); n-hexane as solvent.

Subtraction of the individual quinone and phenol spectra from the combined quinone plus phenol spectrum clearly shows this extra absorbance. The difference spectrum is given in Fig. 31. The additional absorbance band, attributed to a CTC between the phenol and the quinone, has a maximum absorbance at 428 nm and an intensity at this maximum of 0.029 absorbance units (AU). If the added quinone is completely complexed, this spectrum indicates a molar absorptivity of 131 lit/mole-cm for the complex. The slight negative absorption centered at 366 nm is probably caused by a small change in the quinone absorption band due to the CT interaction or to different solvent properties when the phenol is present.

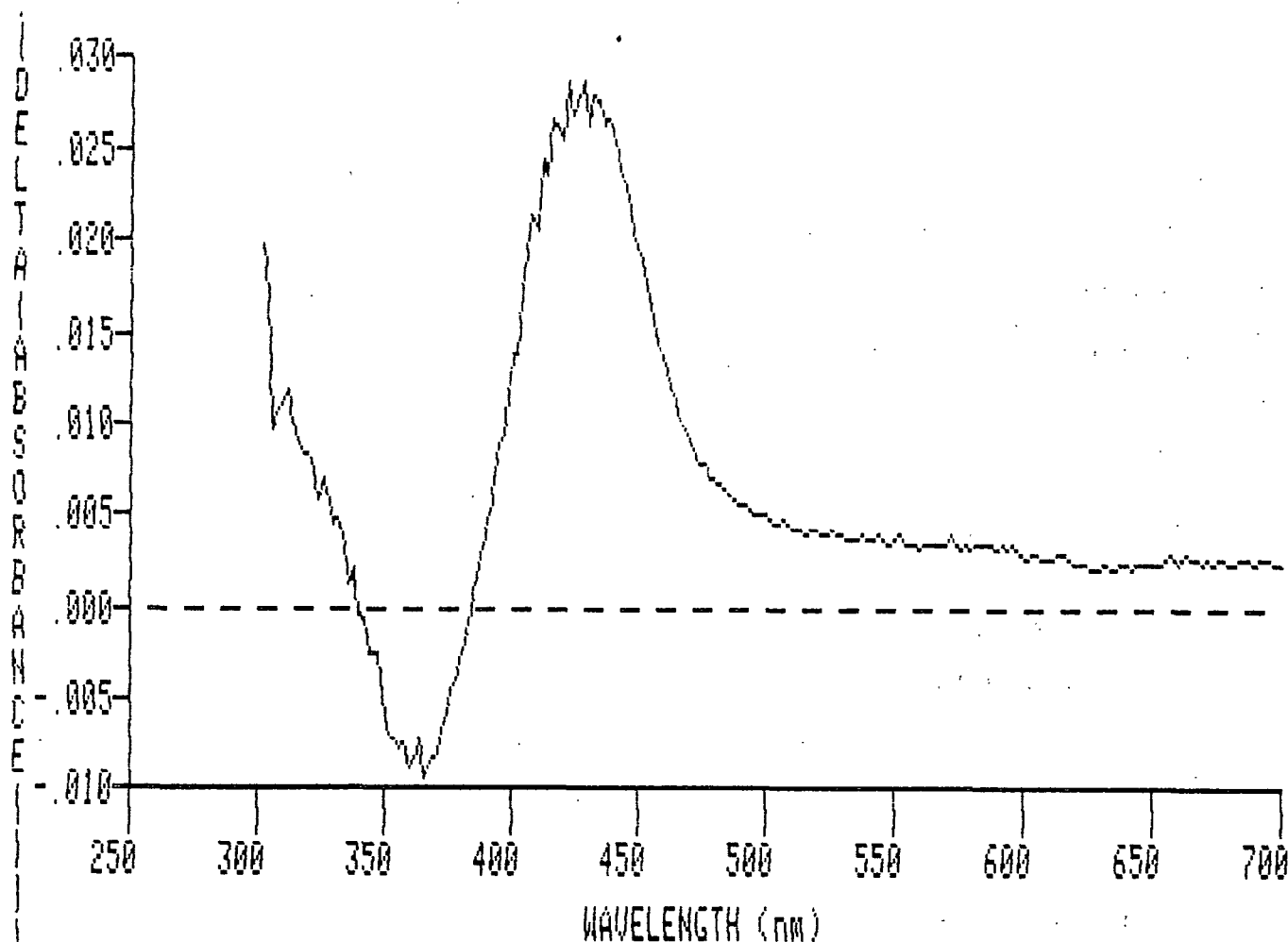


Figure 31. Difference spectrum from Fig. 30.

#### CTC Between Model Acetate and Model Quinone

One of the observations made during the study of the CTC formed between kraft lignin and 3,5-di-tert-butyl-1,2-benzoquinone was that acetylation of the phenolic groups in kraft lignin interrupted complex formation. This acetylation effect was also substantiated through the use of model compounds. Specifically, the phenol used above was acetylated to produce 1-acetoxy-2-methoxy-4-methylbenzene.

Although this model acetate and the model quinone still formed a complex, as shown in Fig. 32 and 33, it was approximately 40% less intense than the phenol complex under the same conditions (see Fig. 34). Figure 32 shows the complex was again evident as a slightly higher absorbance in the quinone plus acetate spectrum compared to the individual quinone spectrum. Subtraction of the individual quinone and acetate spectra from the combined quinone plus acetate spectrum, resulted in the difference spectrum shown in Fig. 33. The CTC band maximum occurred at 424 nm with an intensity at the maximum of 0.0175 AU. If complete complexation of the quinone is assumed, the molar absorptivity of the complex was 79 lit/mole-cm.

As shown by Fig. 33 and 34 the acetate-quinone complex is slightly blue-shifted and about 40% less intense than the comparable phenol-quinone complex. The slight blue shift in the complex absorption band is explained by the fact that acetate is a weaker electron donor than the phenol. The decrease in intensity of the absorption band is probably mostly due to the greater steric hindrance of the acetate group compared to the hydroxyl group. The results from this model compound study, therefore, substantiate the conclusions drawn from the acetylated lignin experiments.

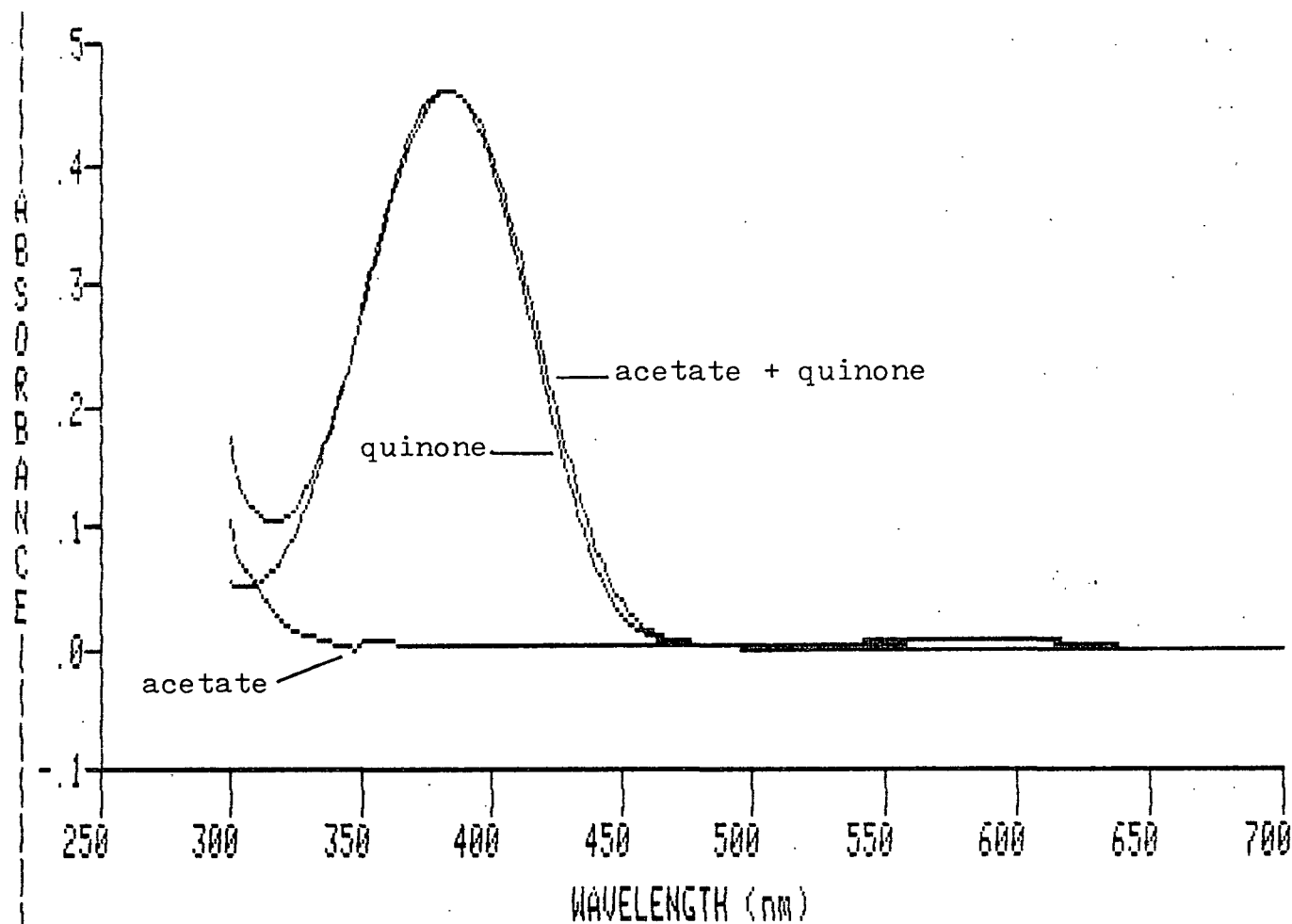


Figure 32. Visible spectra of 1-acetoxy-2-methoxy-4-methyl-benzene ( $1.77 \times 10^{-4}M$ ), 3,5-di-*tert*-butyl-1,2-benzoquinone ( $2.21 \times 10^{-4}M$ ), and acetate plus quinone (same concentrations); n-hexane as solvent.

#### Evidence for CTC's in Periodate Oxidized Kraft Lignins

The objective of the incorporation of quinones into kraft lignin was to enhance the likelihood of CT interactions. Periodate oxidation with ethylene glycol addition proved an acceptable method to accomplish this incorporation. However, the question remained, Did the incorporation of ortho-quinones result in the formation of CTC's and, if so, could they be detected? In Fig. 20 the difference spectrum between the original kraft lignin and a periodate oxidized or "quinone" lignin was presented. The increased absorbance of the periodate lignin provided evidence for the formation of quinone groups in the lignin. However,

the skewed form of this difference band also led to speculation that the band was actually a complex absorption composed of two separate components. One of these components is obviously the quinone absorption. The studies detailed below address the question of whether the second component was a CT absorption.

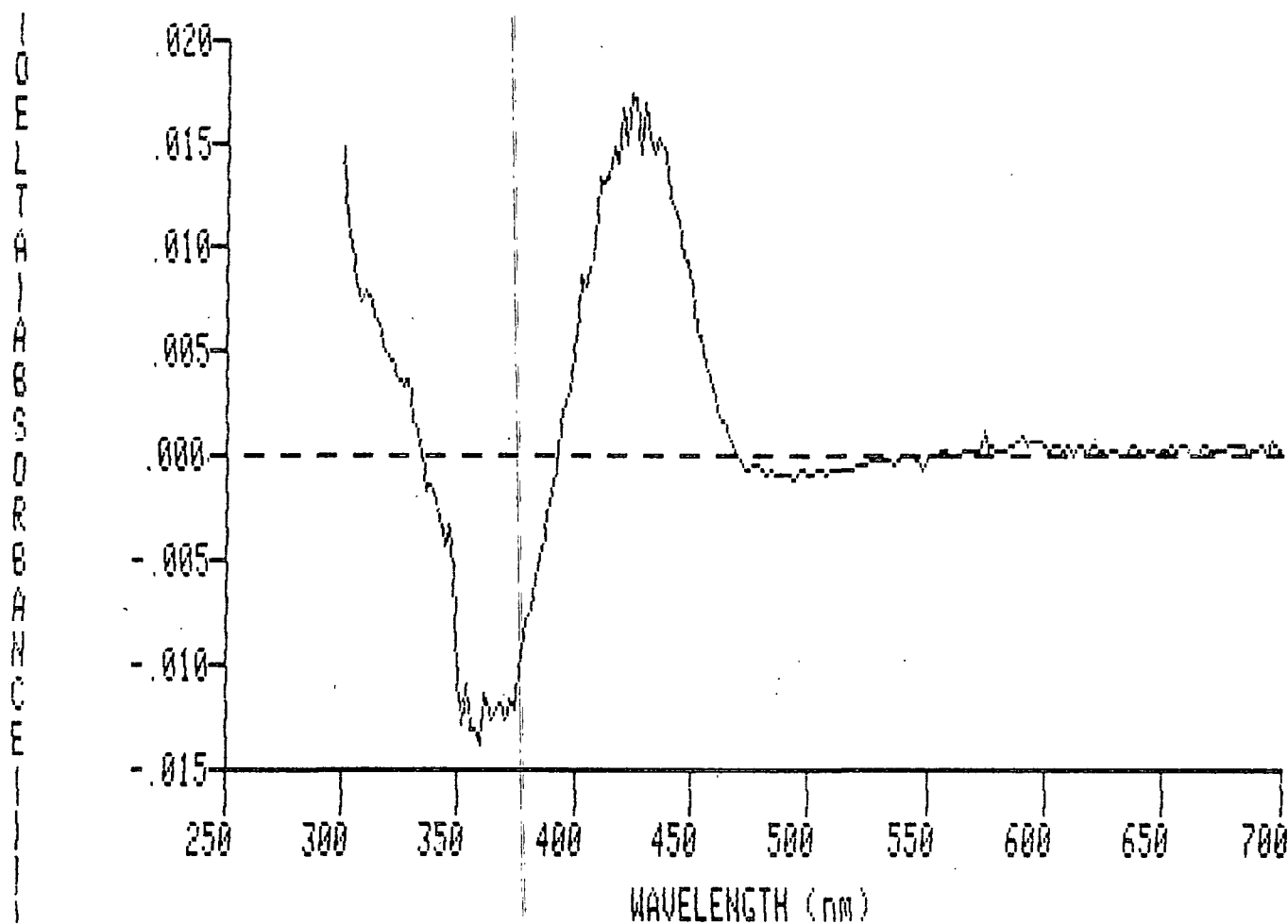


Figure 33. Difference spectrum from Fig. 32.

#### Solvent Effect

Solvent effects on CT absorption frequencies and intensities were discussed earlier. Briefly, for the  $\pi$ - $\pi$  type of complex expected in kraft lignin, the

frequency of the CT band shifts slightly toward longer wavelengths with increasing solvent polarities. Also with increasing solvent polarity, the intensity of the CT band decreases.

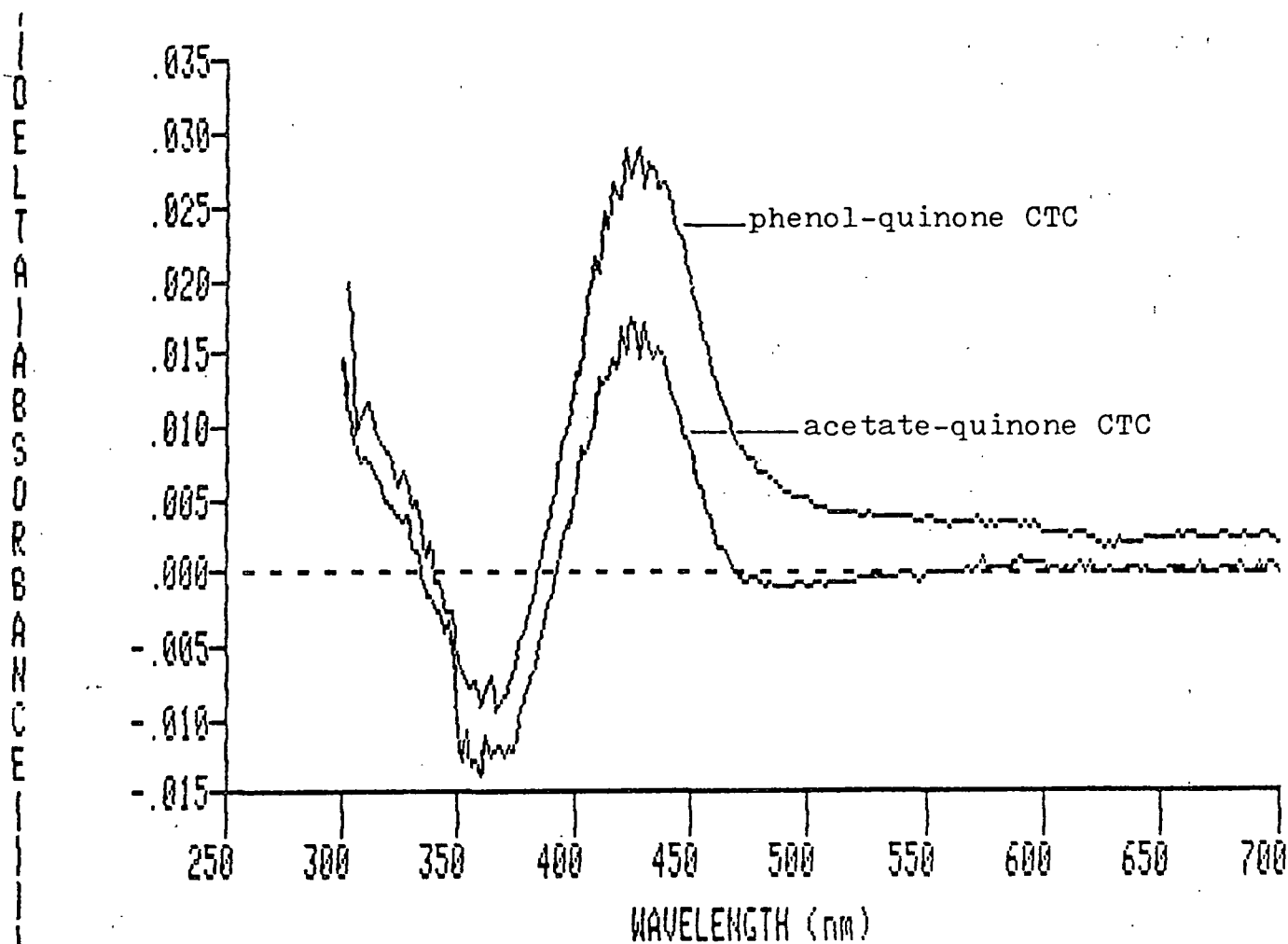


Figure 34. Comparison of difference spectra from Fig. 31 and 33.

Difference spectra between a quinone lignin and the original kraft lignin are shown in Fig. 35 for the two solvents DMF and 2-methoxyethanol. As stated previously, in terms of physical constants DMF is the more polar solvent. As shown in Fig. 35, the difference band was slightly red-shifted when DMF was used as the solvent compared to when 2-methoxyethanol was employed. The absorption maximum occurred at 434 nm in DMF and at 430 nm in 2-methoxyethanol. There was

a more substantial difference in the intensity of the band in the two solvents. At the maximum, the absorbance was 25% more intense in 2-methoxyethanol than in DMF (0.302 vs. 0.242 AU). This solvent behavior was the opposite from that shown for the model quinone-kraft lignin CTC in Fig. 29.

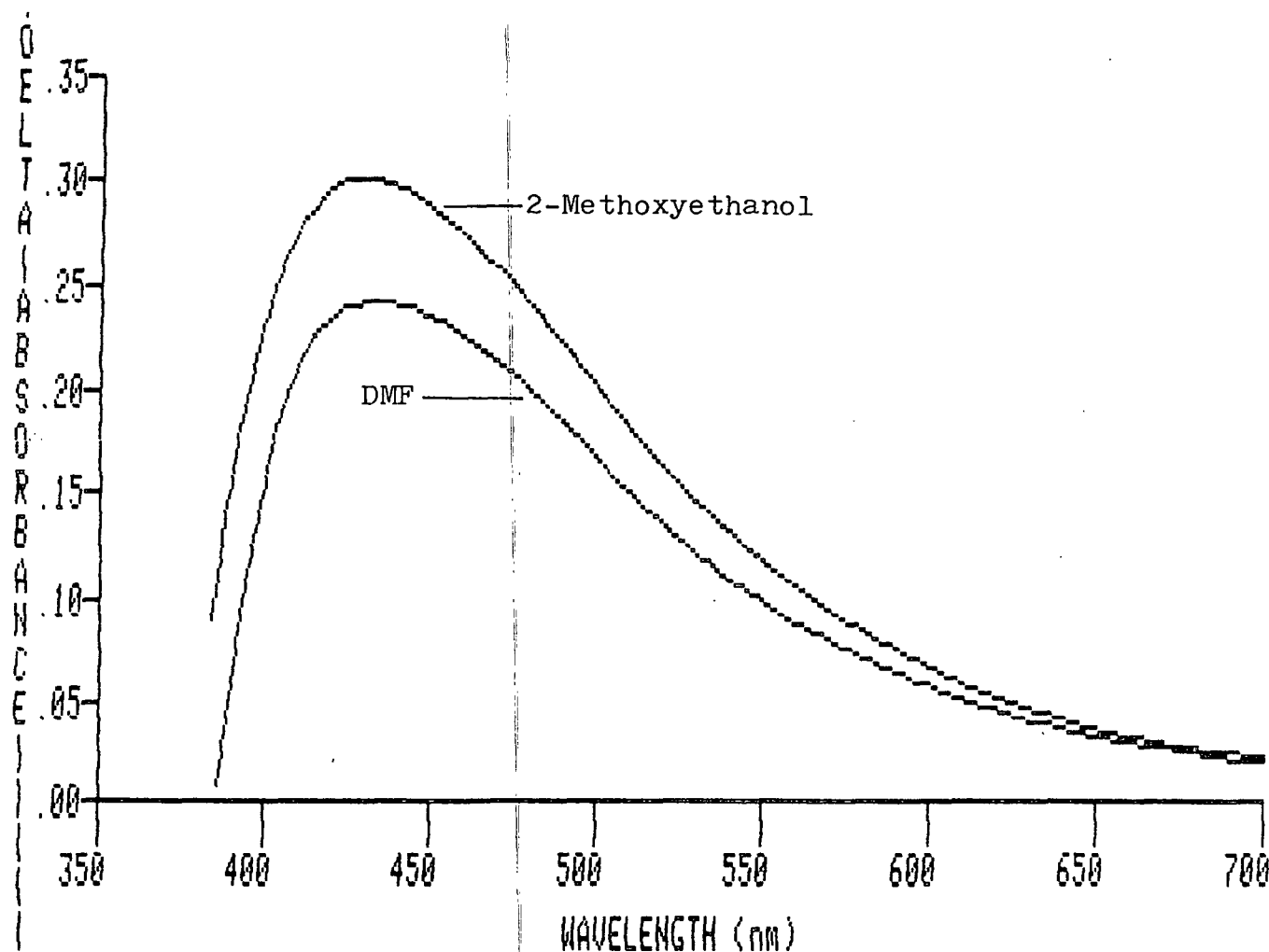


Figure 35. Difference spectra between quinone (periodate oxidized 40 sec, see Table 13) and original kraft lignins; concentrations of subtracted lignins were 7.5 mg/25 mL of solvent.

The origin of the increased intensity of the band in 2-methoxyethanol was investigated by examining the solvent effect on the spectra of the individual quinone and original lignins. Visible spectra of these lignins in the two solvents are given in Fig. 36 and 37, respectively.



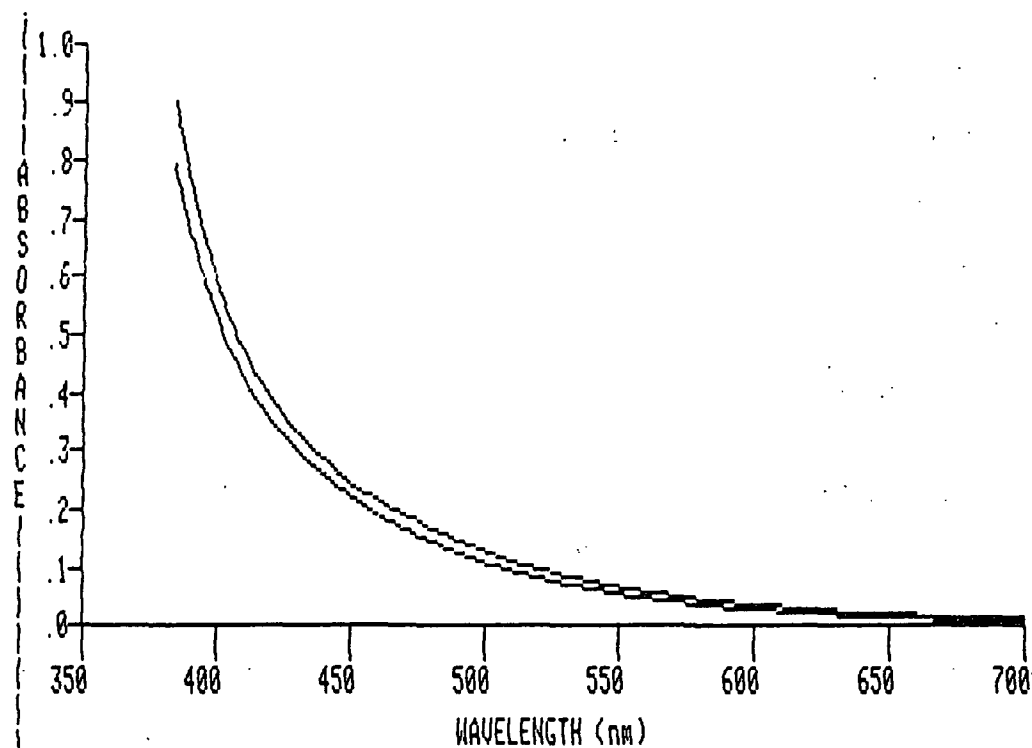


Figure 36. Visible spectra of original kraft lignin in DMF (top curve) and 2-methoxyethanol (bottom curve).

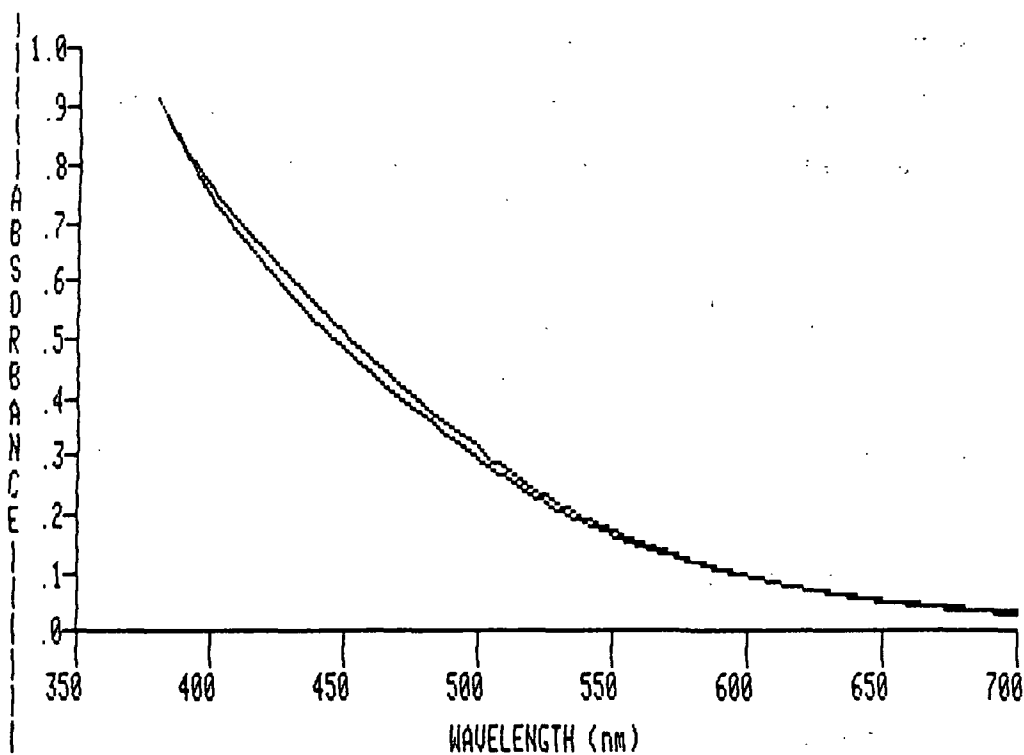


Figure 37. Visible spectra of quinone lignin in DMF (bottom curve) and 2-methoxyethanol (top curve).

The spectra of the original lignin (Fig. 36) show that the lignin absorbed more intensely in DMF. This result was consistent with the earlier findings (Fig. 29). However, the quinone lignin (Fig. 37) demonstrated the opposite solvent behavior, absorbing more intensely in 2-methoxyethanol. In order to explain this behavior, further details concerning the periodate oxidized quinone lignin need to be provided.

Fully reacted periodate lignins are noted for their insolubility in organic solvents.<sup>106</sup> The insolubility is thought to result from crosslinking of the introduced ortho-quinones via Diels-Alder type condensations. In the present study, lignin insolubility problems were encountered when the oxidation was quenched with lead nitrate. Details are provided in Appendix II. Solubility problems with the quinone lignins discussed here were minimized by the use of short reaction times, cold temperatures, and rapid quenching of the oxidation with ethylene glycol. However, the quinone lignins were not as soluble as the original lignins, indicating some crosslinking had still occurred. Furthermore, DMF was observed to be a better solvent than 2-methoxyethanol for the quinone lignins.

The more effective solvating ability of DMF explains the results shown in Fig. 37. DMF was evidently also more effective at solvating and therefore at dissociating the CTC's present in the quinone lignin. Consequently, the quinone lignin absorbed more intensely in the 2-methoxyethanol. If correct, this interpretation implies the complexes in the quinone lignin were intramolecular ones.

Evidence consistent with the above interpretation was obtained from the solvatochromic behavior of the model ortho-quinone, 3,5-di-tert-butyl-1,2-benzoquinone. ortho-Benzoquinones possess two types of absorption bands in the

visible region of the spectrum: relatively intense  $\pi-\pi^*$  bands close to 400 nm ( $\epsilon \approx 1000$ ) and weak, longer wavelength maxima due to forbidden  $n-\pi^*$  transitions near 560 nm ( $\epsilon \approx 40$ ).<sup>107,108</sup> These two types of absorption bands exhibit opposite solvatochromic behavior. The  $\pi-\pi^*$  absorption bands of carbonyls undergo bathochromic (red) shifts with increasing solvent polarity, whereas  $n-\pi^*$  absorption bands undergo hypsochromic (blue) shifts with increasing solvent polarity.<sup>33</sup>

The solvatochromic behavior of 3,5-di-tert-butyl-1,2-benzoquinone was consistent with the literature findings. Spectra of this quinone in the solvents DMF, 2-methoxyethanol, and n-hexane are shown in Fig. 38. Data for the frequencies and molar absorptivities of the absorption band maxima are given in Table 16. The position of the absorption bands did not change appreciably in DMF or 2-methoxyethanol. However, the intensities of the absorption bands changed considerably in going from DMF to 2-methoxyethanol.

Significantly the intensity of the model quinone  $\pi-\pi^*$  absorption band was more intense in DMF than it was in 2-methoxyethanol. However, the spectra in Fig. 37 reveal that the quinone lignin absorbs less strongly in DMF, opposite from the model quinone behavior. This difference can be explained if a CT band was present in the quinone lignin spectra, as previously suggested. The absorbance of the quinone lignin decreases in DMF due to the decreased intensity of the CT band in this solvent.

#### Pressure Effect

As discussed earlier, for weak CTC's increased external pressures result in shifts of the CT band to longer wavelengths. The effect is similar to that of increasing the solvent polarity. Additionally, increased external pressures

result in increased CT band intensities. An example of this behavior is given by the work of Stephens and Drickamer,<sup>60</sup> who investigated the CT absorption band of crystalline quinhydrone. This CT band had a maximum at 559 nm at atmospheric pressure, which shifted to 575 nm at 5000 atmospheres, and to 592 nm at 10,000 atmospheres of pressure. These shifts were accompanied by an increase in the intensity of the absorption, with little or no broadening of the absorption band.

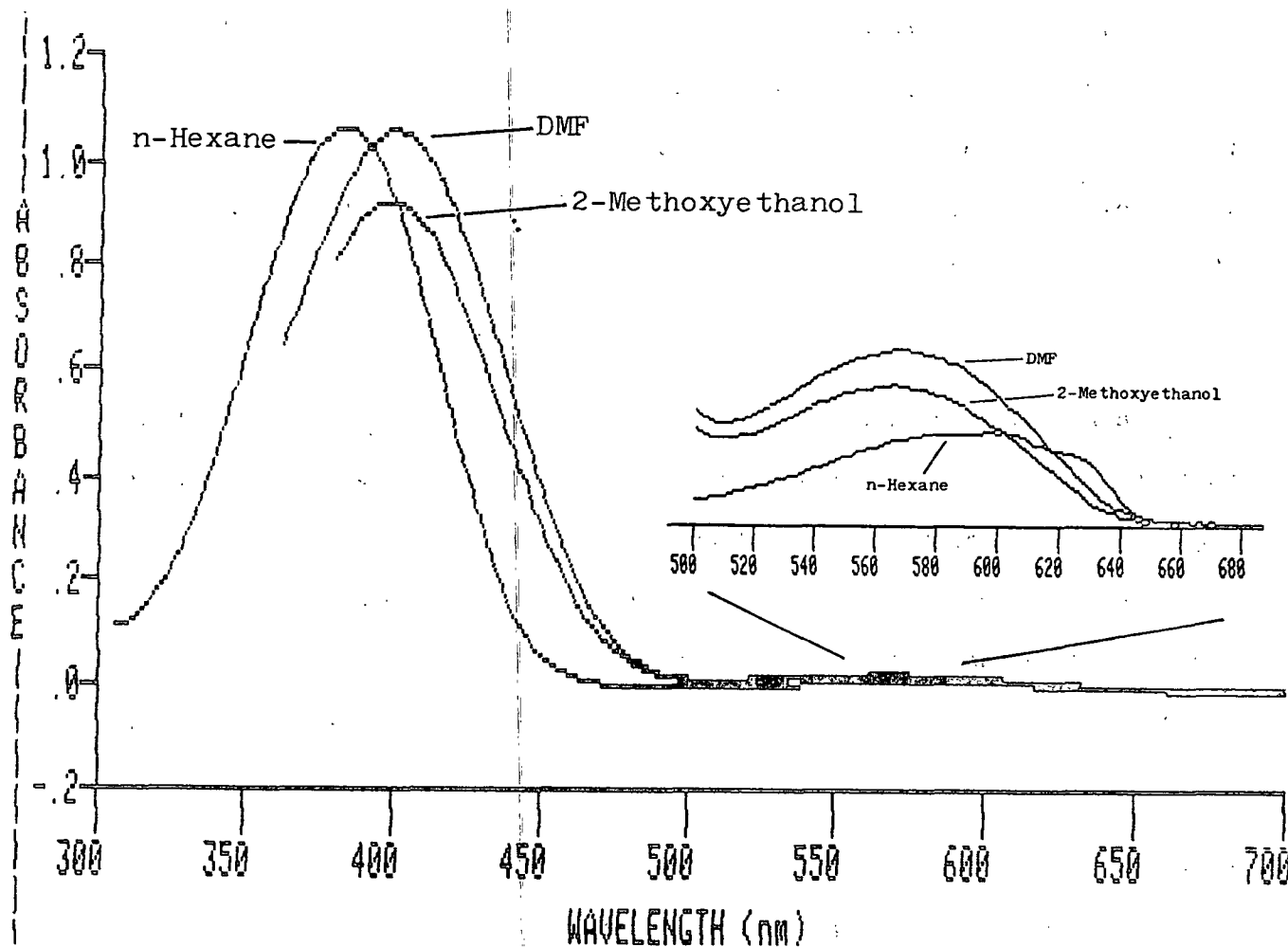


Figure 38. Absorption spectra for 3,5-di-tert-butyl-1,2-benzoquinone in the solvents indicated ( $5.00 \times 10^{-4}M$ ).

Table 16. Solvatochromic behavior of 3,5-di-tert-butyl-1,2-benzoquinone.

Solvent	$\pi-\pi^*$		$n-\pi^*$	
	$\lambda$	$\epsilon$	$\lambda$	$\epsilon$
DMF	400	2117	568	58.2
2-methoxy-ethanol	398	1845	566	46.8
n-hexane	382	2145	590	31.4

In the present study, the original, unmodified kraft lignin and several quinone lignins were investigated by high pressure spectroscopy. The quinone lignins were reduced with sodium borohydride, hydrogenated with diimide, and treated to remove metal ions prior to periodate oxidation. The pretreatments were performed in an attempt to isolate the CT interaction. Spectra were recorded in two solvents, DMF and 2-methoxyethanol, and up to pressures of 360 MPa. In a typical experimental run, lignin spectra were recorded at 0.1 MPa (atmospheric pressure), several points at higher pressures, and once again at 0.1 MPa. In all cases, the spectra returned to their original values; no irreversible pressure effects were observed.

Figures 39-42 show spectra recorded of the original and quinone lignins at 0.1 MPa and 300 (or 360) MPa, in the two solvents. Spectra were also recorded at other pressure intervals (50, 100, 150, 200 MPa), but are not shown for reasons of clarity. In general, these intermediate pressure spectra fell between the initial and high pressure ones in order of the applied pressure, except where experimental difficulties (pressure leaks) distorted the data. The high pressure spectra in Fig. 39-42 are uncorrected for solvent compression effects which would act to decrease the solution volume or increase the concentration. The magnitude of this solvent compression was estimated to be approximately 6.5-7.0% at the upper pressure ranges (see Appendix III).

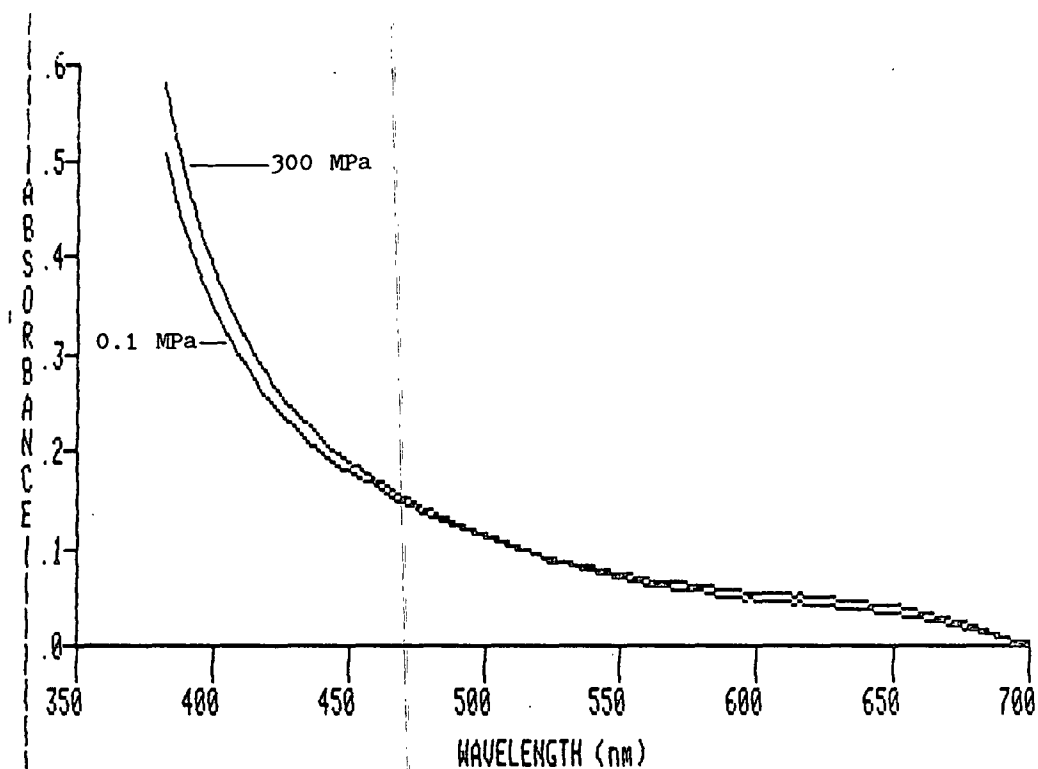


Figure 39. Visible absorption spectra for original kraft lignin in 2-methoxyethanol.

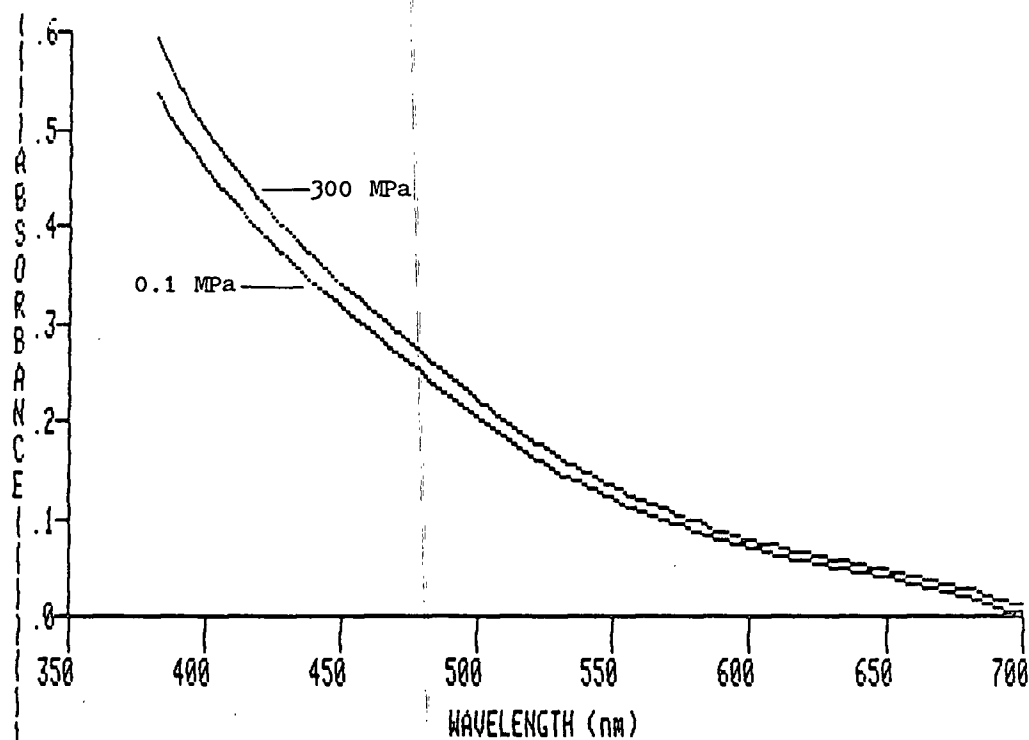


Figure 40. Visible absorption spectra for quinone lignin (40 sec periodate oxidation) in 2-methoxyethanol.

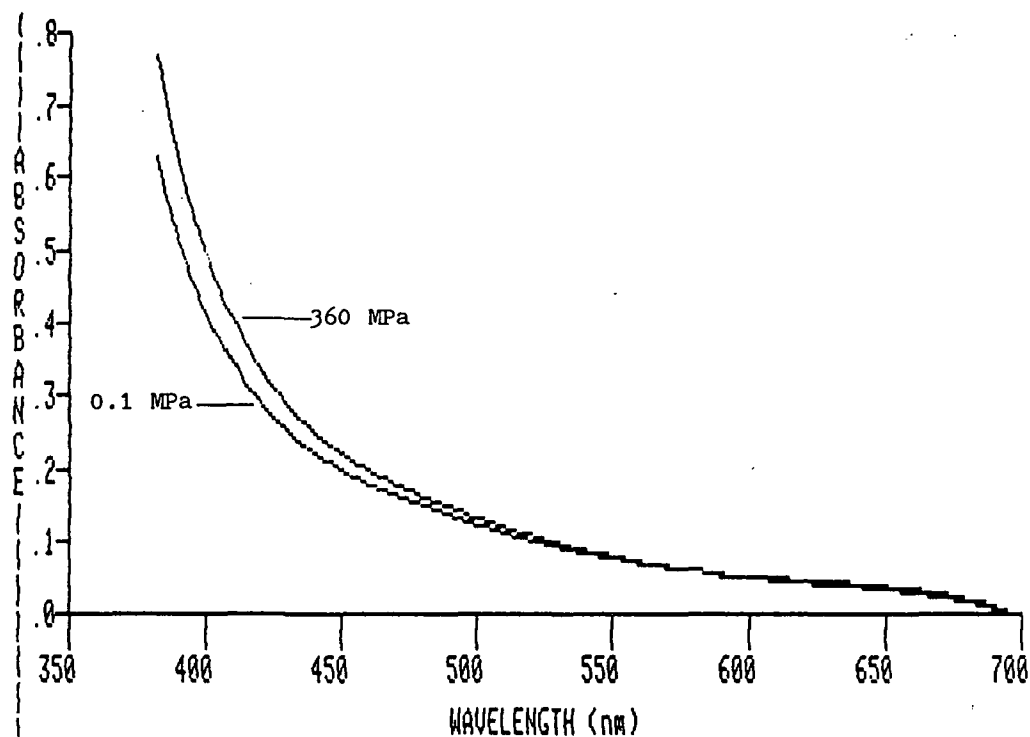


Figure 41. Visible absorption spectra for original kraft lignin in DMF.

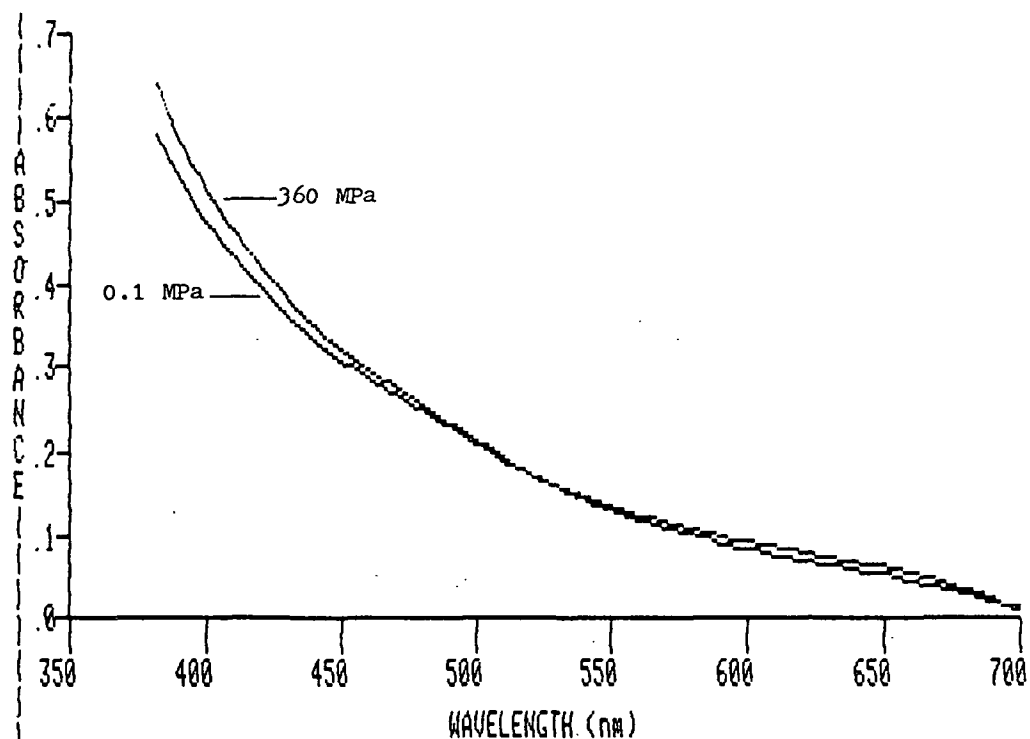


Figure 42. Visible absorption spectra for quinone lignin (same as Fig. 40) in DMF.

The crossovers between the spectra in Fig. 39 and 42 may be explained by the effect of solvent on the various absorption bands which compose the spectra, remembering that with increasing pressure the solvents act as if they were more polar. The decreased intensity of the original kraft lignin in 2-methoxyethanol at 300 MPa vs. 0.1 MPa (Fig. 39) in the long wavelength region can be explained by a shift of the quinone  $n-\pi^*$  band to shorter wavelengths. In Fig. 42, the crossover can be explained by the decreased intensity of the CT absorption band at higher pressures in DMF (see below).

Difference spectra were once again calculated between the quinone and original lignins in order to observe the changes in the spectra clearly. These spectra are presented in Fig. 43 and 44 for 2-methoxyethanol and DMF. In each figure, the difference spectrum at high pressure is compared to the difference spectrum at atmospheric pressure. For the difference spectra calculated at high pressure, the effect of solvent compression is the same for both of the subtracted lignins and, thus, cancels out.

In Fig. 43, the effect of high pressure (300 MPa) was to cause a slight red shift of the absorption maximum, and a noticeable broadening of the long wavelength side of the absorption. In addition, there was an approximately 8.4% increase in the intensity of the absorption maximum over that at atmospheric pressure. This type of behavior, a red shift and increase in intensity, is the behavior expected for a weak CT band under pressure. These observations, therefore, were consistent with the interpretation that the difference band between the quinone and original lignins contained a CT component.

In Fig. 44, the difference band is shown at high pressure (360 MPa) in DMF. In this solvent, application of high pressure caused a more significant red



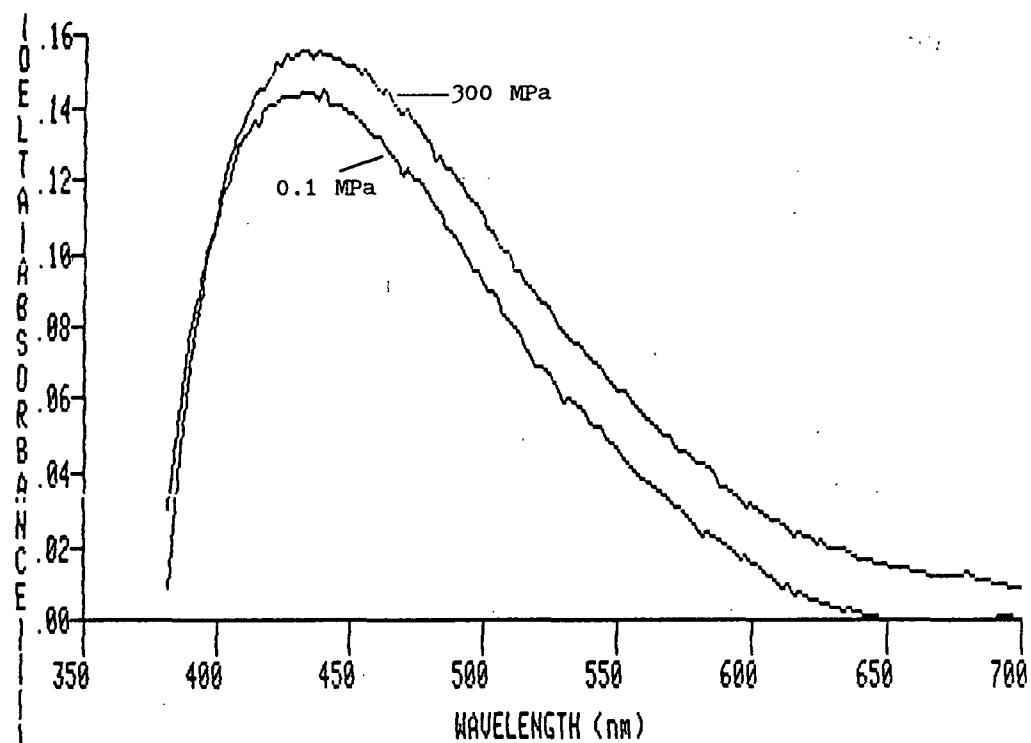


Figure 43. Quinone lignin minus original lignin in 2-methoxyethanol.

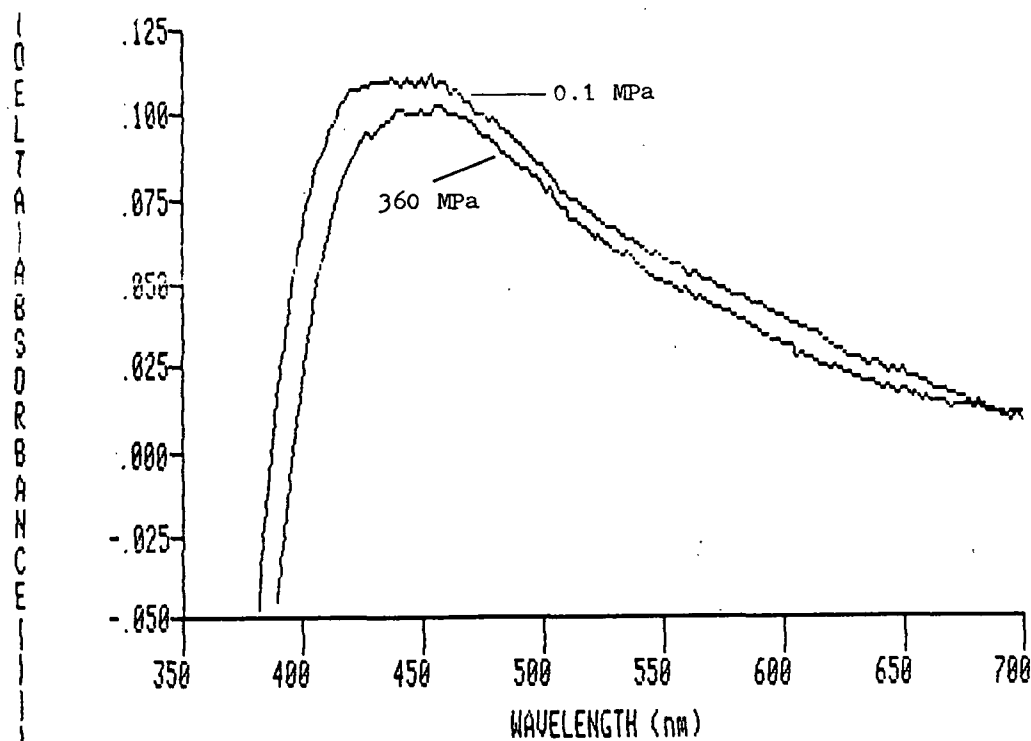


Figure 44. Quinone lignin minus original lignin in DMF.

shift of the absorption maximum (approximately 10 nm), but there was actually a slight decrease in the intensity of the difference band. The red shift of the absorption band is again consistent with the interpretation that this difference band contained a CT component. The decrease in intensity of the band is not consistent but fits with the earlier solvent study which demonstrated that DMF was effective in dissociating CTC's in the quinone lignin. Figures 41 and 42 indeed revealed that under high pressure the intensity of the original lignin in DMF increased to a greater extent than did the intensity of the quinone lignin. Apparently, under high pressure the dissociative effect of DMF on the CTC's in the quinone lignin was increased. This effect naturally results in the formation of fewer complexes and explains the decreased intensity of the difference band in Fig. 44.

The vast majority of high pressure studies on CTC's have been conducted with discrete model compounds. On the other hand, the lignin systems studied here are exceedingly complex. While not totally conclusive, the results from these high pressure studies favored the presence of CTC's in the quinone lignin.

#### Derivatization Experiments

Evidence was also sought from derivatizations of the quinone lignin that the difference band between the quinone and original lignins was a complex absorption composed of both a quinone and a CT band. The derivatizations which were employed included acetylation and reductive acetylation. Both acetylation techniques reduced the visible absorbance of the quinone lignin, as shown in Fig. 45. Reductive acetylation proved to be the more effective technique in reducing this absorbance. Obviously, both derivatizations removed some chromophore(s) from the lignin, resulting in the decreased absorbance. The chromophores which were removed are considered below.

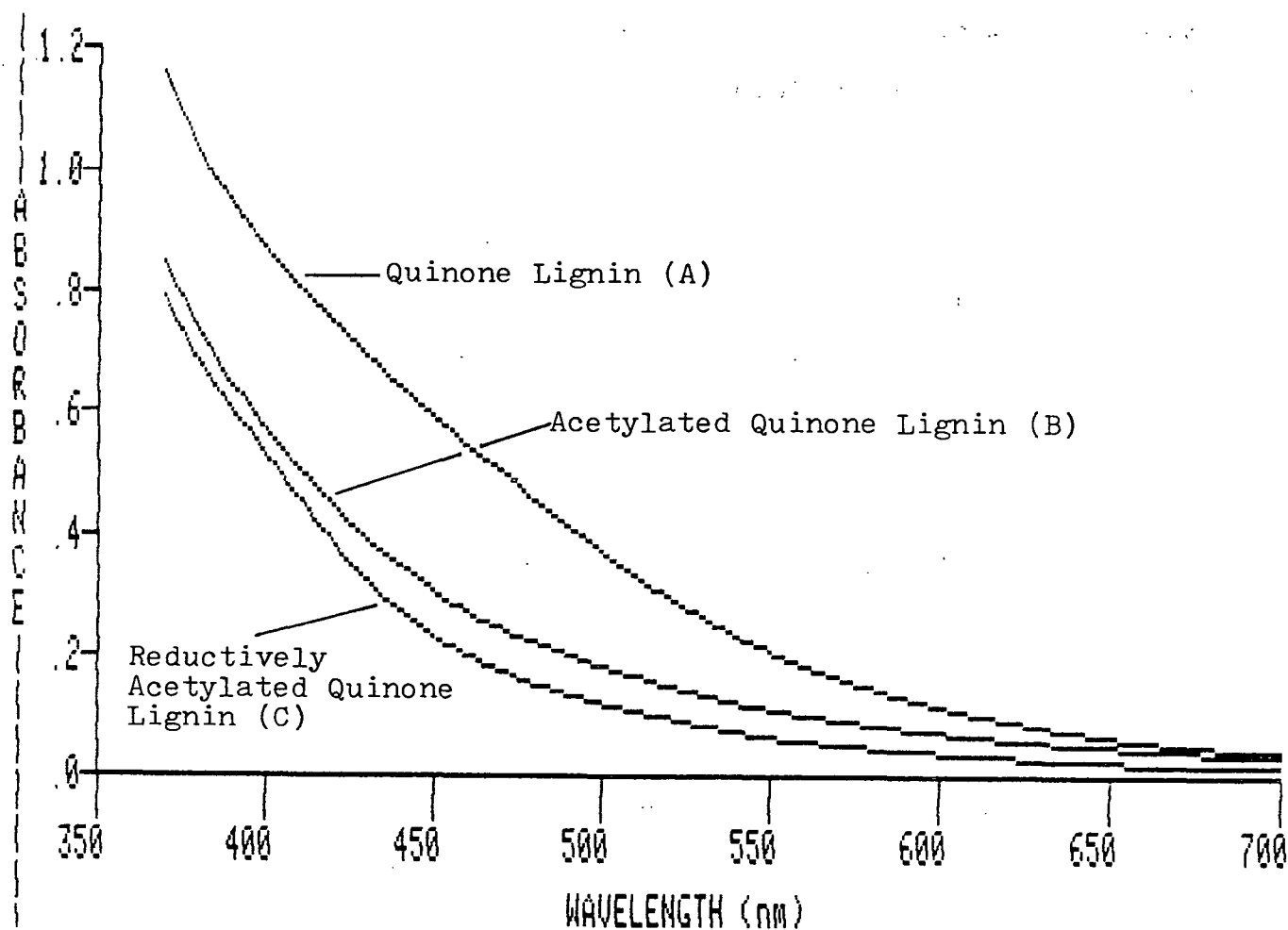


Figure 45. Visible absorption spectra of quinone lignin (pretreated; 40 sec periodate oxidized), acetylated quinone lignin, and reductively acetylated quinone lignin; concentration, 7.6 mg/25 mL DMF.

Acetylation of the quinone lignin was conducted in the usual manner, employing pyridine and acetic anhydride. During acetylation of the lignin, free phenolic and hydroxyl groups were derivatized to form acetates. This modification of the phenolics in lignin has a profound effect on the ability of CTC's to form. For the case of the CTC between kraft lignin and the model quinone, 3,5-di-tert-butyl-1,2-benzoquinone, acetylation of the lignin completely eliminated the formation of this CTC. Likewise, acetylation was expected to have a similar effect in disrupting CTC's as visible chromophores in the quinone lignin. Acetylation

should have no other effect on the visible absorbance of the quinone lignin, since the phenolic absorption band is in the ultraviolet (280 nm) region of the spectrum.

Reductive acetylation refers to the addition of zinc dust to the acetylation reaction mixture. Under these conditions, quinone groups are reduced to catechols or hydroquinones and then acetylated.<sup>22,109</sup> Without the added zinc dust, the quinones remain unchanged.<sup>109</sup> Reductive acetylation, therefore, disrupts two types of chromophores in the quinone lignin: the CTC's, as well as the quinones.

According to the above analysis, proper subtraction of the spectra in Fig. 45 should yield spectra representative of the individual quinone and CTC chromophores. These difference spectra are given in Fig. 46. The spectrum (A-C) was obtained by subtraction of the reductively acetylated quinone lignin (C) from the quinone lignin (A). Since the quinone lignin contains both quinones and CTC's as chromophores, and since in the reductively acetylated quinone lignin both chromophores were removed, the difference spectrum is composed of these two chromophores. In fact, the difference spectrum (A-C) is essentially the same as the difference spectrum between the quinone and original lignins which has been presented throughout this section (see, for example, Fig. 35).

The spectrum (A-B) was obtained by subtraction of the acetylated quinone lignin (B) from the quinone lignin (A). Since acetylation removes CTC's, this difference spectrum is a measure for CTC's in the quinone lignin. Finally, the spectrum (B-C) was obtained by subtraction of the reductively acetylated quinone lignin (C) from the acetylated quinone lignin (B). Since the acetylated quinone lignin contains quinones, whereas the reductively acetylated quinone lignin does not, this difference spectrum is a measure for the quinones in the quinone lignin.

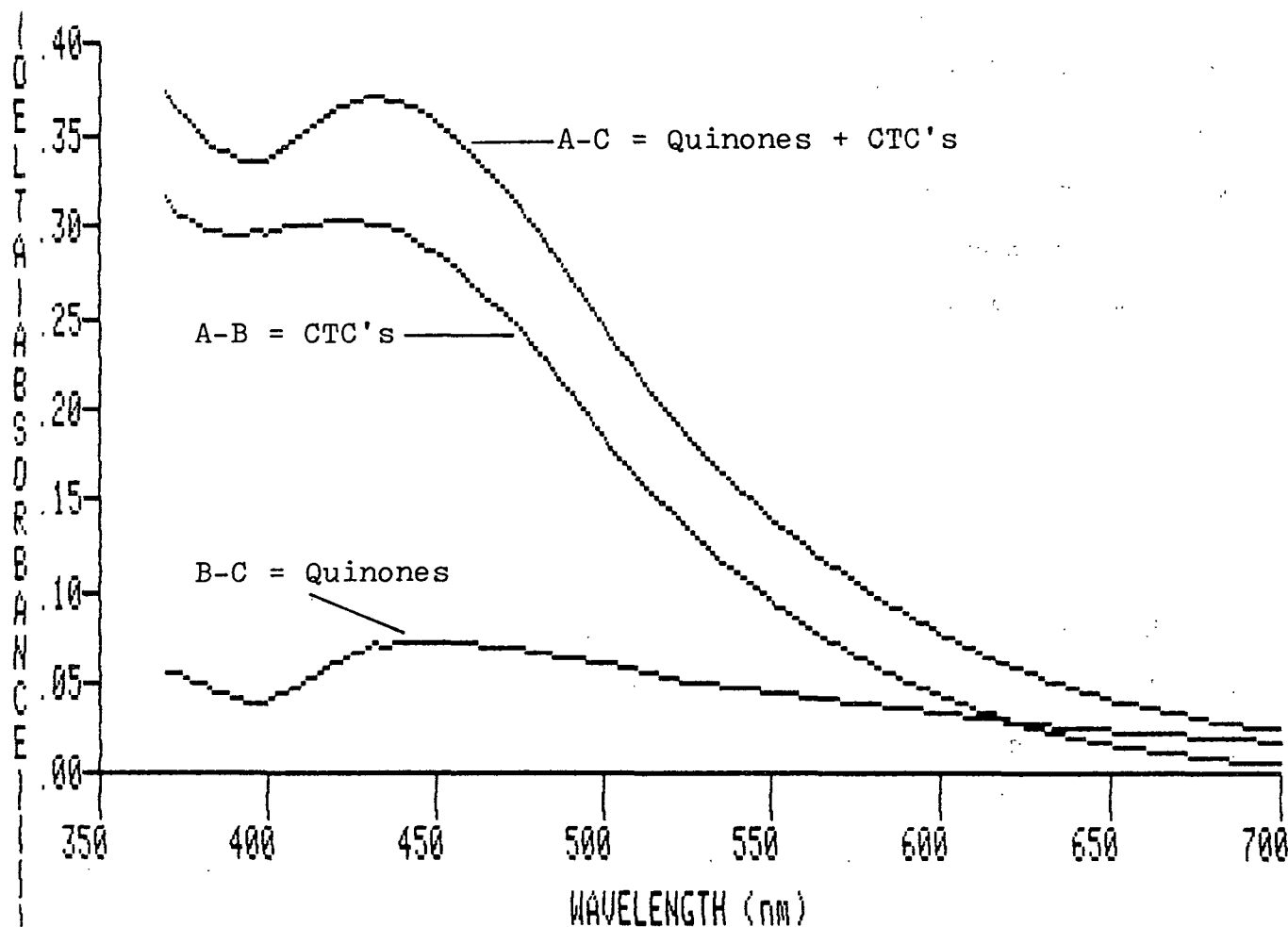


Figure 46. Difference spectra from Fig. 45.

The derivatizations, therefore, were successful in separating the additional absorbance introduced to the lignin by periodate oxidation into its two component bands: a quinone and a CT band. These spectra are only qualitative in nature, since an acetylated lignin was compared to a nonacetylated lignin. However, they did indicate the CT band occurred in the vicinity of 420-425 nm, and at a shorter wavelength than the quinone absorption band (approximately 445 nm).

The position of a CT band depends on the substituents attached to the donor and acceptor moieties of the complex and on the amount of orbital overlap between

the donor and acceptor. The effect of substituent groups was documented in the introduction. In short, substituents which increase the ionization potential of the donor (or decrease the electron affinity of the acceptor) shift the CT maximum to shorter wavelengths. The effect of orbital overlap between the donor and acceptor components has been investigated by Staab and coworkers<sup>40,42</sup> and Tashiro and coworkers,<sup>43,44</sup> using cyclophane quinhydrones. A compilation of their results is presented in Table 17. The maxima for these CT absorptions occurred throughout a wide range, from 346 to 515 nm. In view of these results, the occurrence of a phenol-quinone CT band in lignin in the vicinity of 420-425 nm is not surprising.

#### Evidence for CTC's in Kraft Lignin

The presence of CTC's in the original kraft lignin was more difficult to discern than in the quinone lignin due to their decreased concentration. The presence of CTC's in the original lignin was determined by a method where first the number of quinones in the lignin was obtained by a carbon-14 labeling technique. In this technique, the kraft lignin was acetylated twice in the normal manner and subsequently reductively acetylated using carbon-14 labeled acetic anhydride,  $(\text{CH}_3^*\text{CO})_2\text{O}$ . The preacetylation steps were necessary in order to prevent free hydroxyl groups from being acetylated during the reductive acetylation step. The reductive acetylation step therefore specifically labeled only the quinone groups in the lignin. The labeling procedure is depicted in Fig. 47.

The amount of activity introduced to the lignins was determined by liquid scintillation counting. The activity of the original kraft lignin in counts per minute (cpm) is given in Table 18. The cpm of the lignin was converted to the actual disintegrations per minute (dpm) by dividing by the efficiency of the sample. Efficiencies were determined by the internal standard method as detailed in the "Materials and Methods" section. The column titled "DPM/mg" was simply obtained by dividing the dpm by the lignin sample weight in milligrams.

Table 17. Effect of orbital overlap on CT bands in cyclophane quinhydrones.<sup>40,42-44</sup>

Complex	$\lambda_{\max}$ , nm	$\epsilon_{\max}$	Solvent
	495	1600	MeOH
	515 375	170 790	MeOH
	500(sh) 346	105 1904	Dioxane
	462	3210	Dioxane
	459	260	EtOH
	490	676	THF

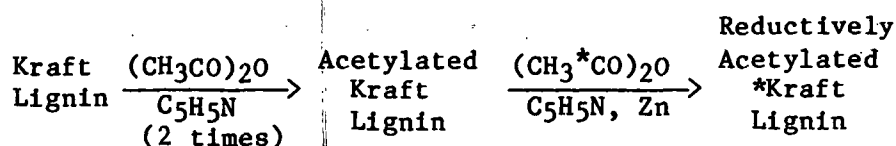


Figure 47. Carbon-14 labeling of quinones in kraft lignin.

Also given in Table 18 are values for what are termed "control lignins" or original kraft lignins which were subjected to acetylation with radioactive acetic anhydride, but without the zinc present. The control samples served to determine the activity introduced into the lignins from traces of radioactive chemicals not removed during the purification procedure, and also from any exchange of nonlabeled acetates with labeled ones.

Table 18. Activities and quinone concentrations of kraft lignins.

Lignin Type	Sample No.	CPM <sup>a</sup>	% Efficiency	DPM	DPM/mg	Net DPM/mg <sup>b</sup>	Actual DPM	mmol of *Ac <sub>2</sub> O <sup>c</sup>	Quinone Conc., %
Control	1	882	5.91	14,924	350.3	--	--	--	--
	2	942	5.90	15,966	366.2	--	--	--	--
Original Kraft Lignin	3	3466	16.28	21,290	481.7	123.45	5456	5.61	3.13
	4	3937	18.20	21,632	475.4	117.15	5330	5.48	2.97
NaBH <sub>4</sub> Reduced	5	6147	37.85	16,240	384.8	26.55	1120	1.15	0.67
	6	6113	35.12	17,406	381.7	23.45	1069	1.10	0.60
Quinone Lignin <sup>d</sup>	7	1212	3.53	34,334	725.9	367.65	17,390	17.9	10.61
	8	1807	13.76	13,132	795.9	437.65	7,221	7.42	12.61
	9	2307	6.70	34,433	812.1	453.85	19,243	19.8	13.09

<sup>a</sup>At least three separate determinations each; at 95% confidence level, values within 1% of the mean.

<sup>b</sup>Net DPM = (sample DPM) - (average control DPM).

<sup>c</sup>Values multiplied by 1000.

<sup>d</sup>Lignin was previously treated with sodium borohydride, diimide, and EDTA, then periodate oxidized 40 seconds.



Other data given in Table 18 include the net dpm values, which were calculated by subtracting the control dpm values from the desired sample dpm values. "Total DPM" is the dpm of the sample on a total weight basis. From this value and the specific activity of the radioactive acetic anhydride ( $1.62 \times 10^4$  Bq/mmol), the number of millimoles of labeled acetic anhydride incorporated in the lignin sample was calculated. This value was equal to the millimolar quantity of quinones in the sample, since each acetic anhydride molecule contained two radioactive carbons, and since there were two sites for acetylation in each quinone. Finally, the concentration of quinones in each sample was calculated by dividing the molar quantity of quinones by the molar quantity of acetylated lignin in that sample. Unit molecular weights for the acetylated lignins were calculated as shown in Appendix IV.

Data are also given in Table 18 for a sodium borohydride-reduced kraft lignin and for a periodate-oxidized lignin. The values for these lignins lend credibility to the method, since the quinone concentrations which were determined followed the expected trends. Borohydride reduction reduces quinones to catechols, thereby removing quinones from the lignin. The value determined for the quinone concentration of the reduced lignins reflects this removal. The quinone concentration would have probably been even lower except for the time lag between reduction of the lignin and the measurement for the quinones. The catechol groups are not stable and readily reoxidize. Also as expected, the increased quinone content of the periodate-oxidized lignin (average value of 12.1%) reflects the incorporation of quinones caused by the oxidation.

The absorbance due to the quinones in the original kraft lignin was determined from the difference spectrum between its acetylated and reductively acetylated derivatives. Direct comparison of the lignins obtained by running the

acetylated lignin in the spectrophotometer sample cell vs. the reductively acetylated lignin in the reference cell produced the spectrum given in Fig. 48. This direct method of obtaining the difference spectrum provided a sensitive measure of the location of the maximum difference between the two lignin spectra. In 2-methoxyethanol, the maximum occurred at 431 nm. However, the magnitude of the difference in Fig. 48 is subject to the errors which are introduced by the weighing out of the samples and by the assumption of their similar molecular weights. Therefore, the two spectra were subtracted after correction to the same concentration at 280 nm. This difference spectrum is shown in Fig. 49.

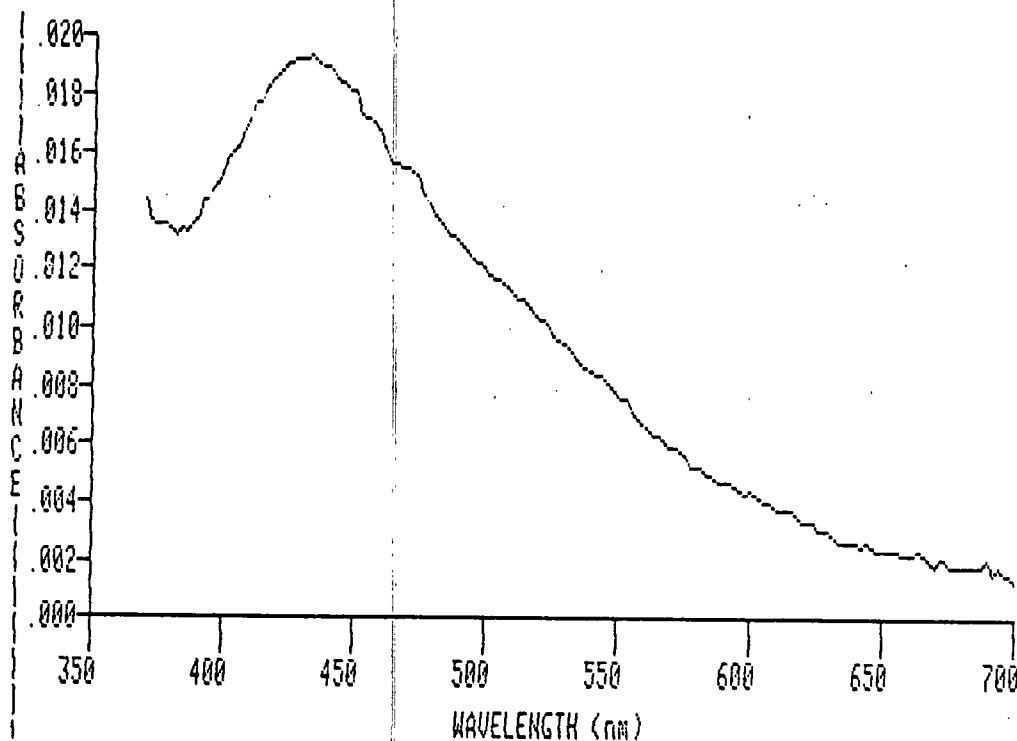


Figure 48. Visible absorption spectrum; acetylated kraft lignin (sample cell) vs. reductively acetylated kraft lignin (reference cell); concentration, 7.6 mg/25 mL 2-methoxyethanol.

At 431 nm, the difference in absorbance between the two lignins amounted to 0.026 AU. The estimated error in the magnitude of this difference was only

approximately 3%. The error is based on the difference in phenolic content between the acetylated and reductively acetylated lignins (about 5%). However, about one-third of this 5% reduction is regained from the corresponding quinone absorption at 280 nm (based on measurements of the reduced form of the quinone, 3,5-di-tert-butyl-1,2-benzoquinone).

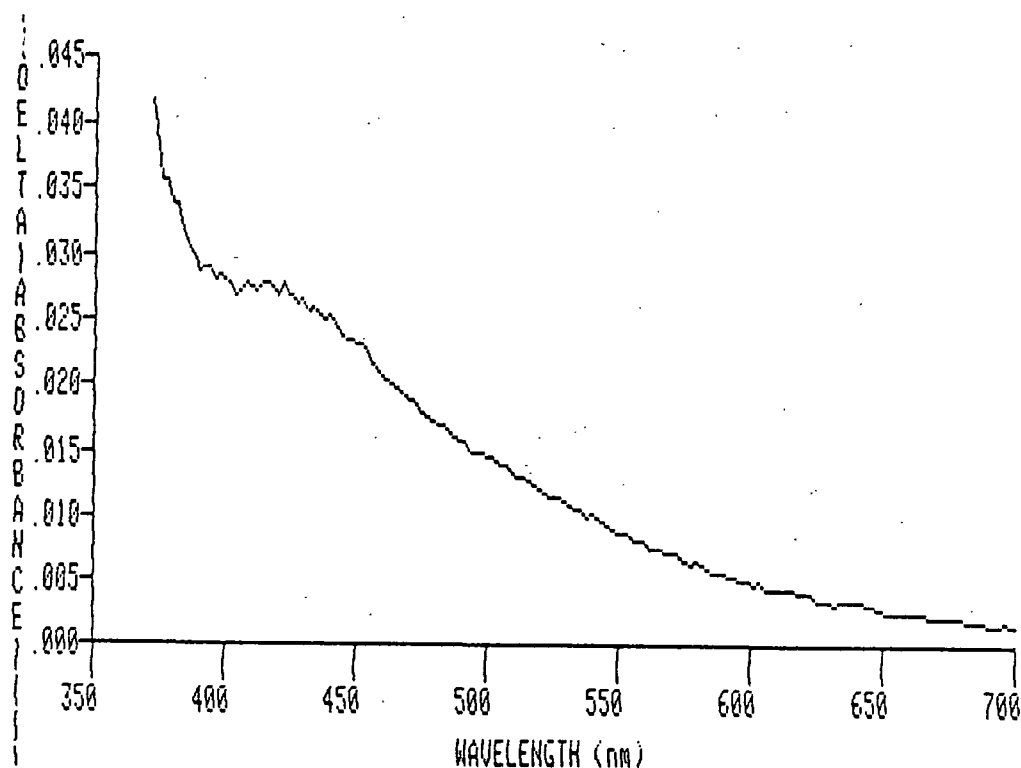


Figure 49. Acetylated kraft lignin minus reductively acetylated kraft lignin after correction to same 280 nm absorbance values.

From the values obtained for the quinone concentration and absorbance and utilizing Beer's law, the molar absorptivity of the quinones in kraft lignin was calculated. This calculation (see Appendix V) yielded a value of 528 lit/mol-cm in 2-methoxyethanol. Although this molar absorptivity was significantly lower than the average molar absorptivity of the  $\pi-\pi^*$  band (1479 lit/mol-cm) for ten ortho-benzoquinones found by Teuber and Staiger,<sup>110</sup> it agreed well with other

literature data. Imsgard, et al.<sup>12</sup> reported molar absorptivities of 600 and 741 lit/mol-cm for the  $\pi-\pi^*$  band of the ortho-quinones synthesized from the lignin model compounds acetoguaiacone and isoeugenol, respectively. Also of interest is the reported 430-435 nm absorption band for the dimer of ortho-benzoquinone, which has a molar absorptivity of 130 lit/mol-cm.<sup>111</sup>

Having determined values for the molar absorptivity and the concentration of the quinones in the original kraft lignin, the amount of absorbance at the quinone maximum due to these quinones was calculated. Spectra resulting from the sodium borohydride reduction of the lignin, which removed quinones and therefore CTC's also, were used to calculate the total absorbance due to both the quinones and CTC's. A difference spectrum resulting from the subtraction of a reduced lignin from the original kraft lignin appears in Fig. 50. At the quinone maximum (431 nm) the total drop in absorbance caused by the reduction amounted to 0.091 AU (average of two determinations). The proportion of the absorbance drop resulting from the reduction of the quinones, shown in Fig. 50, was calculated to be 0.0284 AU, or 31.2% of the total absorbance decrease.

The proportion of the absorbance which could not be accounted for by the quinones was then assigned to CTC's. The quinones apparently participated in these CTC's as the acceptor species. The results meant the major portion (two-thirds) of the absorbance at 431 nm was in fact due to CTC's. If every quinone is assumed to be participating in a CTC, the molar absorptivity of the complex can be calculated to be 1163 lit/mol-cm. This assumption is reasonable, considering the relatively low quinone and high phenol concentrations in the original kraft lignin. The molar absorptivity is in the range of other molar absorptivities determined for phenol-quinone complexes (see Tables 3 and 17). The calculations used for obtaining the percent absorbances due to the quinones

and CTC's, and for obtaining the molar absorptivity of the CTC, are given in Appendix VI.

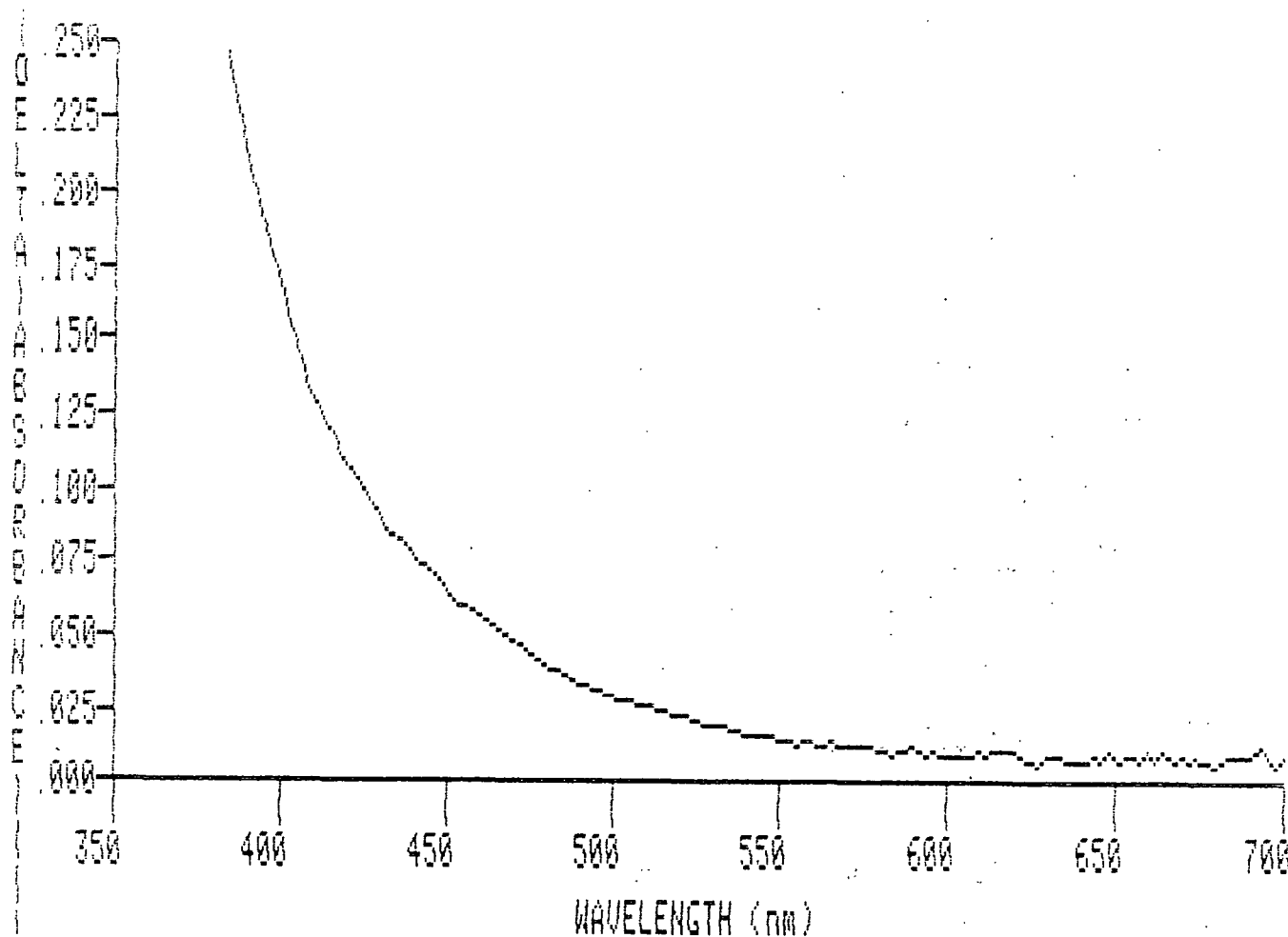


Figure 50. Original kraft lignin minus sodium borohydride reduced kraft lignin; 2-methoxyethanol as solvent.

For comparison, similar calculations were performed for the periodate-oxidized kraft lignin given in Table 18. Again, the absorbance from the quinones in this oxidized lignin was determined from spectra of the acetylated and reductively acetylated oxidized lignin. The difference spectrum between these acetylated lignins is shown in Fig. 51. The spectrum had a maximum absorbance at 447 nm, at which an intensity of 0.072 AU was measured. From this absorbance

and the concentration of quinones in the lignin (12.1%), the molar absorptivity of the quinones was calculated to be 435 lit/mol-cm.

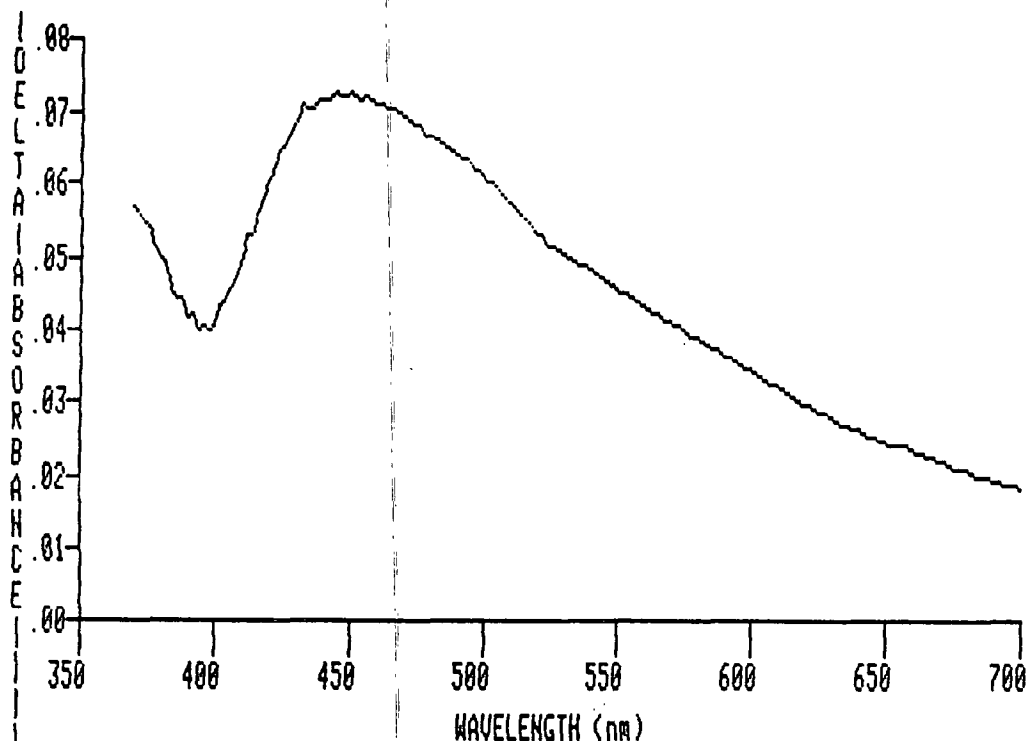


Figure 51. Acetylated quinone lignin (pretreated; 40 sec periodate oxidation) minus reductively acetylated quinone lignin; DMF as solvent.

Sodium borohydride reduction of the periodate oxidized lignin produced the absorbance drop shown by the difference spectrum in Fig. 52. The maximum drop in absorbance (0.0989 AU) occurred at 446 nm. Of this total drop in absorbance, 71.8% was attributed to the quinones in the sample, while 28.2% was attributed to CTC's.

The decreased percentage of absorption due to CTC's in going from the original lignin to the quinone lignin may be explained by several factors. First, the solvent employed for spectral measurement of the reduced quinone lignin was a 2:1 DMF/water mixture. Because of the small quantity of sample available, the reduction was done directly in the spectrophotometer cell, and this necessitated the addition of an aqueous borohydride solution to the DMF lignin solution. DMF

had to be employed, since the acetylated periodate-oxidized lignin was partially insoluble in 2-methoxyethanol. As shown earlier, the CTC absorbs less intensely in DMF; dilution of DMF with water would be expected to enhance this effect. Secondly, as the concentration of quinones is increased in the lignin, the availability of good donor sites to complex those quinones is decreased. In the periodate oxidation quinones were formed by the oxidation of phenolic sites. As a consequence, the number of donor sites available was reduced. Also, due to steric reasons, only a limited number of phenolic sites should be expected to be suitable sites for complexation. Thirdly, a side effect of the periodate oxidation was some crosslinking of the lignin. This would reduce the mobility, or freedom, of the individual donor and acceptor sites to assume conformations conducive for interaction.

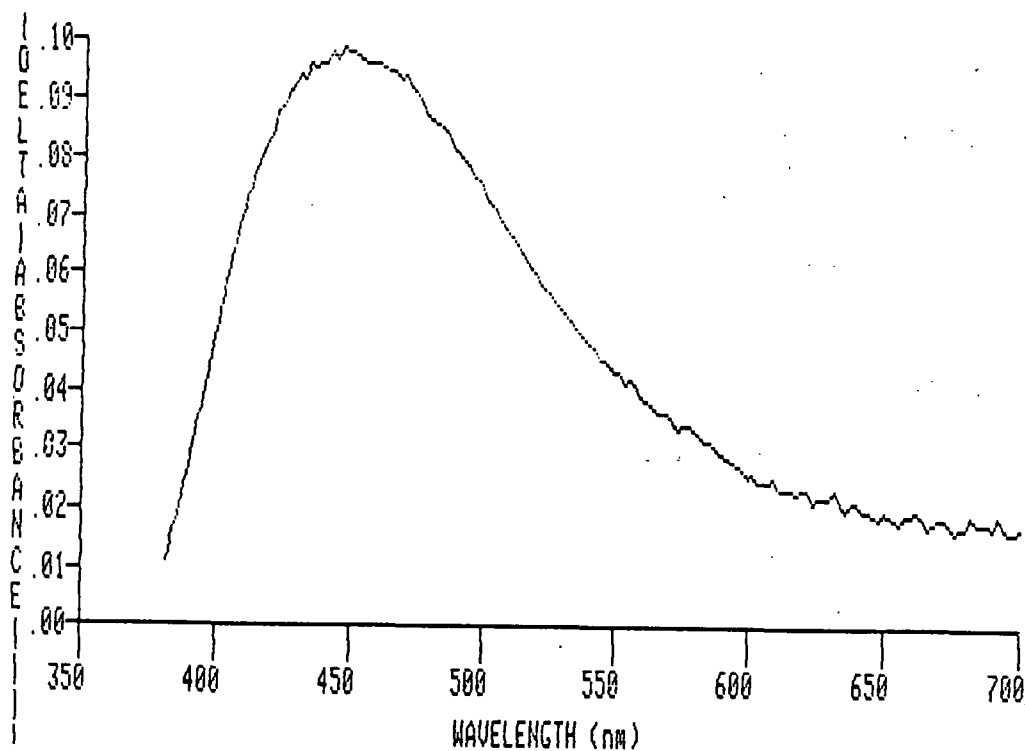


Figure 52. Quinone lignin (pretreated; 40 sec periodate oxidation) minus sodium borohydride reduced quinone lignin; DMF/H<sub>2</sub>O (2:1) as solvent.

## THE CONTRIBUTION OF VARIOUS CHROMOPHORE TYPES TO THE COLOR OF KRAFT LIGNIN

The contribution of quinones and CTC's to the overall absorbance of kraft lignin is discussed below. Also included are evaluations of the contributions of transition metal-lignin complexes and extended conjugated systems.

### Transition Metal Complexes

The contribution of transition metal-lignin complexes to the visible absorption spectrum of kraft lignin was investigated by the removal of these metals. Metals were removed by chelation with ethylenediaminetetraacetic acid (EDTA) and the subsequent extraction of the metal chelates from the lignin by electro-dialysis. EDTA is a hexacoordinate ligand which is able to complex a wide variety of metals.<sup>112</sup> The electrodialysis setup was previously diagrammed in Fig. 13 and 14 of the "Materials and Methods" section.

Table 19 shows the average content of six transition metals found in the original kraft lignin. As can be seen, iron was the transition metal present in largest abundance. The metal content of this laboratory-produced kraft lignin was relatively low when compared to metal contents reported for industrial kraft lignins. Industrial kraft lignins have been found to contain iron in the level of hundreds of parts per million.<sup>17</sup> Also given in Table 19 are the metal levels found in the lignin after the treatment with EDTA. The values shown are the lowest levels which were obtained, compiled from several experimental runs. These results demonstrate the effectiveness of the EDTA chelation combined with electrodialysis in removing metals from kraft lignin.

Figure 53 shows the visible absorption spectra of a kraft lignin before and after the metal removal treatment. The iron content of this lignin was 9.33 ppm



after treatment. As related in the introduction, iron is the most important metal found in lignin in terms of color development. The lignin shown in Fig. 53 was treated with sodium borohydride and diimide prior to the removal of the metals. Both treatments had no effect on the metal content of the original lignin. The spectra in Fig. 53 demonstrate that the metal removal did not produce a detectable drop in absorbance and in fact caused a slight increase in absorbance toward shorter wavelengths. This increase was probably caused by the reoxidation of some of the reduced quinones during the electrodialysis procedure.

Table 19. Metal content of laboratory kraft lignins.

Metal	Quantity Found, ppm	
	Original Kraft Lignin <sup>a</sup>	EDTA Treated Kraft Lignin <sup>b</sup>
Chromium	8.18 ± 1.64	3.2
Manganese	0.55 ± 0.18	< 0.002
Iron	37.67 ± 12.0	9.33
Cobalt	0.70 ± 0.64	< 0.05
Nicke	17.14 ± 1.71	2.0
Copper	8.47 ± 0.81	2.85

<sup>a</sup>Average of three determinations.

<sup>b</sup>Best values.

The results obtained for the laboratory kraft lignin were contrary to other work dealing with industrial kraft lignins<sup>17</sup> and may have been due to the initially low metal content of this lignin. This possibility was investigated by performing the metal removal procedure on an industrially obtained kraft lignin (Indulin AT from Westvaco). The Indulin AT contained a significantly higher quantity of iron and manganese than the laboratory kraft lignin did (see Table 20). After treatment with EDTA, however, these levels were again reduced below 10 ppm.

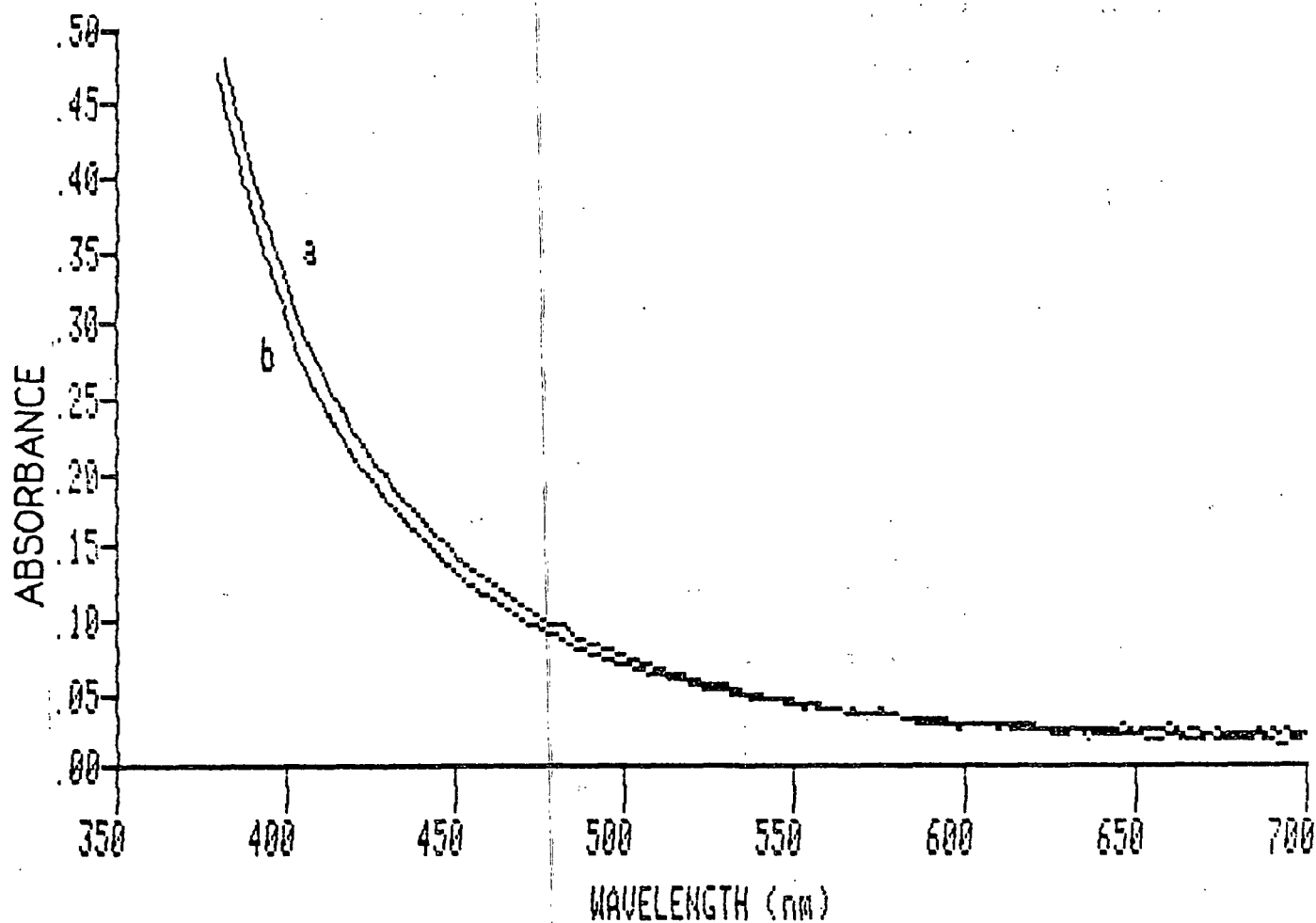


Figure 53. Visible absorption spectra of (a)  $\text{NaBH}_4$  reduced,  $\text{N}_2\text{H}_2$  hydrogenated, and EDTA treated kraft lignin (9.33 ppm Fe) and (b)  $\text{NaBH}_4$  reduced,  $\text{N}_2\text{H}_2$  hydrogenated kraft lignin; concentration, 7.5 mg/25 mL of 2-methoxyethanol.

Table 20. Metal content of Indulin AT.

Metal	Quantity Found, ppm	
	Before Removal	After Removal
Chromium	2.34	1.71
Manganese	56.7	0.09
Iron	176	8.28
Cobalt	1.14	0.81
Nickel	2.78	1.56
Copper	1.26	0.72

Analysis of the EDTA-treated Indulin AT yielded the visible absorption spectrum given in Fig. 54. In this case, reducing the metal content produced a small, but noticeable drop in the spectrum, starting at approximately 450 nm and continuing toward longer wavelengths. This drop in absorbance reached a maximum at approximately 520 nm, as shown in Fig. 55. Meshitsuka and Nakano<sup>17</sup> similarly found that the EDTA treatment of a thiolignin produced a decrease in absorbance centered at 500 nm. Ferric complexes of model lignin catechols and phenols have also been observed to have absorption maxima in this long wavelength region (550-590 nm).<sup>12</sup>

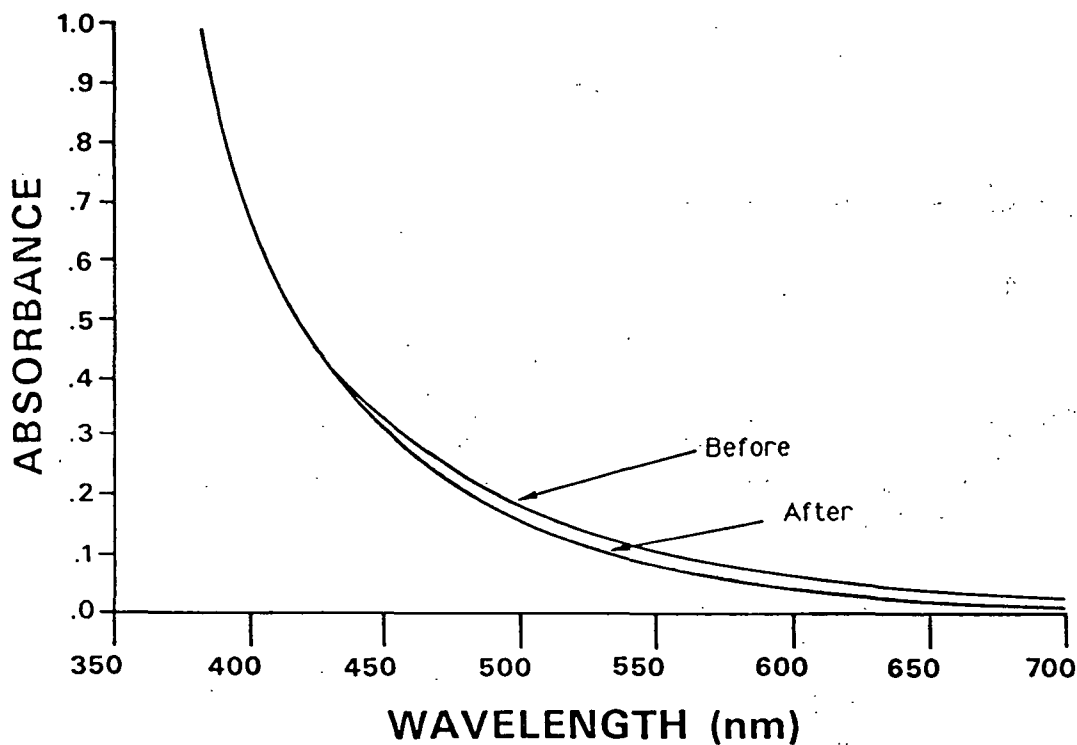


Figure 54. Visible absorption spectra for Indulin AT before and after metal removal; concentration, 7.6 mg/25 mL of 2-methoxyethanol.

The different behavior of the laboratory and industrial kraft lignins may be the result of the much lower initial metal content of the former. If true, this would indicate a certain threshold level for the metals, below which, further

decreases in metal content of the lignin would not produce a corresponding color decrease. This possibility was examined by adding ferric ions to the EDTA-treated laboratory kraft lignin. At an addition level of 400 ppm iron, however, no change in the lignin spectrum was observed. Another possibility was that the two lignins contained different chelation sites for the metals and the chelation sites in the Indulin AT were the more effective color producers.

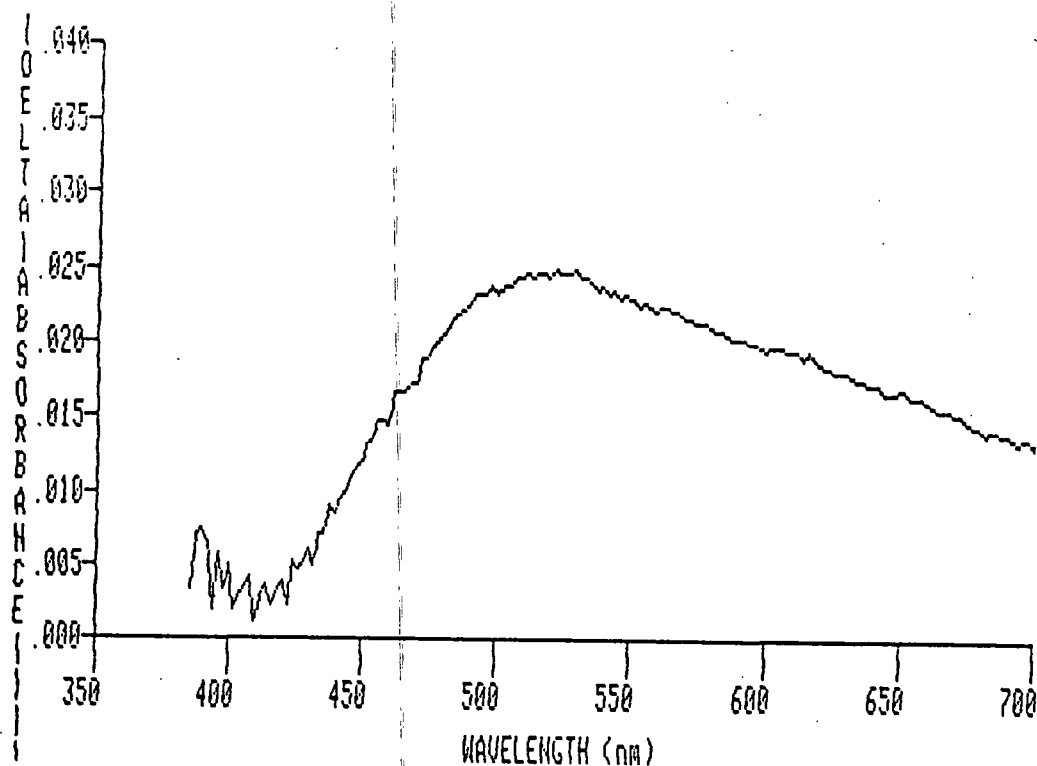


Figure 55. Difference spectrum from Fig. 54.

#### Extended Conjugated Systems

The contribution of extended conjugated systems of the type proposed by Marton<sup>23</sup> to the color of kraft lignin was examined by interrupting the conjugation in these systems through hydrogenation of their connecting carbon-carbon double bonds with diimide. A novel hydrogenating agent for lignin,

diimide,  $N_2H_2$ , was chosen for a number of reasons. First, catalytic hydrogenations of kraft lignin were expected to be difficult due to poisoning of the catalyst by the sulfur groups present in the lignin. However, the presence of sulfur groups in a molecule does not affect diimide's ability to function as a reducing agent.<sup>113</sup> Secondly, in a polymeric substance such as lignin, double bonds located in the interior of the molecule may not be able to approach the catalyst surface due to steric considerations, thus preventing the hydrogenation from taking place. Diimide, being a small molecule, should be able to reach all carbon-carbon double bonds within the lignin macromolecule. Finally, catalytic hydrogenations may result in degradations of the lignin and also may cause reductions of carbonyl groups.<sup>114</sup> Diimide only reduces nonpolar C-C and N-N multiple bonds.<sup>113,115</sup> Polar functional groups, including  $-C=O$ ,  $-C=N$ ,  $-NO_2$ ,  $-N=C$ , and  $S=O$  are inert.

The yield of hydrogenated product from diimide reductions decreases with increasing substitution and crowding around the multiple bond. Mono- and disubstituted olefins are usually reduced in yields of 70-90%, whereas trisubstituted olefins are reduced in yields of 20-40%.<sup>113</sup> Aromatic nuclei are stable toward diimide, but conjugated dienes, for example 1,3-cyclopentadiene, are reduced.  $\alpha,\beta$ -Unsaturated carbonyl compounds are expected to be somewhat less reactive toward diimide due to the polarity of their double bonds.<sup>113</sup>

Diimide hydrogenates multiple bonds at least 97-98% by a cis-addition mechanism.<sup>115</sup> The hydrogenation is usually formulated as a concerted reaction involving a cyclic transition state and the simultaneous transfer of two hydrogen atoms, as depicted in Fig. 56.

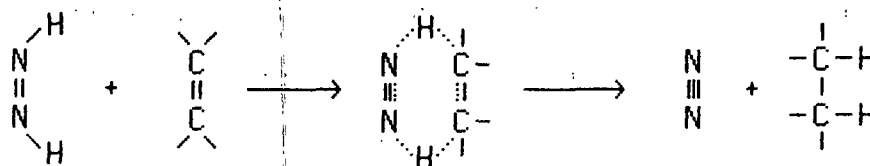


Figure 56. Mechanism of diimide hydrogenation.

In hydrogenating kraft lignin, diimide was generated in situ from the cleavage of meta-nitrobenzenesulfonyl hydrazide, using the conditions given in Fig. 57. Hydrogenation by diimide is a competing reaction with both its own decomposition and disproportionation.<sup>115</sup> The decomposition of diimide is base catalyzed and probably occurs via the diimide anion, ultimately yielding nitrogen and hydrogen. The disproportionation of diimide may be viewed as a self-hydrogenation, yielding nitrogen and hydrazine.

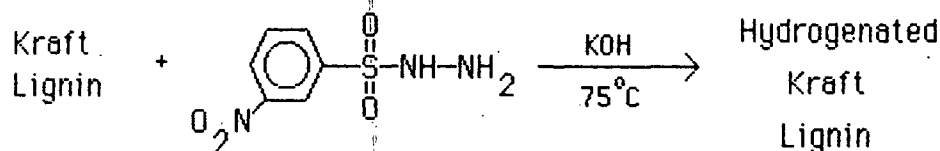


Figure 57. Hydrogenation of kraft lignin.

Hydrogenation was performed on both original and sodium borohydride reduced kraft lignins. The progress of the hydrogenations was monitored by UV spectroscopy. When no further decreases in the UV spectra were detected, the hydrogenations were considered complete. This technique is illustrated by the results given in Table 21. In this example, the molar ratio of diimide to lignin was approximately 1:2.

Table 21. Hydrogenation of kraft lignin with diimide.

Length of Reaction, hr	$\Delta$ Absorbance (decrease in AU)	Wavelength at which Maxi- mum Decrease Occurred, nm
1	0.0525	341
2	0.0620	340
4	0.0685	340
8	0.0655	342
2 x 4 <sup>a</sup>	0.131	337
3 x 4 <sup>b</sup>	0.131	338

<sup>a</sup>New charge of hydrazide added after 4 hours.

<sup>b</sup>New charges of hydrazide added after 4 and 8 hours.

The diimide appeared to be active for a period of four hours, and a total of three 4-hour treatments were necessary to completely hydrogenate the lignin. Difference spectra between the original and hydrogenated lignins as a function of time appear in Fig. 58. The maximum decrease in absorbance occurred at approximately 340 nm. The shapes of the curves suggested more than one type of C-C double bond was hydrogenated. Of the double bond types found in lignin, those conjugated with an aromatic ring have an absorption band near 300 nm, phenylcoumarones absorb near 310 nm, and stilbenes near 330 nm.<sup>18</sup> Disappearance of the 966  $\text{cm}^{-1}$  band in FTIR spectra of the hydrogenated lignins also confirmed the removal of C-C double bonds. This band is caused by =C-H out-of-plane deformations.<sup>93</sup>

Evidence was obtained from difference spectra of ionized lignins which indicated the predominant type of double bond hydrogenated was a stilbene. Subtraction of an ionized, borohydride-reduced and diimide-hydrogenated lignin from an ionized, borohydride-reduced lignin produced a difference spectrum which had a

maximum at approximately 366 nm. The absorption bands of ionized hydroxy stilbenes have been reported to occur between 370 and 380 nm.<sup>18</sup>

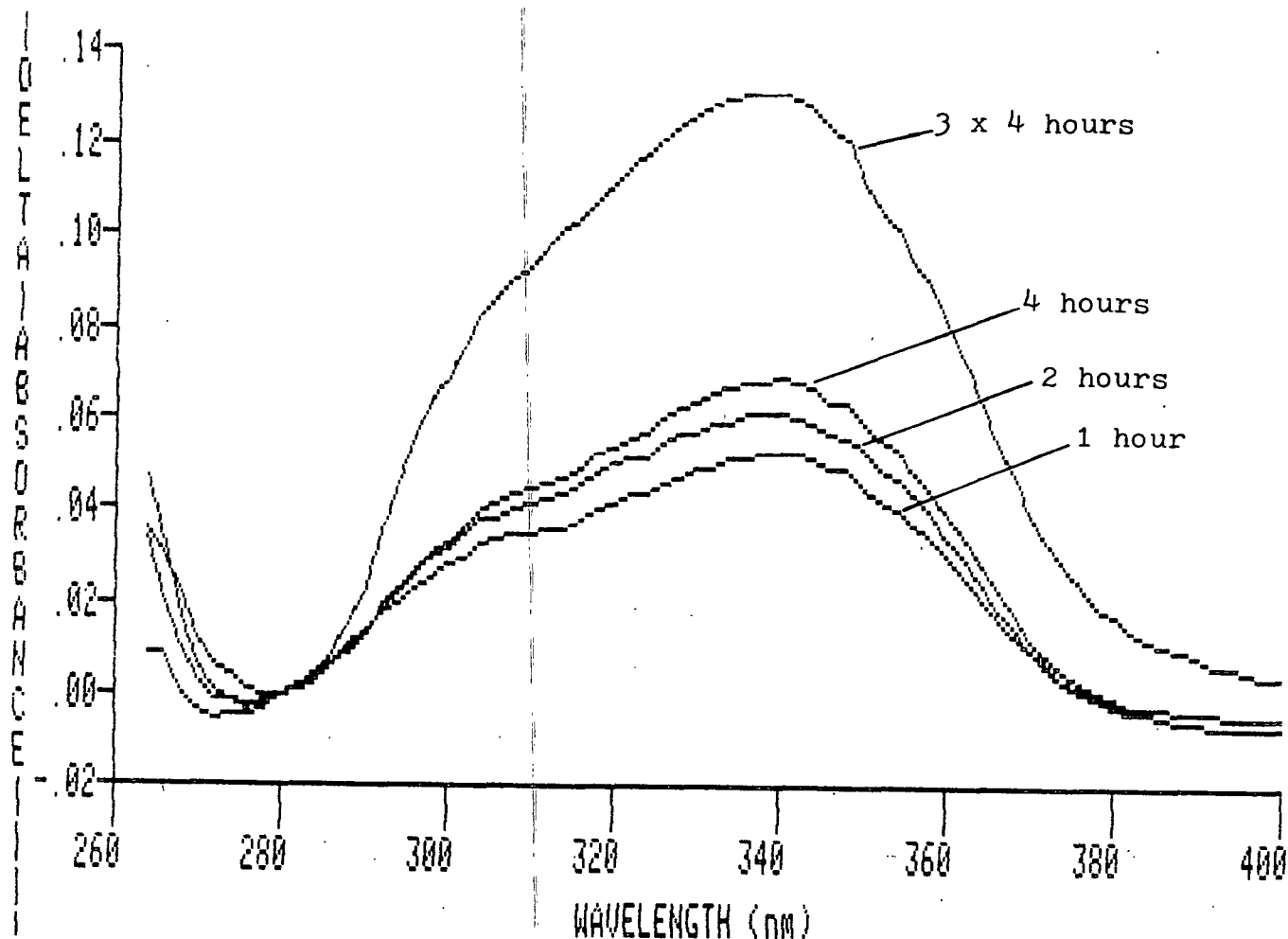


Figure 58. Difference spectra resulting from the subtraction of hydrogenated kraft lignins (length of hydrogenation shown) from the original untreated lignin.

Remarkably, even though hydrogenation resulted in such a large decrease in the UV absorbance of the kraft lignin, no decrease in absorbance was detected in the visible region of the spectrum (see Fig. 59). Significantly, these spectra indicate extended conjugated systems are probably not present in kraft lignin. The hydrogenation of a sodium borohydride reduced kraft lignin gave similar results.



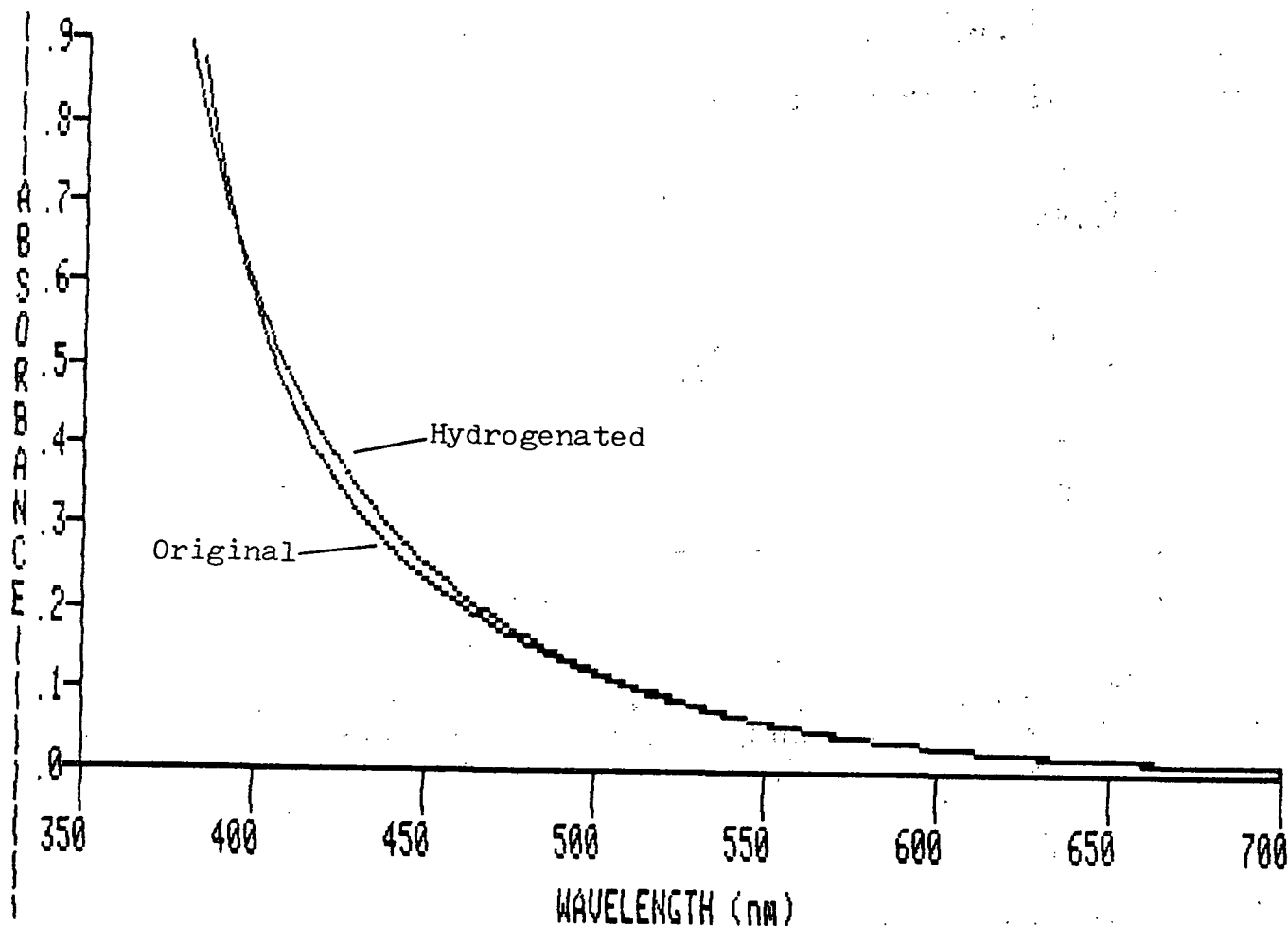


Figure 59. Visible absorption spectra of original and hydrogenated kraft lignins; concentration, 7.5 mg/25mL DMF.

The combined effect of both borohydride reduction and diimide hydrogenation on the UV spectrum of kraft lignin is shown in Fig. 60 and 61. Obviously, hydrogenation had a substantially greater effect in reducing the lignin's absorbance. Overall, there was little absorbance left in this region of the UV spectrum, except for the 280 nm phenolic maximum. The maximum decrease in absorbance caused by the two treatments occurred at 328 nm, as shown in Fig. 61. In the visible region of the spectrum, sodium borohydride reduction had a much greater effect than diimide hydrogenation in reducing the lignin's absorbance; this result will be discussed in the following section.

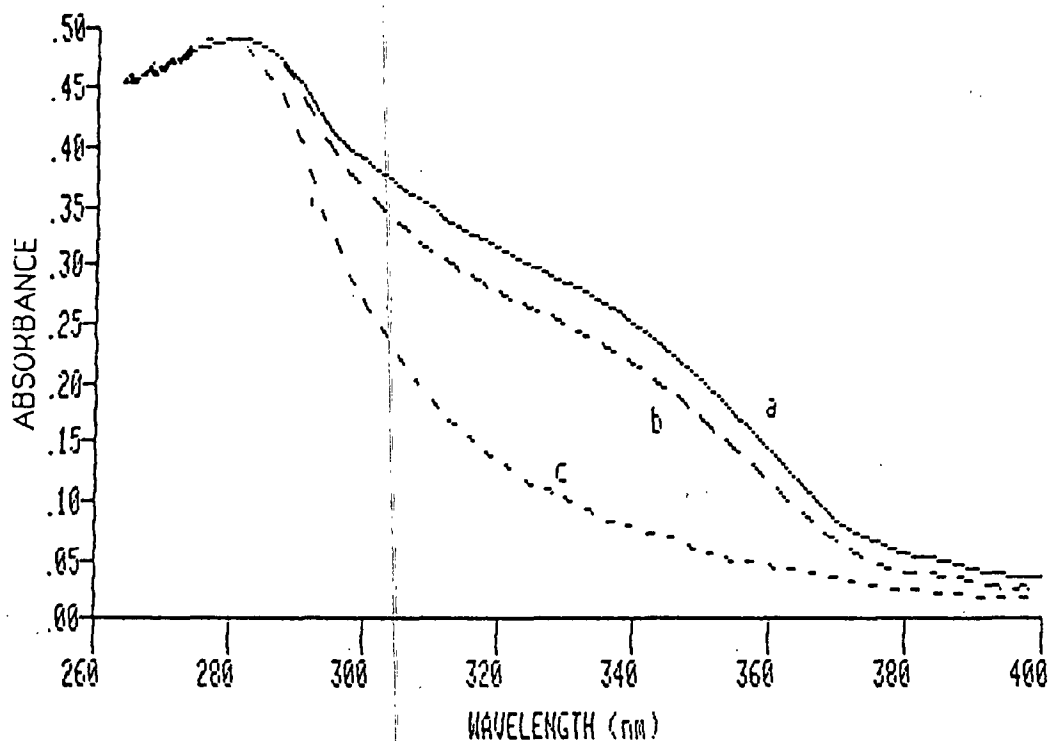


Figure 60. UV spectra of (a) original kraft lignin, (b) NaBH<sub>4</sub> reduced kraft lignin, and (c) NaBH<sub>4</sub> reduced and N<sub>2</sub>H<sub>2</sub> hydrogenated kraft lignin; concentration, 0.375 mg/25 mL 2-methoxyethanol.

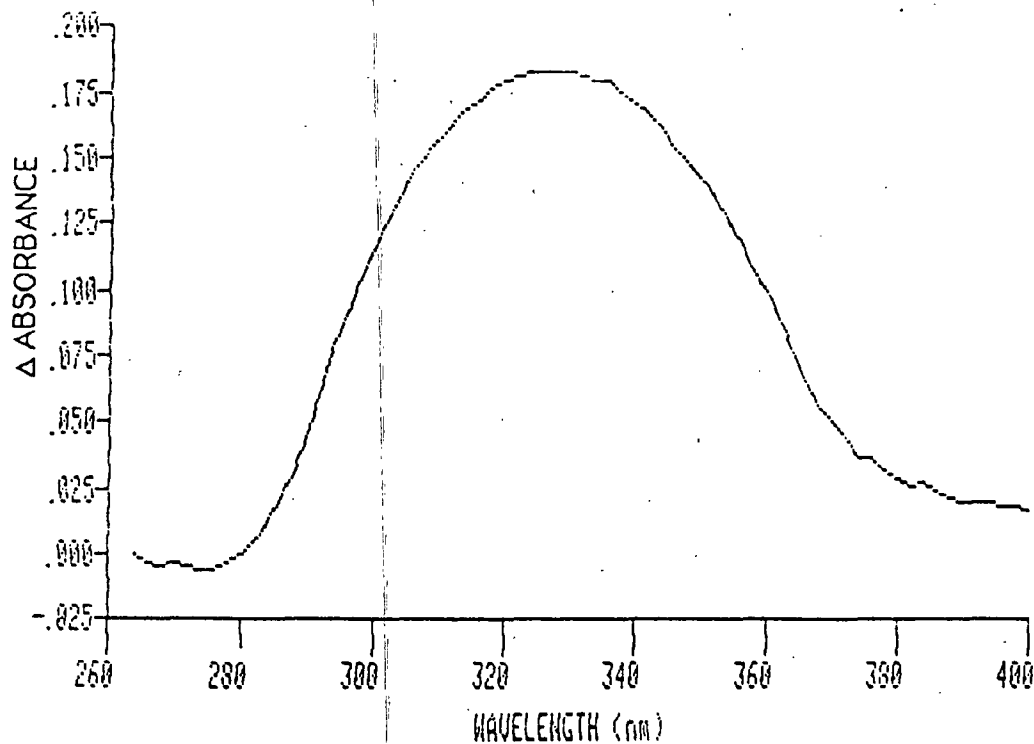


Figure 61. Difference spectrum of original kraft lignin minus NaBH<sub>4</sub> reduced and N<sub>2</sub>H<sub>2</sub> hydrogenated kraft lignin.

## Quinones

The dual role quinones play as a chromophore in kraft lignin was delineated earlier with the use of carbon-14 labeling. Sodium borohydride reduction of the kraft lignin yielded some additional information on the nature of the carbonyl groups as chromophores.

Sodium borohydride reduction of the kraft lignin resulted in decreased absorption in both the UV and visible spectral regions. The difference spectrum, shown in Fig. 62, reveals a broad band centered at approximately 320 nm, whose intensity gradually decreases toward longer wavelengths. Studies of guaiacyl lignin model compounds have shown  $\alpha$ -carbonyls absorb between 280 and 310 nm, whereas conjugated aldehydes have an absorption band near 350 nm.<sup>18</sup> Difference spectra of the ionized original and sodium borohydride reduced lignins gave results very similar to the ones published by Marton.<sup>88</sup> In the ionized difference spectrum a maximum was found at 353 nm. This absorption band has been attributed to phenolic, conjugated  $\alpha$ -carbonyl groups.<sup>88</sup>

In the visible region of the spectrum, sodium borohydride reduction produced the decrease in absorbance shown in Fig. 63. Difference spectroscopy revealed only a smooth curve, with increasing intensity at shorter wavelengths. An example of this was given by Fig. 50 earlier. The decrease in the visible absorbance of the lignin was caused by the removal of the quinone and CTC chromophores.

Infrared spectra of the sodium borohydride reduced kraft lignin were also obtained (see Fig. 64). Compared to the original lignin (see Fig. 10), borohydride reduction decreased the intensity of the  $1709\text{ cm}^{-1}$  band and shifted it to higher wavenumbers ( $1721\text{ cm}^{-1}$ ). These results were due to the removal of nonconjugated carbonyl groups. The absorption remaining at  $1721\text{ cm}^{-1}$  was due to

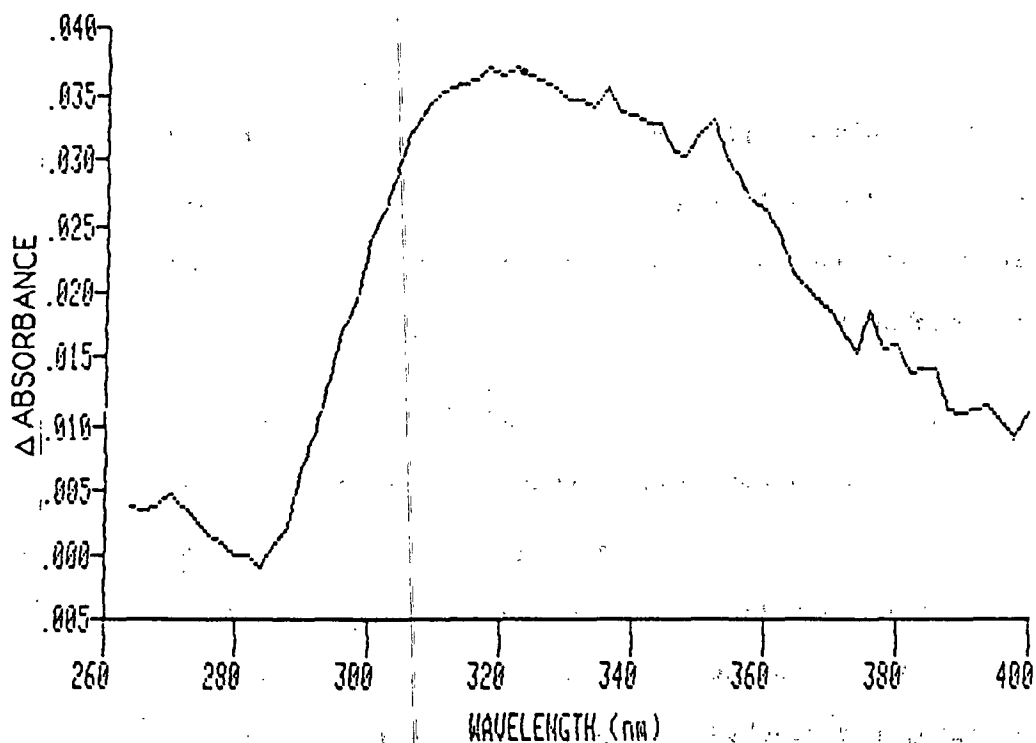


Figure 62. Difference spectrum of original kraft lignin minus NaBH<sub>4</sub> reduced kraft lignin; the sharp peaks were caused by excessive noise in the subtracted spectra.

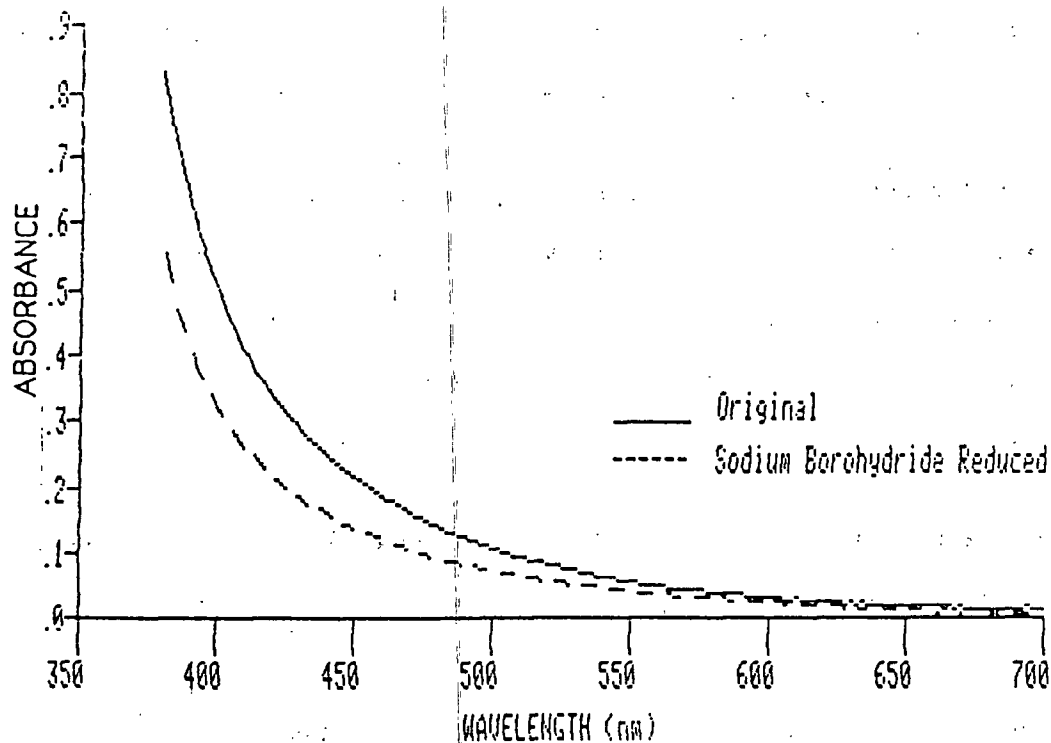


Figure 63. Visible absorption spectra for original and NaBH<sub>4</sub> reduced kraft lignins; concentration, 7.6 mg/25 mL 2-methoxyethanol.

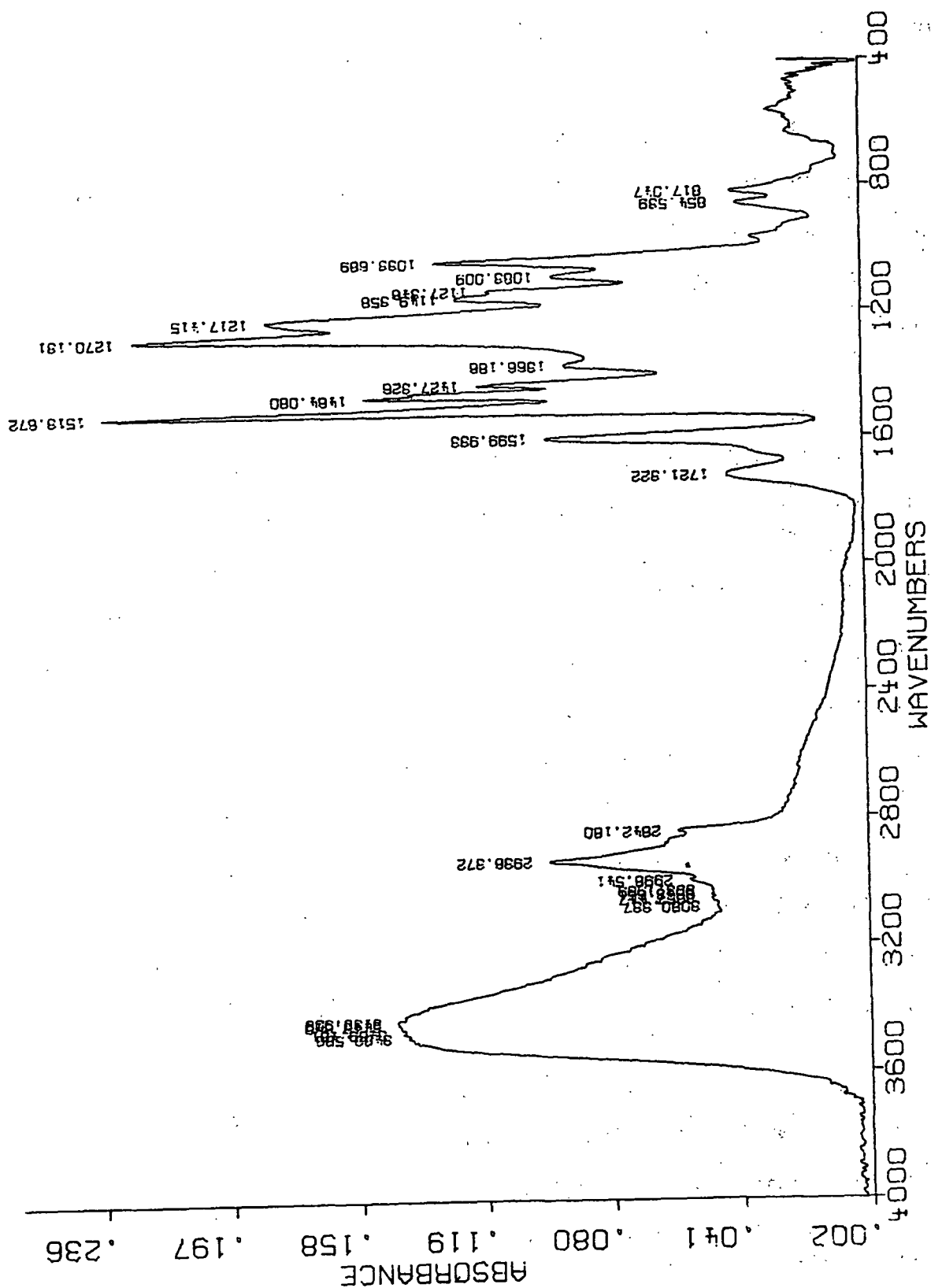


Figure 64. FTIR spectrum of NaBH<sub>4</sub> reduced kraft lignin.

carboxylic acid groups.<sup>88</sup> The quinone carbonyl stretch was previously shown to occur at  $1663\text{ cm}^{-1}$  (see Fig. 17). A shoulder which occurred in the original kraft lignin spectrum (see Fig. 10) between the  $1709$  and  $1599\text{ cm}^{-1}$  absorption bands appeared a likely candidate for this quinone stretch. Closer inspection revealed this shoulder occurred at  $1653\text{ cm}^{-1}$ . However, it could not be removed by reduction. The shoulder is still present in Fig. 64. The quinone carbonyl stretch, therefore, was hidden under other absorption bands in this region of the infrared spectrum. The inability to detect this band in the original kraft lignin is not surprising considering its small concentration of quinones.

#### Summary of Chromophore Contributions

For the laboratory kraft lignin which was investigated, transition metal complexes were insignificant contributors to the lignin's visible absorption spectrum. When the iron content in the lignin was decreased from approximately 40 to 9 ppm, no corresponding decrease in visible absorbance occurred. On the other hand, for an industrial kraft lignin, which had a significantly higher iron content, decreasing this content from approximately 176 to 8 ppm produced a noticeable decrease in its visible absorption spectrum. This decrease in visible absorbance amounted to approximately 4% of the total absorbance near 450 nm, but steadily increased to about 20% at 550 nm, and close to 50% at 700 nm. If metal complexes are present in a particular kraft lignin, their impact is obviously most significant in the longer wavelength region of the spectrum.

Again, for the laboratory kraft lignin, extended conjugated systems did not contribute to its visible absorption spectrum. Hydrogenation of the lignin with diimide, with and without prior reduction by sodium borohydride, did not produce a detectable decrease in the lignin's visible absorbance.

Quinones were the major visible-light absorbing chromophores in the kraft lignin used in this study. Importantly, the contribution of the quinones to the visible absorption spectrum was greatly enhanced by their participation in CTC's as accepting moieties. Reduction of the quinones resulted in a decrease in absorbance throughout the visible spectral range. This decrease amounted to approximately 36% of the total absorbance at 400 nm, gradually decreasing to about 30% at 500 nm, and then leveling off at about 25% throughout the remainder of the visible range. Approximately two-thirds of the overall reduction in absorbance, at 430 nm, resulted from the disruption of CTC's. The proportion of the quinone absorbance resulting from CT interactions may be expected to gradually decrease at longer wavelengths.

## CONCLUSIONS

The occurrence of charge-transfer complexes in various kraft lignin systems was concluded from the acquired data. The charge-transfer interaction appeared to occur between free phenolic and ortho-quinone structures acting as the donor and acceptor halves of the complex. The spectral behavior of the lignins with respect to solvent and derivatization pointed to the probability that the complexes were intramolecular in composition. Hydrogen-bonding may play a contributing role by attracting the donor and acceptor halves of the complex into close enough proximity for their differences in electron density to be felt.

Quinones were the major visible-light absorbing chromophores which were identified in the studied kraft lignin. Their color contribution was significantly enhanced by their participation in charge-transfer complexes. Quinones, therefore, may be envisioned as contributing to the color of kraft lignin by two mechanisms.

Transition metal complexes did not contribute to the color of the kraft lignin used in this study. However, metal complexes may be significant color contributors in other lignins. Their contribution appears to be dependent upon the initial metal content of the lignin and the type of chelation sites available within the lignin material.

Extended conjugated systems were not a source of color in this lignin and probably are not a structural feature of kraft lignin.



## RECOMMENDATIONS

The results of this work demonstrated that charge-transfer interactions occur in kraft lignins. The occurrence of CTC's in other lignin systems may also be expected, provided suitable donor and acceptor sites are present. Hopefully, the findings of this thesis will heighten awareness as to the possibility of charge-transfer phenomena in lignin systems and stimulate investigation into the possible roles such complexes play in these systems.

A recommended area of investigation is the study of charge-transfer interactions in solid lignin systems. The results reported in this thesis were only for dissolved lignin samples. Quite possibly these CT interactions will be enhanced in the solid state, when removed from the dissociative effects of solvents. Studies of CT phenomena in solid lignins would have a more direct bearing on the problem of dark-colored residual lignins in chemical pulps. A closely related area is the yellowing of mechanical pulps. Quinones formed from the lignin have been identified as one of the major chromophores contributing to this brightness loss. Participation of these quinones in CTC's would enhance the yellowing effect.

Diimide was shown to be a mild and effective hydrogenating agent for kraft lignin. This reagent may be useful for further structural investigations of kraft and other lignin types.

#### ACKNOWLEDGMENTS

The author wishes to acknowledge the assistance and guidance provided by his thesis advisory committee: Dr. W. F. W. Lonsky, chairman, Dr. D. R. Dimmel, and Dr. R. H. Atalla. The author is especially grateful to Dr. Lonsky for his encouragement, support, and friendship throughout the course of this work.

Financial support from the member companies of The Institute of Paper Chemistry is gratefully acknowledged. The use of equipment and the assistance of Dr. H. W. Offen and Mr. M. Fetterolf of the University of California at Santa Barbara is sincerely appreciated.

The author would also like to thank members of the Institute faculty and staff, too numerous to mention individually here, for their efforts in support of this thesis. Thanks, also, to my fellow students whose friendship made the last few years a genuinely enjoyable time.

I would like to thank my family for their love and encouragement, especially my mother and father, whose inspiration brought me to this point. Finally, I would like to express my sincere gratitude to my wife, Ginny, for her love, understanding, and sacrifice during this time, without which this work would have been impossible.

LITERATURE CITED

1. American Paper Institute. 1983 Statistics of Paper, Paperboard, and Wood Pulp. New York, 1983:52.
2. Kirkman, A. G.; Gratzl, J. S.; Edwards, L. L., Tappi J. 69(5):110(1986).
3. Yamasaki, T.; Hosoya, S.; Chen, C.; Gratzl, J.; Chang, H., The Eckman Days. Vol. II. p. 34-42. International Symposium on Wood and Pulping Chemistry, Stockholm, June 9-12, 1981.
4. Gellerstedt, G.; Lindfors, E., Holzforschung 38:151-58(1984).
5. Gellerstedt, G.; Lindfors, E.; Lapierre, C.; Monties, B., Svensk Papperstid. 87(9):R61-7(1984).
6. Robert, D.; Bardet, M.; Gellerstedt, G.; Lindfors, E., J. Wood Chem. Technol. 4(3):239-63(1984).
7. Gellerstedt, G.; Lindfors, E., Svensk Papperstid. 87(15):R115-18(1984).
8. Pigman, W. M.; Csellak, W. R., Tappi 31:393-9(1948).
9. Falkehag, S. I.; Marton, J.; Adler, E. Chromophores in kraft lignin. In Lignin Structure and Reactions. Adv. in Chem. Ser. 59:75-89, Amer. Chem. Soc., Washington, DC, 1966.
10. Iiyama, K.; Nakano, J.; Migita, N., J. Jap. Wood Res. Soc. 13(3):125(1967).
11. Norrström, H., Svensk Papperstid. 75(22):891-9(1972).
12. Imsgard, F.; Falkehag, S. I.; Kringstad, K. P., Tappi 54(10):1680-4(1971).
13. Paden, C. A.; Frank, A. S.; Wieber, J. M.; Pethica, B. A.; Zuman, P.; Jurasek, L. Properties of wood lignin. In Furda's Unconventional Sources of Dietary Fibers. ACS Symposium Ser. 214:241-50, Amer. Chem. Soc., Washington, DC, 1983.
14. Polcin, J.; Rapson, W. H., Pulp Paper Mag. Can. 73(1):86-92(1972).
15. Marton, J.; Marton, T.; Falkehag, S. I. Alkali-catalyzed reactions of formaldehyde with lignins. In Lignin Structure and Reactions. Adv. in Chem. Ser. 59:125-44, Amer. Chem. Soc., Washington, DC, 1966.
16. Iiyama, K.; Nakano, J., Japan Tappi 27:182-89(1973).
17. Meshitsuka, G.; Nakano, J., Tappi 56(7):105(1973).
18. Goldschmid, O. Ultraviolet spectra. In Sarkanen and Ludwig's Lignins Occurrence, Formation, Structure and Reactions. New York, Wiley-Interscience, 1971:241-66.

19. Gierer, J., *Svensk Papperstid.* 73(18):571-96(1970).
20. Enkvist, T., *Svensk Kem. Tidskr.* 72:93(1960).
21. Hon, D. N.; Glasser, W., *Polym. Plast. Technol. Eng.* 12(2):159-79(1979).
22. Lonsky, L.; Lonsky, W.; Kratzl, K.; Falkehag, I., *Monatshefte Chemie* 107(3):685-95(1976).
23. Marton, J. Reactions in alkaline pulping. In Sarkanen and Ludwig's *Lignins Occurrence, Formation, Structure and Reactions.* New York, Wiley-Interscience, 1971:679.
24. Pew, J. C.; Connors W. J., *Tappi* 54(2):245-51(1971).
25. Harkin, J. M.; Obst, J. R., *Tappi* 57(7):118-21(1974).
26. Iiyama, K.; Nakano, J., *Japan Tappi* 27(11):530-42(1973).
27. Harkin, J. M. *o*-Quinonemethides as tentative structural elements in lignin. In *Lignin Structure and Reactions.* Adv. in Chem. Ser. 59:65-74, Amer. Chem. Soc., Washington, DC, 1966.
28. Rex, R. W., *Nature* 188:1185(1960).
29. Steelink, C.; Reid, T.; Tollin, G., *J. Amer. Chem. Soc.* 85:4048-49(1963).
30. Steelink, C. Stable free radicals in lignin and lignin oxidation products. In *Lignin Structure and Reactions.* Adv. in Chem. Ser. 59:51-64, Amer. Chem. Soc., Washington, DC, 1966.
31. Slifkin, M. A. Charge-transfer interactions of biomolecules. New York, Academic Press, Inc., 1971:1-24.
32. Mulliken, R. S.; Person, W. B. Molecular complexes: a lecture and reprint volume. New York, Wiley-Interscience, 1969; 5-22, 307-8.
33. Reichardt, C. Solvent effects in organic chemistry. New York, Verlag Chemie, 1978; 15-16, 270, 189-203.
34. March, J. Advanced organic chemistry. 2nd ed. New York, McGraw-Hill, Inc., 1977; 79, 459-63.
35. Foster, R., *J. Phys. Chem.* 84:2135-41(1980).
36. Foster, R. Organic charge-transfer complexes. New York, Academic Press, 1969; 110-11, 230-8, 33-92, 125-78.
37. Staab, H. A.; Herz, C. P., *Angew. Chem. Int. Ed. Engl.* 16(6):392-93(1977).
38. Pasman, P.; Rob, F.; Verhoeven, J. W., *J. Amer. Chem. Soc.* 104:5127(1982).

39. Kuboyama, A.; Nagakura, S., J. Amer. Chem. Soc. 77:2644-6(1955).
40. Staab, H. A.; Rebafka, W., Chem. Ber. 110:3333-50(1977).
41. Staab, H. A.; Herz, C. P.; Henke, H. E., Chem. Ber. 110:3351-7(1977).
42. Staab, H. A.; Herz, C. P., Angew. Chem. Int. Ed. Engl. 16(11):799-801(1977).
43. Tashiro, M.; Koya, K.; Yamato, T., J. Amer. Chem. Soc. 104:3707-10(1982).
44. Tashiro, M.; Koya, K.; Yamato, T., J. Amer. Chem. Soc. 105:6650-3(1983).
45. Staab, H. A.; Herz, C. P., Angew. Chem. Int. Ed. Engl. 16(6):394(1977).
46. Bauer, H.; Briaire, J.; Staab, H. A., Angew. Chem. Int. Ed. Engl. 22(4):334 (1983).
47. Miyahara, Y.; Inazu, T.; Yoshina, T., Tetra. Lett. 23(21):2189-90(1982).
48. Effenberger, F.; Agster, W.; Fischer, P.; Jogun, K.; Stezowski, J. J.; Daltrozzo, E.; Kollmannsberger-von Nell, G., J. Org. Chem. 48:4649-58(1983).
49. Kalninsh, K., J. Chem. Soc., Faraday Trans. 2, 78:327-37(1982).
50. Kalninsh, K., J. Chem. Soc., Faraday Trans. 2, 80:1529-38(1984).
51. Benesi, H. A.; Hildebrand, J. H., J. Amer. Chem. Soc. 71:2703(1949).
52. Pearson, J. M.; Turner, S. R.; and Ledwith, A. The nature and applications of charge-transfer phenomena in polymers and related systems. In Foster's Molecular Association. Vol. 2. New York, Academic Press, 1979:79-169.
53. Andrews, L. J.; Keefer, R. M. Molecular complexes in organic chemistry. San Francisco, Holden-Day, Inc., 1964; 15-43, 102-8.
54. McGlynn, S. P., Chem. Rev. 58(4):1113-56(1958).
55. Davis, K. M. C. Solvent effects on charge-transfer complexes. In Foster's Molecular Association. Vol. 1. New York, Academic Press, 1975:151-213.
56. Nagy, O. B.; Nagy, J. B.; Bruylants, A., J. Chem. Soc., Perkin II 1972:968-71.
57. Prochorow, J.; Tramer, A., J. Chem. Phys. 44(12):4545-9(1966).
58. Trotter, P. J., J. Amer. Chem. Soc. 88(24):5721-6(1966).
59. Ham, J., J. Amer. Chem. Soc. 76:3881-5(1954).
60. Stephens, D. R.; Drickamer, H. G., J. Chem. Phys. 30(6):1518-20(1959).

61. Gott, J. R.; Maisch, W. G., J. Chem. Phys. 39(9):2229-35(1963).
62. Offen, H. W., J. Chem. Phys. 42(1):430-4(1965).
63. Offen, H. W.; Kadhim, A. H., J. Chem. Phys. 45(1):269-74(1966).
64. Offen, H. W.; Studebaker, J. F., J. Chem. Phys. 47(1):253-5(1967).
65. Offen, H. W.; Nakashima, T. T., J. Chem. Phys. 47(11):4446-50(1967).
66. Kadhim, A. H.; Offen, H. W., J. Chem. Phys. 48(2):749-53(1968).
67. Ewald, A. H., Trans. Faraday Soc. 64:733-43(1968).
68. Offen, H. W. Electron-donor-acceptor complexes at high pressures. In Foster's Molecular Complexes. Vol. 1. London, Elek Science, 1973:117-49.
69. Offen, H. W. Absorption and luminescence of aromatic molecules at high pressures. In Birk's Organic Molecular Photophysics. Vol. 1. London, John Wiley and Sons, 1973:103-47.
70. Tsubomura, H., Bull. Chem. Soc. Jap. 26:304-11(1953); CA 50:5402h.
71. Moser, R. E.; Cassidy, H. G., J. Amer. Chem. Soc. 87(15):3463-7(1965).
72. Desiraju, G. R.; Sarma, J. A. R. P., J. Chem. Soc., Chem. Commun. 1983:45-6.
73. Aihara, J.; Kushibiki, G.; Matsunaga, Y., Bull. Chem. Soc. Jap. 46(11):3584-5(1973).
74. Mansson, P., Holzforschung 37:143-6(1983).
75. McDonald, K. L., Tappi 62(1):80-1(1979).
76. Borchardt, L. G.; Piper, C. V., Tappi 53(2):257-60(1970).
77. Kursanov, A. L.; Zaprometer, M. N., Biokhimiya 14:467-75(1949); CA 44:978b.
78. Beilstein 6(2), 843.
79. Beilstein 6(2), 784.
80. Beilstein 6(3), 4519.
81. Beilstein 6(1), 542.
82. Ludwig, C. H.; Nist, B. J.; McCarthy, J. L., J. Amer. Chem. Soc. 86:1186-96(1964).
83. Cremlyn, R. J. W., J. Chem. Soc. Sect. C Org. Chem. 1966:1229.

84. Vogel, A. I. Practical organic chemistry. 3rd ed. New York, John Wiley and Sons, Inc., 1956:553.
85. Shriner, R. L.; Fuson, R. C.; Curtin, D. V. The systematic identification of organic compounds. 5th ed. New York, John Wiley and Sons, Inc., 1964:303-4.
86. CRC handbook of tables for organic compound identification. 3rd ed. Cleveland, Ohio, CRC Press, 1967:383.
87. Davies, W.; Storrie, F. R.; Tucker, S. H., J. Chem. Soc. 1931:624-9.
88. Marton, J., Tappi 47(11):713-19(1964).
89. Lyttle, D. A.; Jensen, E. H.; Struck, W. A., Anal. Chem. 24:1843-4(1952).
90. Dawson, D. R.; Offen, H. W., Rev. Sci. Instrum. 51(10):1349-51(1980).
91. Guide for users of labelled compounds. 3rd ed. Arlington Heights, Il, Amersham Corp., 1979:31.
92. Peng, C. T. Sample preparation in liquid scintillation counting. Review 17. Arlington Heights, Il, Amersham Corp., p.32.
93. Hergert, H. L. Infrared spectra. In Sarkanen and Ludwig's Lignins Occurrence, Formation, Structure, and Reactions. New York, Wiley Interscience, 1971:267-97.
94. Ludwig, C. H. Magnetic resonance spectra. In Sarkanen and Ludwig's Lignins Occurrence, Formation, Structure, and Reactions. New York, Wiley Interscience, 1971:299-344.
95. Kringstad, K. P.; Mörck, R., Holzforschung 37:237-44(1983).
96. Mörck, R.; Kringstad, K. P., Holzforschung 39:109-19(1985).
97. Ritchie, P. F.; Purves, C. B., Pulp Paper Mag. Can. 48:74-82(1947).
98. Adler, E.; Hernestam, S., Acta Chem. Scand. 9(2):319-34(1955).
99. Adler, E.; Hernestam, S.; Wallden, I., Svensk Papperstid. 61(18):641-47 (1958).
100. Adler, E.; Falkehag, I.; Smith, B., Acta Chem. Scand. 16:529-40(1962).
101. Sklarz, B., Quart. Rev. 21:17-20(1967).
102. Otting, W.; Staiger, G., Chem. Ber. 88(6):828-33(1955).102.
103. Shriner, R. L.; Fuson, R. C.; Curtin, D. V. The systematic identification of organic compounds. 5th ed. New York, John Wiley and Sons, Inc., 1964:98-9.

104. Levy, G. C.; Nelson, G. L. Carbon-13 nuclear magnetic resonance for organic chemists. New York, Wiley Interscience, 1972:24.
105. Klæboe, P., Acta Chem. Scand. 18:27(1964).
106. Lai, Y. Z.; Sarkanen, K. V. Isolation and structural studies. In Sarkanen and Ludwig's Lignins Occurrence, Formation, Structure, and Reactions. New York, Wiley Interscience, 1971:182.
107. Rubin, M. B., Fortschr. Chem. Forsch. 13(2):251-306(1969).
108. Pasto, D. J.; Johnson, C. R. Organic structure determination. Englewood Cliffs, NJ, Prentice-Hall, Inc., 1969:99.
109. Hayashi, A.; Kinoshita, K.; Taniguchi, A. Polyoxidiphenoquinone structure as a chromophore in alkali lignin. Chromophore Seminar, Raleigh, NC, April 17-19, 1972.
110. Teuber, H.; Staiger, G., Chem. Ber. 88(6):802-27(1955).
111. Birnbaum, H.; Cookson, R. C.; Lewin, N., J. Chem. Soc. 1961:1224-8.
112. Peters, D. G.; Hayes, J. M.; Hieftje, G. M. A brief introduction to modern chemical analysis. Philadelphia, W. B. Saunders Company, 1976:127-9.
113. Miller, C. E., J. Chem. Educ. 42(5):254-9(1965).
114. Hrutfiord, B. F. Reduction and hydrogenolysis. In Sarkanen and Ludwig's Lignins Occurrence, Formation, Structure, and Reactions. New York, Wiley Interscience, 1971:487-509.
115. Hünig, S.; Müller, H. R.; Thier, W., Angew. Chem. Int. Ed. Engl. 4(4):271-82(1965).
116. Marton, J.; Adler, E., U. S. pat. 3,071,570(Jan. 1, 1963).
117. Snell, F. D.; Snell, C. T. Colorimetric methods of analysis. New York, D. Van Nostrand Company, Inc., 1953:126.
118. Smith, J. M.; Van Ness, H. G. Introduction to chemical engineering thermodynamics. 2nd ed. New York, McGraw-Hill Book Company, Inc., 1959:112-14.
119. Riddick, J. A.; Bunger, W. B. Organic solvents, physical properties and methods of purification. 3rd ed. In Weissberger's Techniques of Chemistry. Vol. 2. New York, Wiley-Interscience, 1970:446.
120. Thomson, G. W. Determination of vapor pressure. In Weissberger's Technique of Organic Chemistry. Vol. 1. Part 1. 3rd ed. New York, Interscience Publishers, Inc., 1959:507-8.



121. Thomson, G. W. Determination of vapor pressure. In Weissberger's Technique of Organic Chemistry. Vol. 1. Part 1. 3rd ed. New York, Interscience Publishers, Inc., 1959:509-12.
122. Riddick, J. A.; Bunger, W. B. Organic solvents, physical properties and methods of purification. 3rd ed. In Weissberger's Techniques of Chemistry. Vol. 2. New York, Wiley-Interscience, 1970:469.

# APPENDIX I

## CARBOHYDRATE ANALYSES

Difficulties were encountered in obtaining accurate carbohydrate analyses using the alditol acetate method<sup>76</sup> for materials in which the total carbohydrate content of the sample was on the order of 1%. Several sources of error were found which were corrected in Table 6 of the "Materials and Methods" section. These sources of error are detailed below.

Initial values for the carbohydrate analysis of the 2-methoxyethanol treated kraft lignin were not the same as those given in Table 6, but rather were those appearing in Table 22. Comparison of these results with those in Table 6 shows a wide difference in the amount of glucose which was determined by the alditol acetate method. Even more disturbing at the time was the glucose content determined for the 2-methoxyethanol treated lignin (Table 22). This was actually larger than that found in Table 6 before carbohydrate removal.

Table 22. Uncorrected carbohydrate values for kraft lignin after removal of 2-methoxyethanol insoluble material.<sup>a</sup>

Carbohydrate	% of Total Sample	% of Total Carbohydrate
Arabinose	0.22 ± 0.01	6.98
Xylose	0.73 ± 0.04	23.17
Mannose	0.13 ± 0.15	4.13
Galactose	0.15 ± 0.12	4.76
Glucose	1.92 ± 0.21	60.95

<sup>a</sup>Average of three determinations.

Naturally, these results called into question the accuracy of the alditol acetate method for use on lignin samples. The accuracy of the procedure for determining the carbohydrate content of lignin samples was tested in two ways. First, the internal standard, which was added during the procedure so a quantitative determination of the carbohydrates could be made, was tested for its contribution, if any, to the total carbohydrate content determined for a particular sample. Secondly, the response factor of the procedure to small quantities of sugars added to correspondingly large lignin samples was tested.

myo-Inositol (Pfanstiehl Laboratories, Inc.), the internal standard, was subjected to the analysis procedure at two levels of addition. The resultant chromatograms were examined for the occurrence of carbohydrate peaks. In both cases, glucose was evident in these chromatograms, as is shown by Table 23. The chromatographic data clearly demonstrated the internal standard may contribute significantly to the glucose concentration calculated for low carbohydrate materials. Furthermore, this contribution appears to be linear, at least in the range which was studied.

Table 23. Carbohydrate analysis of myo-inositol.

Quantity Added, mg	% Glucose Found <sup>a</sup>
10	0.13
100	1.17

<sup>a</sup>Calculated percentage, if based on 200 mg lignin sample.

To check the response factor of the procedure, three different samples were prepared and analyzed. The three samples included a kraft lignin after removal of carbohydrates; a prepared sugar mixture containing the five sugars of interest

(2 mg/1 mL); and a combined sample containing 0.5 ml of the sugar solution added to 200 mg of the lignin. The results of the analyses of these samples are given in Table 24. Theoretically, the sum of the values in the first two columns of Table 24 should equal the value in the third column. In all cases, except for glucose, the calculated and experimental values agreed fairly well. Some additional error may therefore enter into the glucose determinations from this uneven response factor.

Table 24. Response of lignin plus sugar mixture compared to response of separate components.

Carbohydrate	% in Total Sample <sup>a</sup>		
	Lignin	Sugar Mixture	Sugar Mixture + Lignin
Arabinose	0.20	0.43	0.60
Xylose	0.59	0.08	0.73
Mannose	0.12	0.48	0.57
Galactose	0.21	0.42	0.62
Glucose	0.29	0.66	0.57

<sup>a</sup>Average of two determinations.

## APPENDIX II

### PERIODATE OXIDATION OF KRAFT LIGNIN

#### LEAD NITRATE ADDITION

Initial oxidations of kraft lignin with periodate utilized lead nitrate<sup>98</sup> to halt the oxidation after relatively long reaction times (30 minutes to 12 hours). The lignin solutions developed a red color during the reaction, indicating quinone formation. Intriguingly, the isolated oxidized kraft lignins were slightly red to orange-tinged in appearance.

Unfortunately, these lignins were insoluble to varying degrees in the usual lignin solvents, except for sodium hydroxide. Their insolubility in organic solvents hindered their characterization and prevented this oxidation method from being useful for further studies. The insolubility of periodate lignins has been noted previously<sup>106</sup> and is probably caused by cross-linking of the ortho-quinone structures in the oxidized lignin, via Diels-Alder type condensations. The insoluble portions of the periodate-oxidized lignins behaved similarly to cross-linked materials, since they could be swollen in the organic solvents but not dissolved.

In spite of their insolubility, evidence was obtained from the periodate-oxidized lignins which indicated the formation of ortho-quinones. The aqueous filtrates recovered during isolation of these periodate lignins were yellow colored. These filtrates tested negative for iodine, and the yellow color could not be extracted into chloroform. Examination by UV-visible spectroscopy revealed two absorption bands located at 420 and 270 nm, respectively. The presence of the 420 nm band was indicative of quinone structures in the filtrate.<sup>103</sup>

Other evidence included FTIR spectra which were obtained from these lignins. The most prominent feature of these spectra compared to the original kraft lignin spectrum (Fig. 10) was the appearance of a strong new absorption band located between 1720 and 1740  $\text{cm}^{-1}$  (see Fig. 65). In addition, a substantial decrease occurred in the intensity of the 1514  $\text{cm}^{-1}$  aromatic stretching band. The new absorption band appearing between 1720 and 1740  $\text{cm}^{-1}$  evidently is due to the formation of carboxylic acid structures in the lignin. These structures would result from the further oxidation of the ortho-quinones. The decreased intensity of the 1514  $\text{cm}^{-1}$  band supports this view, since it indicates the loss of aromatic ring structures. Also evident in some spectra of the periodate lignins was a filling in of the trough between the new carboxylic acid absorption and the aromatic stretching band at 1598  $\text{cm}^{-1}$ . This additional absorbance provided more direct evidence of the incorporation of ortho-quinones within the periodate lignins, since ortho-benzoquinones have a carbonyl stretching band<sup>102</sup> near 1660  $\text{cm}^{-1}$ .

#### Sulfur Dioxide Addition

A second method of halting the periodate oxidation was suggested from a patent by Marton and Adler.<sup>116</sup> In this method, the periodate oxidation was carried out for only a few minutes in an ice bath and rapidly quenched by the addition of sulfur dioxide. The sulfur dioxide treatment apparently prevents cross-linking of the quinones by reducing them to catechol structures. Marton and Adler claimed lignins oxidized in this manner were more completely soluble in organic solvents.

A number of periodate oxidations of kraft lignin employing sulfur dioxide quenching were performed. The oxidized lignins were indeed soluble in organic

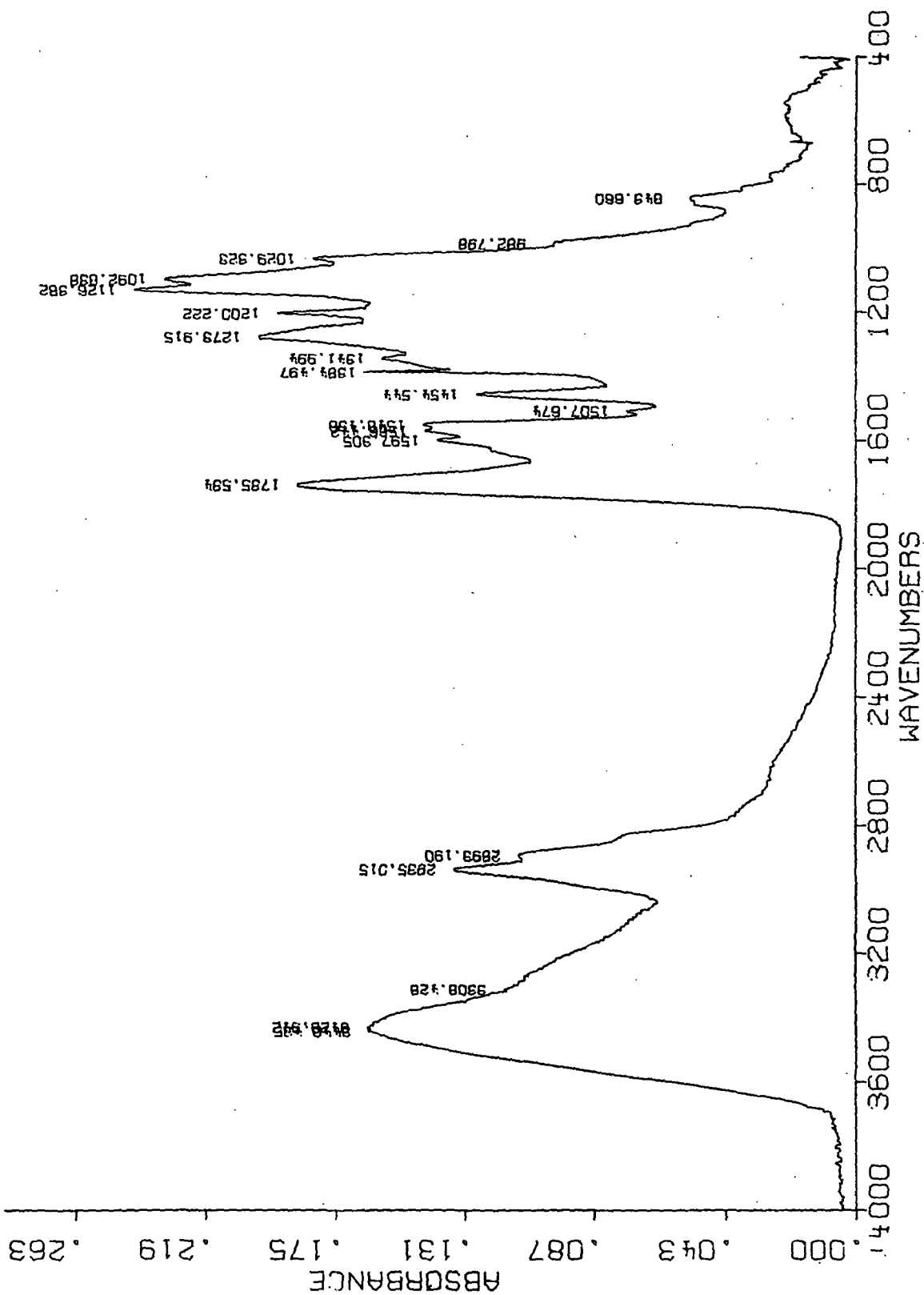


Figure 65. FTIR spectrum of periodate oxidized kraft lignin; isolated by lead nitrate addition after one hour.

solvents as long as the oxidation times were kept relatively short. The improved solubility of these oxidized lignins permitted their further characterization by acetylation and subsequent  $^1\text{H}$  NMR analysis. The quantities of different proton types in the acetylated, periodate-oxidized lignins were estimated from their  $^1\text{H}$  NMR spectra.

Data for some of the periodate oxidized, sulfur dioxide reduced lignins appear in Table 25. Included in the table are the reaction conditions and the  $^1\text{H}$  NMR analysis of the acetylated lignin. Other lignins, not shown, were oxidized in mixtures of organic solvents and acetic acid. In short, the organic solvent mixtures were poor at promoting demethoxylation of the lignins.

Table 25. Acetylated periodate lignins.

Sample	Reaction Conditions				$^1\text{H}$ NMR Analysis		
	Mole $\text{NaIO}_4$ Mole $\text{OCH}_3$	Solvent % $\text{HOAc}$	Temp., $^\circ\text{C}$	Time, min	OMe Arom	OAc <sub>arom</sub> Arom	OAc <sub>aliph</sub> Arom
1	1	82.5	4	2	0.72	0.75	0.85
2	1	82.5	4	2	0.71	0.80	0.94
3	1	82.5	4	2	0.74	0.77	0.87
4	1	82.5	2	2	0.73	0.83	0.88
5	2	78.0	3-4	2	0.72	0.79	0.88
6	1	82.5	2	5	0.63	0.90	0.90
7	0	90.0	4	--	0.87	0.66	0.96
8	0	90.0	2	--	0.95	0.82	0.80
9	0	82.5	2	--	0.84	0.73	0.86

The samples in Table 25 are grouped according to similar reaction conditions. The first four samples were reacted at an equimolar concentration of



periodate to methoxyl groups in the lignin and for an oxidation time of two minutes. Sample 6 was also reacted at the same periodate concentration, but for a time of five minutes. Sample 5 was reacted at twice the periodate concentration used in the previous samples. The last three samples in Table 25 were run as controls. These samples were dissolved in the acetic acid solvent; however, no periodate was added.

The methoxyl contents of the samples shown in Table 25 were also determined by the Zeisel method and appear in Table 26. There was an average 22.4% reduction in the methoxyl contents of the lignin samples reacted for two minutes and with an equimolar amount of periodate compared to the control lignins. When the reaction time was increased to five minutes (sample 6), the methoxyl loss increased to 32.1%. Doubling of the periodate concentration (sample 5) had no effect on the methoxyl loss. The control samples showed essentially no methoxyl loss compared to unreacted, acetylated lignin (10.62% OMe) within the error of the measurements.

The data in Table 26 agreed with the NMR results given in Table 25. Decreases in the OMe/Arom ratio parallel the decreases shown by the Zeisel methoxyl determinations.  $^1\text{H}$  NMR results can therefore at least be used as a qualitative tool in predicting methoxyl losses in these lignins. From the data in Tables 25 and 26, the molar amounts of various substituent groups per 1000 grams of lignin were calculated. These values, for the lignins reacted for two minutes and with an equimolar amount of periodate, and for the control samples, appear in Tables 27 and 28, respectively.

In evaluating the data in Tables 27 and 28, the overall effect on the lignin of the periodate oxidation with sulfur dioxide reduction must be considered.

The loss of methoxyl groups in these lignins should be caused by the formation of ortho-quinone groups. However, with sulfur dioxide addition the quinone groups are immediately reduced to catechol structures. Accordingly, an increase in the amount of phenolic hydroxyl groups in the lignins should be expected. This increase will be indicated by the quantity of aromatic acetates in the oxidized, acetylated lignins. The aliphatic hydroxyl groups in the lignin (represented by the aliphatic acetate content of the oxidized, acetylated lignins) should not be greatly effected by the oxidation. 116

Table 26. Methoxyl contents of acetylated periodate lignins.

Sample	% Methoxyl <sup>a</sup>	Average
1	8.01	
2	8.01	
3	8.18	
4	8.25	
		8.11 ± 0.12
5	8.14	
6	7.10	
7	10.52	
8	10.26	
9	10.58	
		10.45 ± 0.17

<sup>a</sup>Average of two determinations.

Comparison of the values in Tables 27 and 28 demonstrates there was no change in the average aliphatic acetate content, as expected. However, there was also no change in the aromatic acetate content of the two lignins, contrary to expectations. Given the methoxyl loss which occurred, there should have been a

corresponding increase in the phenolic hydroxyl content of the oxidized lignin. A major reason for this unexpected result may have been the incomplete acetylations of the lignins (see section on periodate oxidation dealing with ethylene glycol addition).

Table 27. Substituent groups; periodate lignins, two-minute reaction time.

Sample	Moles per 1000 g Lignin		
	OMe	OAc <sub>arom</sub>	OAc <sub>aliph</sub>
1	2.58	2.68	3.04
2	2.58	2.88	3.40
3	2.64	2.76	3.11
4	<u>2.66</u>	<u>3.04</u>	<u>3.22</u>
	2.64 ± 0.04	2.84 ± 0.16	3.19 ± 0.16

Table 28. Substituent groups; control lignins for periodate oxidation.

Sample	Moles per 1000 g Lignin		
	OMe	OAc <sub>arom</sub>	OAc <sub>aliph</sub>
7	3.39	2.57	3.74
8	3.31	2.84	2.79
9	<u>3.41</u>	<u>2.97</u>	<u>3.46</u>
	3.37 ± 0.05	2.79 ± 0.20	3.33 ± 0.49

A colorimetric method, however, demonstrated there was indeed an increase in the phenolic hydroxyl content of these periodate oxidized, sulfur dioxide reduced lignins. Catechols are known to form violet-colored complexes with ferrous sulfate in the presence of sodium potassium tartrate at approximately pH 8.<sup>117</sup> Falkehag, et al.<sup>9</sup> were successful in applying this method to kraft lignin. They found an absorption maximum for the catechol complex at 560 nm, with a molar absorptivity of 66 lit/mol-cm. From this value, kraft lignin was estimated to contain six catechol structures per one-hundred C<sub>9</sub> units.

This same method was used in order to determine the catechol contents of the original and the periodate oxidized, sulfur dioxide reduced kraft lignins. For the original lignin, an absorbance maximum was observed at 556 nm, with a molar absorptivity of 50 lit/mol-cm (shown in Fig. 66). Using the molar absorptivity at the absorbance maximum and the average molar absorptivity determined for model catechol complexes (1100 lit/mol-cm)<sup>9</sup>, a value of 4.6 catechol structures per one-hundred C<sub>9</sub> units was calculated for the original lignin.

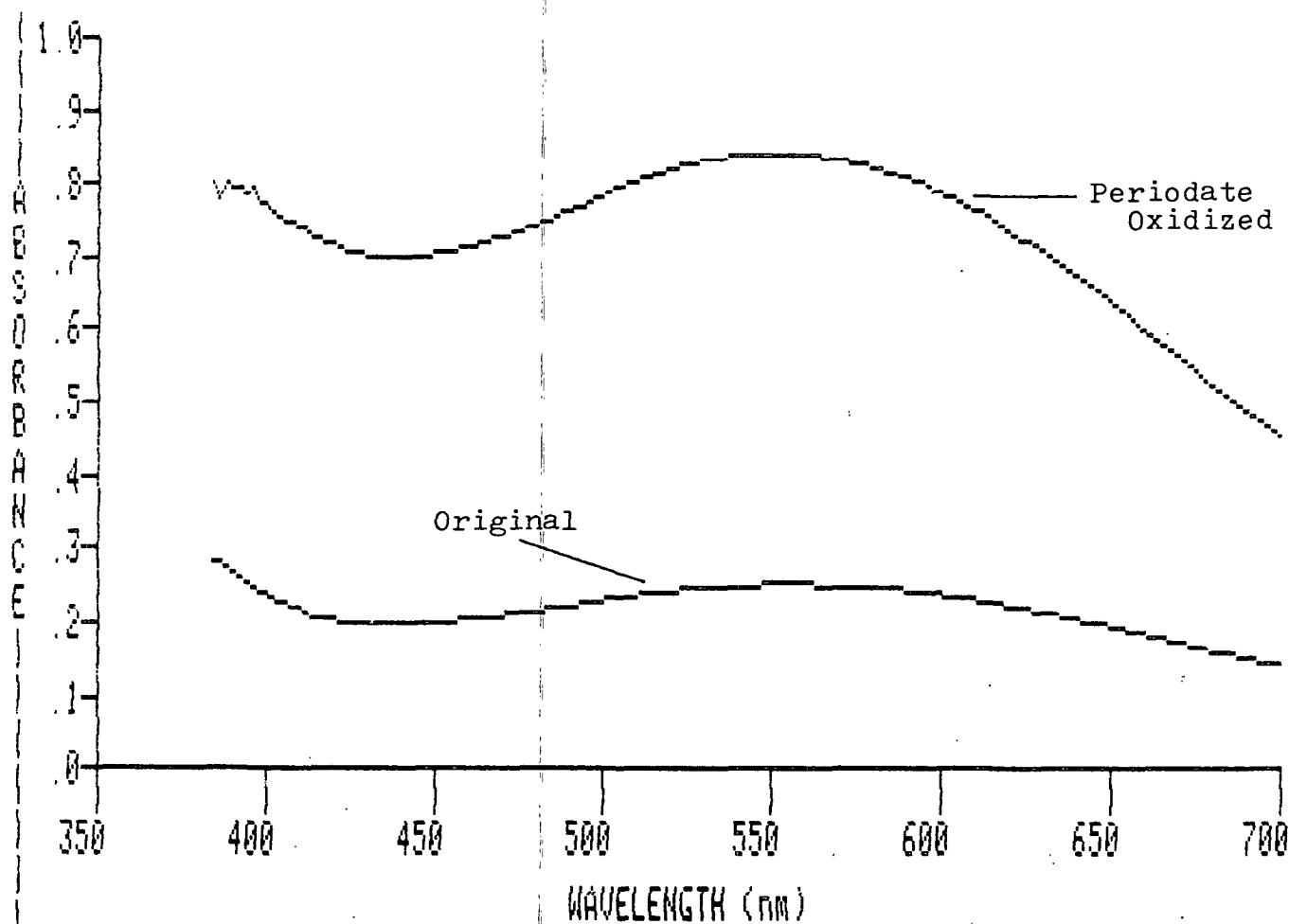


Figure 66. Visible spectra of ferrous sulfate treated original and periodate-oxidized (two minutes), sulfur dioxide-reduced kraft lignins; spectra used for catechol determinations.

An increased absorbance was observed in the 550 nm region for the periodate-oxidized kraft lignin (also shown in Fig. 66). The absorbance maximum occurred at 554 nm with a molar absorptivity of 168 lit/mol-cm. Using this molar absorptivity and the molar absorptivity for model catechols, a value of 15.2 catechol structures per one-hundred C<sub>9</sub> units was calculated for the periodate-oxidized, sulfur dioxide-reduced kraft lignin.

Consequently, the periodate oxidation followed by sulfur dioxide reduction introduced approximately 10.6 catechol structures per one-hundred C<sub>9</sub> units into the original kraft lignin. This value may be compared to the loss of methoxyl groups for the same lignin. The original lignin contained approximately 63 methoxyl groups per one-hundred C<sub>9</sub> units. Periodate oxidation, for a period of two minutes, resulted in the loss of 22.4% of these groups, or a loss of 14.1 methoxyl groups from the original lignin. The loss in methoxyl groups and gain in catechol structures is therefore in rather close agreement. Complete agreement between these two values should not be expected, since at least some of the catechol structures created by demethoxylations probably oxidize further to give carboxylic acid structures.

Finally, the effectiveness of the sulfur dioxide in reducing quinones to catechols was demonstrated by both visible and infrared spectroscopy. The visible spectrum of the oxidized and reduced lignin shown in Fig. 67 may be compared to the spectrum in Fig. 19, where the periodate oxidation was quenched with ethylene glycol.

Similarly, the FTIR spectrum of a periodate oxidized, sulfur dioxide-reduced lignin (Fig. 68) showed no evidence of the quinone absorption band at 1663 cm<sup>-1</sup> found for the oxidized lignin in Fig. 17.

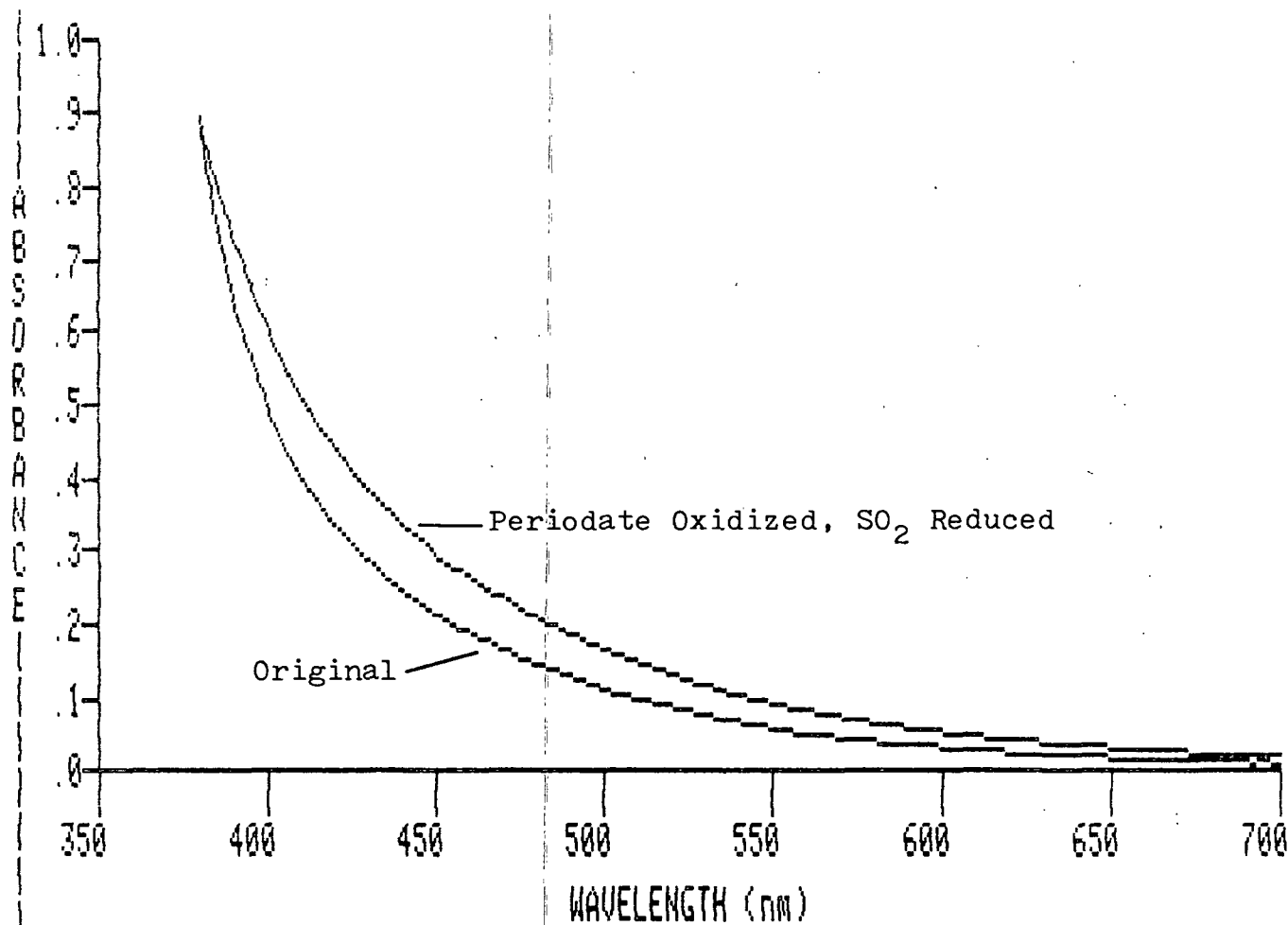


Figure 67. Visible spectra of periodate-oxidized (two minutes), sulfur dioxide-reduced kraft lignin and original kraft lignin.

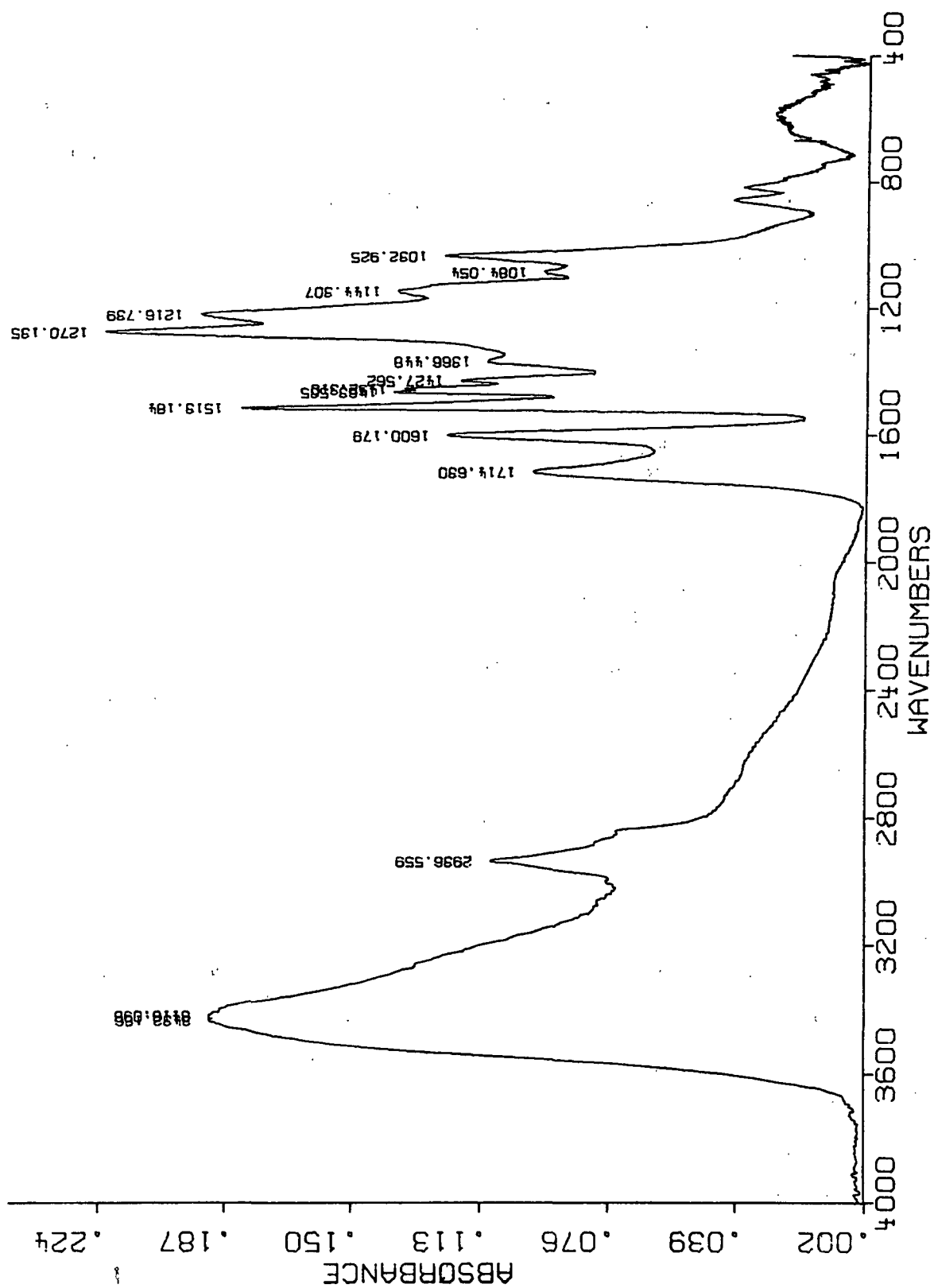


Figure 68. FTIR spectrum of periodate-oxidized (two minutes), sulfur dioxide-reduced kraft lignin.

# APPENDIX III

## ESTIMATION OF SOLVENT COMPRESSION

The change in the liquid densities of DMF and 2-methoxyethanol with pressure were estimated by an empirical method based on the principle of corresponding states.<sup>118</sup> The correlation, which applies to all liquids, is obtained when the reduced density is plotted as a function of the reduced temperature and pressure, as shown in Fig. 69. The reduced density, temperature, and pressure are defined as

$$\rho_r = \frac{\rho}{\rho_c}, \quad T_r = \frac{T}{T_c}, \quad P_r = \frac{P}{P_c}$$

where c refers to the critical point.

Figure 69 may be used directly if an accurate value for the critical density is known. When this value is not available, the relationship given by Eq. (13) may be utilized. Equation (13) makes use of a single known liquid density at any temperature and pressure condition.

$$\rho_2 = \rho_1 \frac{\rho_{r2}}{\rho_{r1}} \quad (13)$$

In Eq. (13),  $\rho_2$  is the required density,  $\rho_1$  is the known density, and  $\rho_{r1}$  and  $\rho_{r2}$  are the reduced densities from Fig. 69 for conditions 1 and 2.

### N,N-Dimethylformamide

The critical temperature and pressure for DMF are 323.4°C and 51.5 atm, respectively.<sup>119</sup> The density of DMF at 25°C is 0.9439 g/mL.<sup>119</sup> Using the method outlined above, the density of DMF at 100 MPa and 25°C was calculated.



The reduced temperature and pressure at condition 1 (25°C and 0.1 MPa) were calculated to be 0.50 and 0.01. Using these values in Fig. 69, the reduced density at condition 1 was found to be 2.92. Similarly, the reduced temperature and pressure at condition 2 (25°C and 100 MPa) were calculated to be 0.50 and 19. Again from Fig. 69, the reduced density at condition 2 was 3.05. Substituting the reduced densities at conditions 1 and 2 into Eq. (13) yielded a value of 0.9859 g/mL for the density of DMF at 100 MPa. This value represented a 4.4% increase in the density of DMF over atmospheric conditions (0.1 MPa).

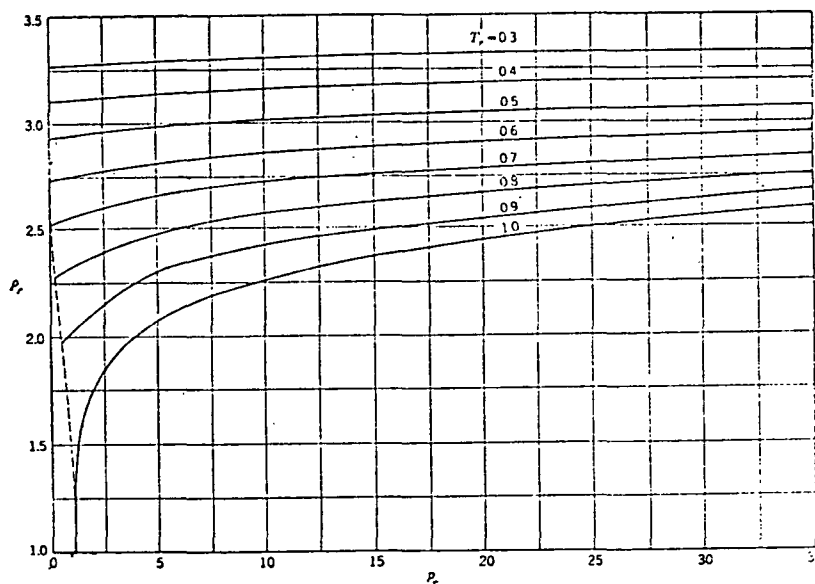


Figure 69. Generalized density correlation for liquids.<sup>118</sup>

Similar calculations to determine the density changes of DMF at other pressure intervals were performed. The results from these calculations are plotted in Fig. 70, where the percentage increase in the density of DMF vs. the applied pressure is shown.

### 2-Methoxyethanol

The change in the density of 2-methoxyethanol with applied pressure was calculated in the same manner as outlined for DMF. Critical constants for

2-methoxyethanol were estimated by two methods, since these values were not available. The Herzog correlation<sup>120</sup> yielded values of 320.5°C and 44.8 atm for  $T_c$  and  $P_c$ , respectively. Values of 324.5°C for  $T_c$  and 51.9 atm for  $P_c$  were obtained from the Heukelom method.<sup>121</sup> The averages (322.5°C and 48.4 atm) from these two sets of values were used in the density calculations. The known density value for 2-methoxyethanol used in these calculations was 0.96024 g/mL at 25°C.<sup>122</sup>

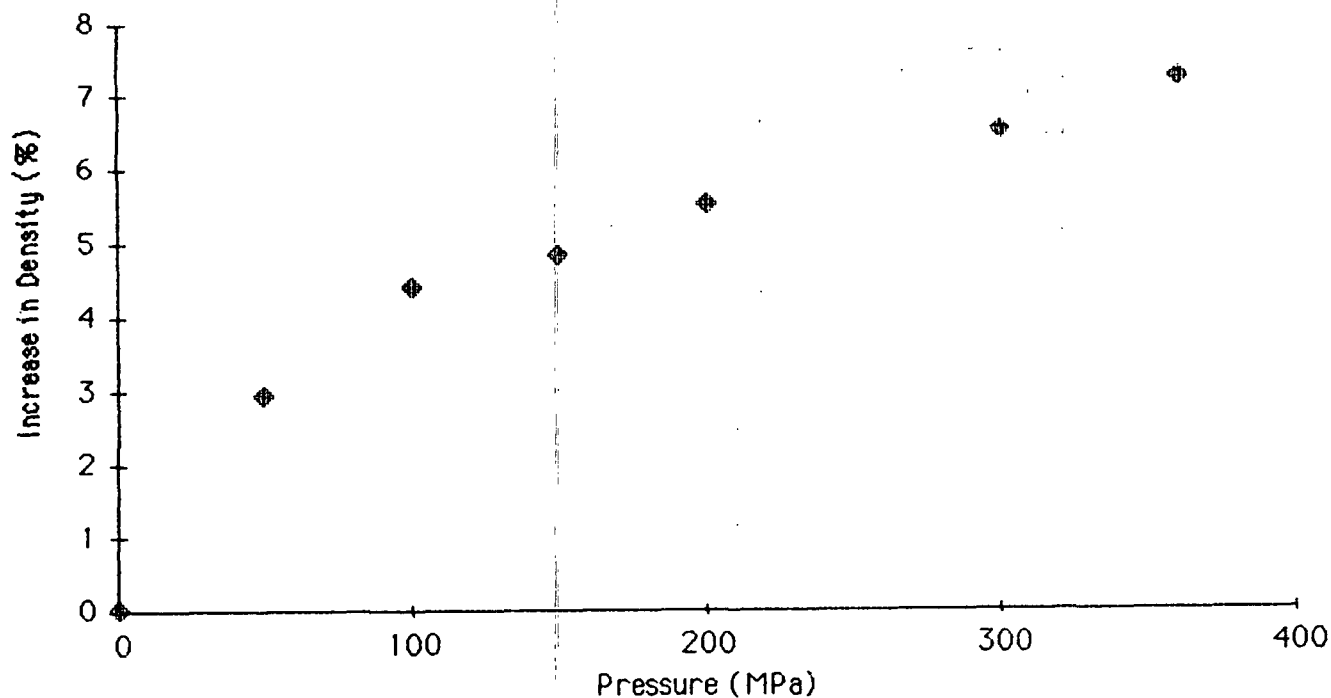


Figure 70. Estimated density change of DMF with applied pressure.

The results from these density calculations appear in Fig. 71, where the percentage increase in the density of 2-methoxyethanol is plotted against the applied pressure.

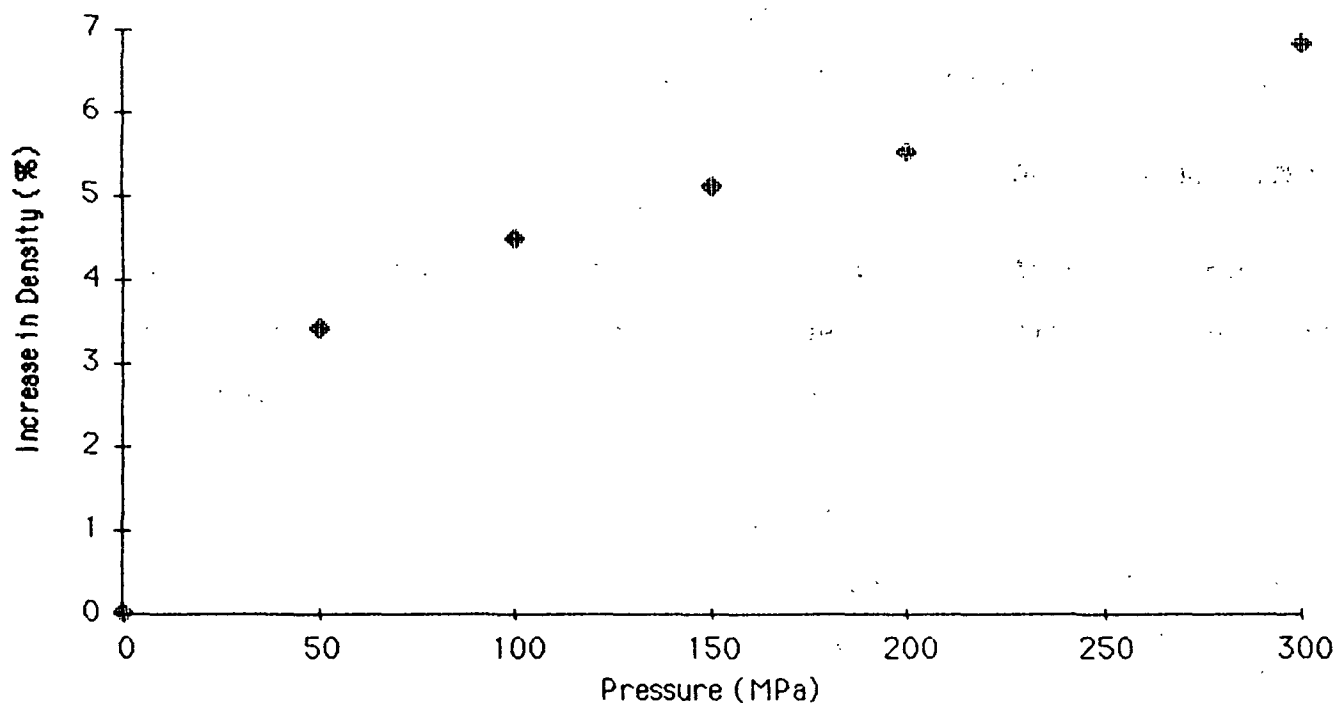


Figure 71. Estimated density change of 2-methoxyethanol with applied pressure.

# APPENDIX IV

## UNIT MOLECULAR WEIGHTS FOR ACETYLATED LIGNINS

### ACETYLATED KRAFT LIGNIN

Before calculating the unit molecular weight of the acetylated kraft lignin, its acetate content had to be determined. This acetate content was not determined directly, but according to the following analysis. For the purposes of this analysis, let the nonacetylated kraft lignin sample be equal to 100 g of material. Also, let  $x$  be equal to the number of grams of acetate present in the acetylated kraft lignin. The weight of the acetylated lignin, therefore, will be  $(100 + x)$  g. The quantity  $x$  may then be determined from the relationship given in Eq. (14), where  $OMe$  is the methoxyl content of the original lignin in grams and  $OMe'$  is the methoxyl content of the acetylated lignin in per cent.

$$\frac{OMe}{100 + x} (100\%) = OMe' \quad (14)$$

The methoxyl contents of the original and acetylated lignins were 14.2 and 10.38%, respectively, for the sample of kraft lignin used in the radioactive labeling experiments. Inserting these quantities into Eq. (14) yielded a value for  $x$  of 36.8 g. This value represented an acetate content in the acetylated kraft lignin of 26.9%.

The method used for calculating the unit molecular weight of the acetylated kraft lignin is summarized in Table 29. In this table, the molecular ratios were calculated by dividing the percentage of a compound or element by its formula weight. Net molecular ratios represent the corresponding molecular ratios minus contributions from the methoxyl and acetate contents. The unit molecular

weight is based on a nine carbon molecular unit. Therefore, the values in the net ratio column were multiplied by a factor of 2.47 in order to yield the correct proportions of these other constituents of the C<sub>9</sub> unit formula. The molecular weight of this C<sub>9</sub> unit formula is 246.6 g/mole.

Table 29. Calculation of unit molecular weight for acetylated kraft lignin.

Element or Compound	% in Lignin	Formula Weight	Molecular Ratio	Amt. of Mol. Ratio From		Net Mol. Ratio	C <sub>9</sub>
				OMe	OAc		
C	62.75	12.01	5.22	0.33	1.25	3.64	9
H	5.51	1.008	5.47	1.00	1.87	2.59	6.40
O	28.29	16.00	1.77	0.33	0.62	0.81	2.00
S	3.19	32.06	0.10	--	--	0.10	0.25
OMe	10.38	31.034	0.33	--	--	0.33	0.83
OAc	26.9	43.044	0.62	--	--	0.62	1.54

#### Acetylated Quinone Lignin

In a similar manner, the acetate content and the unit molecular weight of the acetylated quinone lignin, given in Table 18, were calculated. From the methoxyl contents in the quinone and acetylated quinone lignins of 9.275 and 5.815%, respectively, the acetate content of the acetylated quinone lignin was calculated to be 37.3%. The additional values of 61.455% C, 5.195% H, 1.615% S, and 31.295% O yielded a unit molecular weight of 280.3 g/mole for the acetylated quinone lignin.

APPENDIX V

MOLAR ABSORPTIVITY OF QUINONES IN KRAFT LIGNINS

KRAFT LIGNIN

After obtaining the concentration and absorbance of the quinones in kraft lignin, a value for their molar absorptivity was calculated from Beer's Law. The difference spectrum, shown in Fig. 49, revealed the quinones in this kraft lignin had an absorbance equal to 0.026 AU at the quinone maximum (431 nm; 2-methoxyethanol). Also, from radioactive labeling experiments, the concentration of quinones in this lignin was known to be 3.05%.

The quinone concentration was converted to its molar equivalent, using the weight of the material present in the sample and the estimated unit molecular weight of a quinoidal unit in the lignin. The acetylated lignin samples used to obtain the spectrum in Fig. 49 contained  $7.6 \times 10^{-3}$  g of material. Since the concentration of quinones was 3.05%, the amount of quinoidal material in this lignin sample was equal to  $2.32 \times 10^{-4}$  g. A quinoidal unit in the acetylated kraft lignin will differ from a normal unit by 58 g/mol (-OMe, -OAc). Since the unit molecular weight of the acetylated kraft lignin was 246.6 g/mol (Appendix IV), the unit molecular weight of the quinoidal units in the acetylated kraft lignin was estimated to be 186.6 g/mol. Consequently, the molar quantity of quinones in the acetylated lignin was  $1.23 \times 10^{-6}$  mole, or if based on the 25 mL of sample solution,  $4.92 \times 10^{-5}$  M.

Calculation of the molar absorptivity of these quinones was then performed by substituting the values of concentration and absorbance into Beer's Law. Given the path length of 1 cm, a value of 528 lit/mol-cm was calculated for the quinones in this lignin.

### Quinone Lignin

Similar calculations were performed in order to determine the molar absorptivity of the quinoidal groups in the quinone lignin listed in Table 18. From the difference spectrum in Fig. 51, the absorbance due to the quinones at the quinone maximum (447 nm; DMF) was determined to be 0.072 AU. Also, the concentration of quinones in this sample was known to be 12.1% from radioactive labeling.

The quantity of lignin present in the samples which were used to obtain the spectrum in Fig. 51 was  $7.6 \times 10^{-3}$  g. Since the concentration of quinones was 12.1%, this meant  $9.2 \times 10^{-4}$  g of quinoidal material was present in the sample. The unit molecular weight of the acetylated quinone lignin was determined to be 280.3 g/mol (Appendix IV). Therefore, the unit molecular weight of a quinoidal unit in this lignin equaled 222.3 g/mol. Consequently, the molar quantity of quinones in this lignin sample was  $4.14 \times 10^{-6}$  mole, or taking into account the 25 mL of solution,  $1.65 \times 10^{-4}$  M.

Again, utilizing Beer's Law, the molar absorptivity of the quinoidal structures in this oxidized lignin was calculated to be 435 lit/mol-cm.

APPENDIX VI

SEPARATION OF QUINONE AND CTC ABSORBANCES

Sodium borohydride reduction of the original kraft lignin removed both the quinone and CTC absorbances from the lignin's spectrum. The amount of absorbance removed from this lignin at the quinone maximum averaged 0.091 AU (see Fig. 50). The percentage of this absorbance loss, which was due to the removal of the quinones only, was calculated from the concentration of quinones in the sample ( $5.38 \times 10^{-5}M$ ; determined as in Appendix V) and the molar absorptivity of these quinones (528 lit/mol-cm; Appendix V). Applying Beer's Law, the calculated absorbance due to this quantity of quinones was 0.028 AU.

Out of the total absorbance removed by the  $NaBH_4$  reduction (0.091 AU), this meant 0.063 AU, or 68.8%, of the absorbance decrease was caused by CTC's. Based on this absorbance value for the CTC's, a molar absorptivity was calculated. A concentration for the CTC's was obtained from the assumption that every quinone was participating in a complex. Therefore, the concentration of quinones in the sample equaled the concentration of CTC's. Substituting the values of concentration and absorbance into Beer's Law yielded a molar absorptivity of 1163 lit/mol-cm for the CTC.

Sodium borohydride reduction of the quinone lignin, given in Table 18, resulted in a 0.099 AU decrease at the quinone maximum. Of this total decrease in absorbance, 0.071 AU, or 71.8%, was calculated to be a direct result of the removal of quinones from this sample. This calculation was based on the values of molar absorptivity (435 lit/mol-cm; Appendix V) and concentration ( $1.63 \times 10^{-4}M$ ) for the quinones in this lignin. Of the total absorbance decrease caused by  $NaBH_4$  reduction, this left 0.028 AU, or 28.2% as due to the disruption of CTC's.